POLITECNICO DI MILANO

Scuola di Ingegneria Industriale e Dell'Informazione

Master Thesis in Materials Engineering and Nanotechnology

Dipartimento Di Chimica, Materiali e Ingegneria Chimica "Giulio Natta"

A COMPARATIVE STUDY BETWEEN A SHORT-TERM ANALYTICAL METHOD AND LONG-TERM AGING FOR THERMAL INDEX PREDICTION OF POLYAMIDE 6,6 AND POLYBUTYLENE TEREPHTHALATE

Supervisor: Prof. Roberto Frassine

Tutor: Ing. Loredana Mercante

Giovanni Pallaoro

ID 875269

Academic Year 2017/2018

Abstract

Polymers and composites are versatile and cost-effective materials which play a leading role in the manufacturing industry and are an essential part of our everyday life. Unfortunately, the properties of this class of materials are time and temperature dependent and a measure of their durability in fields of application comprising elevated temperatures and chemically aggressive environments is of the uttermost importance. Techniques which allow for an evaluation of this paramount feature exist, but they are often empirical and rely on prerequisites which may not prove adequate. The main result they provide is a quantity called *thermal index*, which stands for the maximum temperature at which a material can safely perform for a given lifetime without experiencing a decay of some of its key properties greater than 50%. This is an internationally recognized design criterium, often employed in the selection of the most suitable material for a specific application. Therefore, this mere number is of significant interest for manufacturing companies and the development of time- and cost-saving procedures for its prediction is a hot topic. As a matter fact, traditional standardized procedures for the determination of the thermal index rely on long-term thermal aging programs, which extend from 8 to 12 months on average, are labour intensive, and costly. Beside these, the importance of novel alternative procedures represented by short-term analytical methods, which exploit thermogravimetric analysis to achieve kinetic parameters, has recently seen a substantial growth. However, they employ operating conditions which cannot be compared to those in which real plastics undergo degradation, which usually to defects and surface oxidation which could cause catastrophic failure. In this work, a comparison between these two approaches was carried out to define whether they provide acceptable results and whether they could be considered interchangeable in the assessment of polymer durability, if not for all, at least for a specific part of these materials.

Sommario

Polimeri e compositi sono una classe di materiali caratterizzati da basso costo e alta versatilità, che rivestono un ruolo di primo piano nell'industria manifatturiera e che sono ormai una parte essenziale della vita di tutti i giorni. Purtroppo, le loro proprietà sono intrinsecamente dipendenti dal tempo e dalla temperatura di utilizzo e una stima della loro durabilità in ambienti chimicamente aggressivi o caratterizzati da temperature elevate è della massima importanza. Al fine di valutare questa caratteristica, al giorno d'oggi sono utilizzate tecniche spesso empiriche e che si basano su prerequisiti che potrebbero rivelarsi non adeguati. Il risultato principale che queste procedure forniscono è un valore chiamato *thermal index*, che rappresenta la temperatura massima alla quale un materiale può essere utilizzato per un tempo specifico, senza che le sue proprietà principali decadano di più del 50%. Questo valore è visto internazionalmente in fase di progettazione come criterio di selezione del materiale più adatto per una determinata applicazione. Perciò, è evidente come questo numero possegga una fondamentale importanza in campo industriale e come lo sviluppo di procedure a basso costo e a basso dispendio per la sua determinazione siano un argomento scottante. Infatti, le tradizionali procedure standardizzate per il calcolo di questo indice si basano su programmi di invecchiamento a lungo termine, con una durata media dagli 8 ai 12 mesi, che risultano estremamente costosi. Al fianco di queste si stanno sviluppando innovative tecniche di breve durata, che utilizzano l'analisi termogravimetrica per l'ottenimento dei parametri cinetici. Però, queste fanno uso di condizioni operative che non possono essere paragonate a quelle a cui sono sottoposti realmente i materiali plastici, che generalmente causano la formazione di difetti e di ossidazione superficiale che possono portare a fallimenti improvvisi. In questo elaborato, i risultati di questi due approcci sono stati paragonati per determinarne l'accettabilità e l'interscambiabilità nella valutazione della durabilità dei materiali polimerici, se non per tutti, almeno per una parte di essi.

Il progetto di confronto delle due metodologie è stato proposto dall'azienda LATI S.p.A. di Vedano Olona, leader a livello europeo nel compounding di materiali termoplastici. Per lo studio sono stati selezionati due compositi con fibra di vetro, ossia

un grado di poliammide 6,6 ed uno di polibutilene tereftalato. L'elaborato è stato sviluppato nel modo seguente:

- Nel primo capitolo sono stati presentati i concetti di durabilità e degradazione dei materiali polimerici ed è stato delineato lo scopo del lavoro. Inoltre, è stata introdotta l'azienda LATI S.p.A. ed è stata fornita un'analisi dell'attuale stato dell'arte sulle due metodologie di studio. Infine, è stato brevemente presentato un lavoro di tesi magistrale nel quale vengono comparati gli indici ottenuti con i due metodi.
- Nel secondo capitolo sono stati descritti i materiali utilizzati e la tecnica di stampaggio ad iniezione con la quale sono stati ottenuti i provini. In seguito, è stata effettuata un'analisi degli standard in base ai quali si sono svolte le prove sperimentali di caratterizzazione e di invecchiamento.
- Nel terzo capitolo vengono mostrati i risultati ottenuti dalle caratterizzazioni meccaniche ed elettriche, con relativi grafici descrittivi dell'evoluzione di queste proprietà, e dalle analisi termogravimetriche.
- Nel capitolo quattro i dati appena ottenuti sono stati elaborati al fine di ottenere i valori di energia di attivazione del processo degradativo ed i thermal index.
- Nel capitolo cinque sono stati paragonati i risultati ottenuti per mezzo delle due tecniche per determinarne l'accettabilità e l'interscambiabilità. Inoltre, vengono presentate le ulteriori analisi svolte sui due materiali per determinare sinteticamente come il processo degradativo sia avvenuto, in termini di variazione di aspetto esteriore, viscosità e peso molecolare.
- Nel capitolo sesto sono state tratte le conclusioni ed è stato evidenziato come le prove analitiche a breve termine non si prestino alla valutazione dell'energia di attivazione e del thermal index in modo assoluto, ma come in realtà sia necessario che il materiale studiato presenti determinate caratteristiche.

Table of Contents

Table of Figures

CHAPTER ONE
Introduction

1. Chapter Content

In the following chapter, the main purpose of this work will be described and a review of the state of the art at present time will be given. Firstly, a short introduction to the key concept used during this work will be presented, followed by a brief description of the company supporting the project, i.e. LATI S.p.A.

1.1. Polymer Degradation

Degradation is a concept that defines the decay of the properties of polymers related to changes in the chemical structure and molecular weight, due to mechanical, chemical, photochemical or thermal stresses. Conversely, when the decay is caused by physical effects, such as free-volume relaxation, the phenomenon is addressed as *physical aging*. Pure polymers are prone to quick degradation even by simple light exposure under mild condition, a feature which can be explained by the presence of weak bonds and defect, causing spontaneous spreading of the process. Therefore, it has proved necessary to identify and use appropriate processing aids, such as stabilizers, to improve the resistance of the polymer to oxygen and elevated temperatures.

It has been observed that an induction period is always present before the trigger of the degradation processes. Any material possesses its own, but, upon compounding, the process of consumption of stabilizers determines the final induction time. Among the various degradation mechanisms, two are most relevant for the development of this work, hence they will be inspected more comprehensively:

- *Thermal degradation*, which is only assisted by temperature and occurs as soon as thermal energy overcomes bond energy, consequently being difficult to counteract it if not by working on weak bonds. It is possible to distinguish two categories of degradative pathways:
    - Main-chain reactions, which imply the scission of carbon-carbon bonds and lead to an inevitable decrease of molecular weight, up to the point of the formation of volatile products. The most prominent competing mechanisms are *beta-scission* (Figure 1), which can lead to complete *unzipping* up to the monomer, as observed for PMMA, and *back-biting*,

which is a mechanism of radical shifting due to the formation of six-membered rings intermediates.

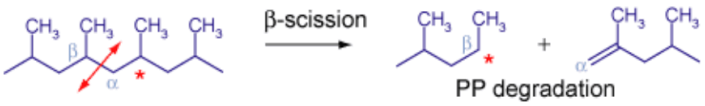

Figure 1 *Example of the mechanism of beta-scission during degradation of PP*

- Side-group reactions, which generally cause little to no variation of mechanical properties, normally only bringing about changes in colours. They occur at constant molecular weight and the main example is the dehydrochlorination of PVC (Figure 2), which leads to the release of HCl with formation of carbon-carbon double bonds along the main chain.

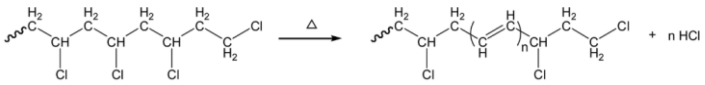

Figure 2 *Ideal depiction of the process of dehydrochlorination of PVC*

Oxidative degradation, which refers to any type of decay occurring in presence of oxygen, a substance that acts as an accelerator and modifies the mechanisms through which the reactions occur. The main effect of oxygen is the reduction of molecular weight and the introduction of carboxyl or hydroxyl groups in the chain (Figure 3).

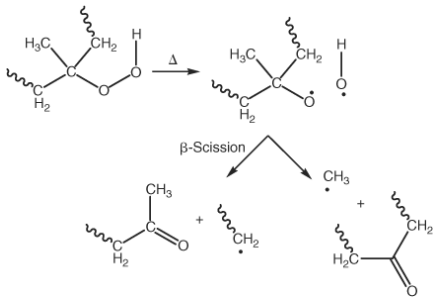

Figure 3 *Example of the main processes occurring during oxidative degradation*

The usual scheme is the following:

- Initiation, which refers to the formation of macroradicals due to the action of heat or light;
- Propagation, when the radical reacts with oxygen to form peroxide radicals, which then subtracts a hydrogen to the chain causing beta-scission and the formation of an hydroperoxide;

- Branching, when the hydroperoxide group is broken to form smaller and more aggressive radicals;
- Termination, which could in principle occur by combination of two reactive groups, even though it generally needs to be induced [1].

1.2. **Durability**

Durability is defined as the retention of properties over time. Polymers and composite materials must always satisfy specific requirements, such as excellent mechanical properties, chemical and thermal stability and suitable dielectric behaviour, all of which play a key role both during manufacturing and application. Under standard operating conditions at a fixed temperature, the planned service lifetime of such materials is of the order of several decades. However, polymeric materials age with an irreversible process characterized by a deterioration of their properties, consequently affecting their lifetime [2].

Therefore, a proper estimation of the durability of this type of materials is required at any industrial level. Such an evaluation proves unfeasible at the operating temperature, since the test would be time intensive and economically unacceptable. As an answer to this issue, various kinds of testing are generally exploited, so as to reduce the overall cost, while still providing acceptable results. The most noteworthy solution is that represented by *accelerated aging tests*, which exploit the action of temperature in accelerating the physical and chemical degradation processes [3].

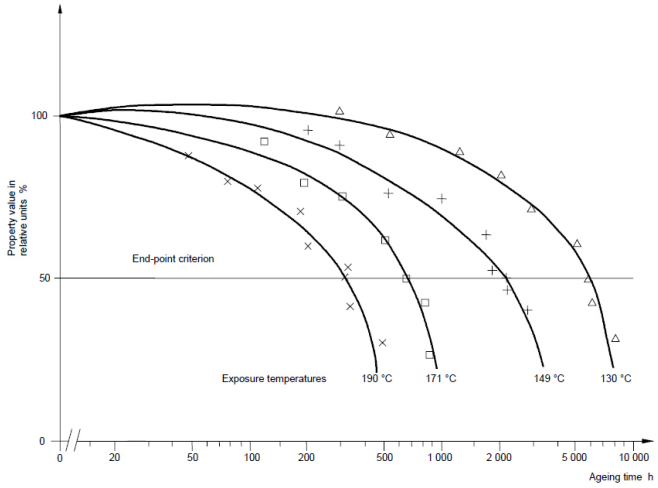

Figure 4 *Typical graph representing the loss of property of a polymeric material due to aging at different temperatures, the end point being set at 50% of the initial property*

In such tests, samples of the desired material are aged at set of different temperatures, each higher than the expected service one, in order to determine the so-called *thermal endurance*. The latter is defined as the time required to reach an end point in the property, i.e. a specific reduction taken as the limiting requirement for service life at each temperature (Figure 4) [4].

1.3. **Purpose of the work**

The concept of durability is of the uttermost importance for industries that deal with polymer production and compounding, since this class of materials is often subject to interactions with different environments and aggressive chemical substances. The main goal of this project is to evaluate and confront some of the existing methodologies exploited to test and determine the durability of polymeric products. As a matter of fact, several different standardized techniques exist nowadays, each of which is mostly empirical and based on prerequisites that are not necessarily representative of the actual working conditions.

The project is aimed at determining the kinetics of degradation and trying to establish the conditions of validity for the distinct types of accelerated thermodynamic analysis. In order to study such phenomena, it is important to introduce a specific quantity which is called *Thermal Index* (TI). This can be defined as "the maximum service temperature for a material where a class of critical property will not be unacceptably compromised through chemical thermal degradation". Notwithstanding its clear reference to a temperature, it is a dimensionless quantity. Generally, a slightly different measure is preferred, that is to say the *Relative Thermal Index* (RTI), which "spans over the reasonable life of an electrical product relative to a reference material having a confirmed, acceptable corresponding performance-defined RTI" [5]. It is usually associated to three properties, one of which is electrical while the others are mechanical. Specifically, the three addressed properties are the dielectric strength, the mechanical impact resistance and the mechanical strength. The end-of-life of a material at a selected temperature is assumed to be the decrease of a property to 50% its original value.

The definition and computation of such an index is paramount for all plastic manufacturers as it is part of the *UL (Underwriters Laboratories) Yellow Card* (Figure 5),

which represents a globally recognised safety and quality guarantee for all industries. This lists multiple safety and performance-related properties for a polymeric material tested by UL to appropriate standards, and can also include additional performance credentials, which verify industry requirements. It provides substantiation that a material is appropriate for specific applications and helps ensure that the manufacturer is using a tested and certified material, as well as being monitored at regular intervals by an independent test laboratory.

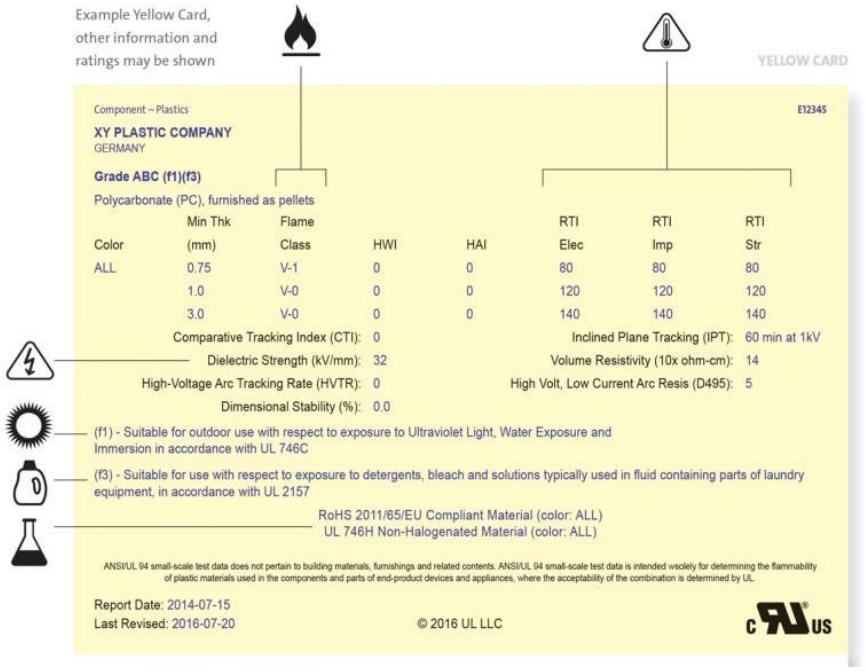

Figure 5 *Example of a UL Yellow Card for a polymeric material*

Polymer manufacturers use the UL Yellow Card to promote the safety and quality of products to markets and existing or potential customers. Yellow Cards are listed in several databases, which are exploited by designers, engineers, and suppliers to find providers of verified materials and components. Therefore, the Thermal Index is truly a selective criterion in the choice of which material to buy and use for one's projects. This is what makes the search for a quicker, yet still reliable, way to determine it one of the main concerns for this kind of industries [6].

Actually, abiding by distinct standards and exploiting different techniques and end-points, it is possible to determine two specific types of thermal index, the second taking the name of temperature index. Nonetheless, both can be equally addressed as thermal indices. As a matter of fact, they are:

- Thermal index obtained from *long-term testing* and relying on the standard UL 746B. This procedures consists in studying the decay of the three properties recalled above due to thermal aging in ovens at selected temperatures. The end point of the test is the degradation of those properties up to the 50% of the initial value. Once the times corresponding to that feature are obtained, by means of regressions, it is possible to estimate the activation energy of the degradative phenomenon, i.e. the minimum amount required to initiate the chemical process, and to compute the temperature at which the properties are retained for at least $6 \cdot 10^4$ hours. This value is defined TI and the specific methodology to obtain it will be examined in the following chapter.
- Temperature index obtained from *thermogravimetry*, either standard or modulated one, which introduces an additional subdivision in the computation. This procedure is by far shorter than the previous one in terms of time, but it is based on dissimilar assumptions. As a matter of fact, not only is the end-point different, being generally between 5% and 10%, but also the controlled feature varies. Precisely, this technique monitors the mass loss and not the decay of a specific property, relying principally on ASTM standards. Apart from these distinctions, the definition of TI is basically the same and the time of retention of mass used in the computation is still $6 \cdot 10^4$ hours.

Consequently, as stated above in terms of evaluation of durability, one of the main aims of this project is to provide a comparison between these two methods, trying to give insight on the pros and cons of each of them.

1.4. **LATI S.p.A.**

The will to find a way to forecast the durability of polymeric materials is one of the main interests for any manufacturer dealing with such materials. In this context, it is important to introduce the company supporting this project, i.e. LATI S.p.A from Vedano Olona (VA). Nowadays, this company is among the most important European manufacturers of technical thermoplastics for engineering purposes. It is active in creating new solutions providing thermoplastic compounds to the main industrial sectors. Officially established in 1945, though already active in 1943, LATI S.p.A.

enjoyed an authentic economic boom in the 50's and 60's. In the following decades, the decision to invest in the development of high-performance products led to the consolidation at an international level.

The innovation comes from the work of the R&D team, which offers superior customer support for the development of new materials, for the resolution of applicative problems and for the research of solutions in new and high technological fields and sectors. Moreover, the concepts of observance to legislation, respect for the environment and for the mental and physical integrity of the individual thrusts the company to always seek to comply to the latest safety and quality standards and regulations and to enforce and adopt an appropriate quality management system.

The most relevant products developed by LATI S.p.A are reinforced plastics, self-extinguishing, self-lubricating, density-controlled and electrically conductive compounds. Therefore, the interest in the prediction of durability and estimation of polymer compounds lifetime is clear and legitimate. With a turnover of 147 million Euro and over 2400 active formulations, the sales network of the company is widespread all around the world, in the face of only two production sites (Figure 6) [7].

Figure 6 *LATI S.p.A. production site in Vedano Olona*

1.5. **Long Term Aging**

After outlining the main aims of this project and the interests lying behind it, it is necessary to examine the current state of the art. Still, it is important to always keep in mind that forecasts are essentially made by following precise standards and that any result is only meant to be a qualitative indication of the quality of the product. Therefore, papers and books related to the use of these procedures only provide an analysis of the

degradation products and the kinetics of decomposition of such materials, instead of any improvement or development of the techniques themselves. Such techniques are based on different standards and rely on dissimilar phenomena to compute the thermal index, namely it is possible to speak of long-term aging and thermogravimetric analysis, as stated above. However, the results of these techniques have never been properly compared, so that no similar work exists. On the contrary, the two are usually examined separately and no difference or correlation is ever highlighted.

Let's start to examine the state of art of long-term aging in ovens. The first important thing to underline is that temperature has the strongest influence on the aging of polymeric materials, causing an increase of the molecular mobility and an acceleration of all degradative phenomena. Namely, temperatures below the glass transition temperature promote *physical aging*, characterized by structural relaxation, while temperatures above it foster *chemical aging*, which implies an action on the chemical bonds themselves, still favoured by the even higher mobility of the chains [3]. In order to examine the decay of the material and to infer information about the modification of the structure, *Differential Scanning Calorimetry* (DSC), *Thermogravimetric Analysis* (TGA), *Dynamic Mechanical Analysis* (DMA) and *Fourier Transform Infrared Spectroscopy* (FTIR) are exploited and they will all be examined in the following chapter.

As an example of that, Guilherme Cybis Pereira et al. could spot the degradation of the polymeric structure of short glass fibre reinforced Polybutylene Terephthalate (PBT) after aging at 180°C in oil. As a matter of fact, they noticed the broadening of the melting peak of aged samples under DSC analysis (Figure 7) and could attribute it to mechanisms of chain scission instead of interaction with the oil.

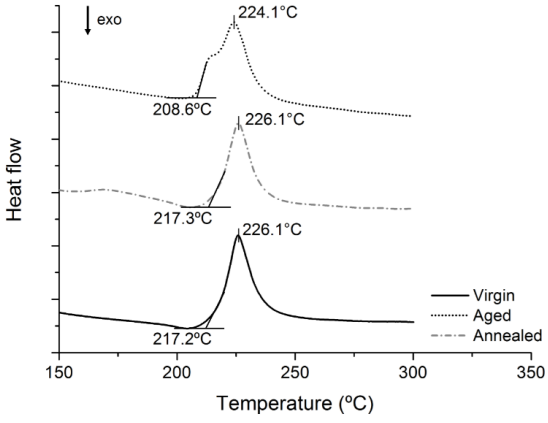

Figure 7 *DSC analysis of samples of PBT after annealing and aging*

Smaller molecules have enhanced mobility and melt before larger ones, causing the melting process to begin earlier. The identification of the reason for this was made possible by coordinating this technique with TGA, thus spotting that no reaction enthalpy was observed at those temperatures in the case of pure oil droplets. Moreover, these analyses put the emphasis on a phenomenon which will be of the uttermost importance throughout this project, i.e. the insurgence of a second melting peak before the original one. In this case, this event was attributed to the reorganization of the crystalline structure and to the crystallization of previously amorphous material [8].

Kenneth T. Gillen and Roger L. Clough carried out accelerated thermal-aging experiments at the university of Akron, Ohio. They could demonstrate that the oxygen consumption rate is relatively constant over the entire mechanical degradation lifetime in the case of elastomers. This statement is of paramount importance as it pinpoints the fact that the degradation curves at any two temperatures will have the same shape when plotted versus the log of the aging time and will be related by a constant multiplicative factor, in accordance with the time-temperature superposition principle. The latter is a representation of the ratio between the two oxidation rates and can be taken into account by considering it as a *shift factor* described by an Arrhenius function:

$$\alpha_T = \exp\left[\frac{E_a}{R}\left(\frac{1}{T_{ref}} - \frac{1}{T}\right)\right] \qquad \textbf{(Eq.1)}$$

In Eq.1, E_a [J/mol] stands for the activation energy of the degradation process, while R [J/K · mol] is the gas constant. However, deviation from this law are not uncommon.

These reasonings can be easily extended to the case of non-crosslinked polymers, too. However, when extrapolating to lower temperatures, this model can prove inaccurate since changes in the dominant reaction can cause the activation energy to vary. At excessively high temperatures, an additional feature of oxidative aging is that if the oxygen reaction is too quick and cannot be sustained in the interior of the material, the concentration will drop, causing reduced or non-existent oxidation in these regions. This phenomenon of diffusion-limited oxidation depends on the oxygen permeability coefficient, the rate of oxygen consumption, but also on the geometry of the specimen, which could lead to heterogeneity and further complications [9].

In their work, R. Polansky et al. emphasised some of the limits of the long-term approach, underlining how the methodologies do not distinguish between oxidative and inert degradation processes. Moreover, in accordance with Kenneth T. Gillen and Roger L. Clough, they stated that any extrapolation of the behaviour of the material at different temperatures can give accurate predictions only in the range of 25°C, because of possible variations of the activation energy of the process outside this. In their work, particular importance was given to the methods of analysis, namely TGA and DSC, which were also directly employed to determine the thermal life. As a matter of fact, parameters such as the evolution of the temperatures corresponding to the maximum peak in the derivative of such curves were monitored throughout the aging process to build the degradation curves. Lastly, to keep track of the ongoing oxidation, FTIR was exploited and the change in peak intensity at 1737 cm^{-1} was controlled, since it corresponds to the stretching vibration of the carbonyl group. This last feature showed a distinguished increase the higher the aging time, as expected (Figure 8) [3].

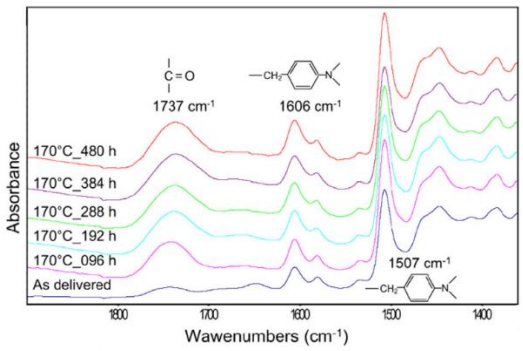

Figure 8 *FTIR spectrum of PCB FR4 epoxy laminates treated at 170°C*

In his studies, M. C. Celina outlined how the behaviour of polymeric material upon oxidation depends on their chemical nature and provided examples in the case of polyolefins, which decay by chain scission, thus decreasing the molecular weight, and elastomers, which are subject to initial crosslinking. In addition, he pinpointed the existence of a critical molecular weight as the threshold between a ductile and a brittle behaviour, meaning that the brittleness of materials rises with increasing oxidation. This latter reasoning, however, is further complicated by heterogeneity in the degradation process and must necessarily be examined case by case. Nonetheless, this provides the general guidelines to understanding the phenomena which occur to materials subject to ageing [10].

All of this is confirmed by M. Nedjar, who focused his study on the evolution of the dielectric strength of polyesterimides upon aging in ovens. Along with highlighting how the breakdown is an essentially random phenomena, thus requiring a statistical treatment, he emphasised how this property is first subject to an increase in value before degradation. This feature is common also for purely mechanical properties, although the reasons lying behind it may differ. In this specific case, Nedjar proposed an explanation which takes into account an initial crosslinking of the material, followed by a weakening of the molecular bonds (Figure 9). The former leads to a decrease in the mean free path of charge carriers, while the latter brings about an increase in mobility. This behaviour is intrinsically dependent on temperature and may not always occur as other phenomena such as the introduction of defects can be dominant [2].

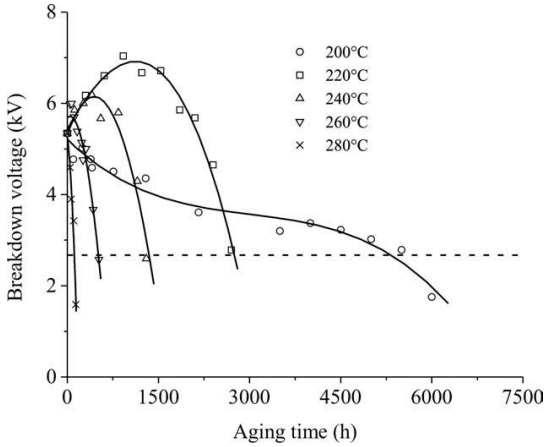

Figure 9 *Typical representation of the evolution of the dielectric breakdown voltage*

1.6. **Thermogravimetry**

Thermogravimetric analysis is usually exploited to study the mass loss curve of a material with increasing temperature, in order to derive information about its nature and structure. However, recently, this technique is starting to be employed to gather information about the kinetics of degradation and to build thermal endurance curves. As a matter of fact, it is possible to use a modulated thermogravimetric analysis (MTGA) to obtain the values of activation energy for the degradation process, along with other data necessary to compute the thermal index. The methodologies lying behind this technique will be examined in the following chapter, while an overview of its recent uses will be provided here.

The most important feature of this type of analysis is that it is a time-saving experiment, as it enables users to obtain information in a single run. Therefore, this technique could be a valuable tool to determine polymer lifetime, being a short-term testing. In case MTGA cannot be taken advantage of, it is possible to use conventional runs of TGA at different heating rates to obtain the same parameters. All the data required to compute the desired kinetic parameters is obtained by deconvolution of the oscillatory temperature programme by means real-time discrete Fourier transforms. The reaction rate is generally expressed as a function of conversion and temperature in the form of:

$$\frac{dC}{dt} = k(T)f(C) = Af(C)\exp\left(-\frac{E}{RT}\right) \quad \textbf{(Eq.2A)}$$

$$C = 1 - \frac{W}{W_o} \quad \textbf{(Eq.2B)}$$

In Eq.2, $k(T)$ is an Arrhenius temperature-dependent rate constant, A is the temperature-independent pre-exponential factor, while $f(C)$ is the conversion dependence function, which is a function of the reaction rate itself [11][12]. Moreover, Eq.2B defines the a as the conversion with respect to the weight of the initial material.

As opposed to long-term testing, it is generally possible to identify several decomposition steps while heating a specimen. Specifically. The TGA plots generally show at least two different slopes, which refer to two separate ongoing mechanisms. The first relates to the proper degradation of the chains, generally occurring by means of chain scission, while the following one, at higher temperatures, denotes the stage of carbonization, comprising the volatilization of char and other residues. This behaviour is emphasized even more when the analysis is carried out in air instead of an inert atmosphere.

In case of non-modulated thermogravimetry, as pointed out by Brems in his studies about the use of the Flynn-Wall-Ozawa method for polyethylene-terephthalate and polystyrene, some limitations can be found. As a matter of fact, the activation energy is only a function of the heating rate, but at low ones some non-linearities may occur, causing an over-estimation of this value. As a matter of fact, the activation energy becomes constant at higher heating rates. Therefore, the author recommends using various heating rates, but mostly high ones, generally above 1°C/min. By using this

approach, he obtained values which are comparable with those coming from literature in case of PET and PS [13].

In a similar study, Lopes et al. investigated the thermal decomposition kinetics of guarana seed residue, both in inert and oxidizing atmosphere, using isoconvertional methods at three different heating rates. By means of thermogravimetry, they could identify three stages in the decomposition, i.e. dehydration, pyrolysis and carbonization or combustion, for inert and oxidizing atmosphere. The first stage takes place below 200°C and comprises the loss of moisture and low molecular weight compounds such as oils. The second one is the preeminent since it is characterized by the greatest mass loss and maximum reaction rates, while the last is significantly different depending on the atmosphere. The main features they pinpointed are:

- A small shift of the peak temperatures towards the right in case of the mass loss derivative plots for the oxidative atmosphere;
- Higher reaction rates in case of oxidative atmosphere, which can be ascribed to the reactivity of the environment, resulting in greater rates the higher the oxygen concentration;
- An increase of the activation energy with the increase of conversion level;

Furthermore, they determined that the application of a simple model comprising a simple-step reaction of the first order was not suitable in case of oxidative atmosphere, due to the presence of simultaneous reactions. Therefore, a better description would call for a more complex scheme of analysis, able to account for parallel reactions. Nevertheless, such a model requires knowledge of the single reactions and of the temperature range in which they occur, leading to a deconvolution of the thermogravimetric curves [14].

In a similar study on the thermal degradation of sugar cane, Rueda-Ordóñez and Tannous pinpointed the influence of the heating rate on the final remaining mass. It was observed that, decreasing the heating rate, the reaction time is increased, allowing the occurrence of more reactions, breaking the polymeric linkages of biomass compounds and increasing the volatile production, thus causing greater biomass decomposition [15].

In their work, Vasconcelos et al. studied, among other topics, how the choice of the end-point affects the results of thermogravimetric tests, both in case of inert atmosphere and in case of a synthetic air one. According to standards, the recommended final conversion value is generally set between 5% and 20% mass loss. What they found was that the values of activation energy computed for different conversion values slightly vary when nitrogen was exploited as atmosphere, while they were much more dispersed in the case of air (Figure 10). This was accounted for by reasonably supposing that a much broader range of reactions take place at the beginning of the decomposition in air than in nitrogen. In addition, in the second case, the computed activation energies were much lower, due to a different initial reaction. As a matter of fact, a non-inert atmosphere prompts oxidation reactions which do not occur in nitrogen. As for the end-point, they suggested to use the value of 5% mass loss as it generally corresponds to the beginning of the degradation process and such a conversion can cause a significant decrease of the mechanical properties of the material [16].

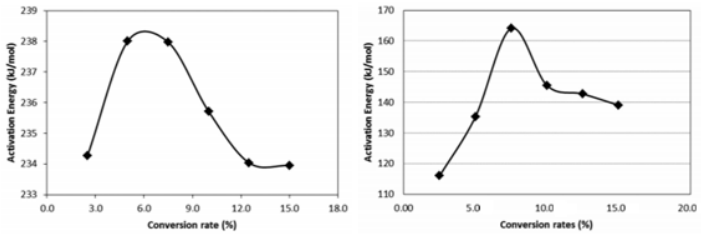

Figure 10 *Computed values of the activation energy at different conversion rates in nitrogen (left) and air (right)*

C. Liu et al. studied the thermal degradation of cyclic olefins copolymers and underlined how the chemical structure has a deep influence in defining the thermal stability of polymeric materials. The phenomena they brought to attention were:

- The improvement in thermal stability given by cyclic structures, whose stiffness reduces the mobility of the chains;
- The increase of the reaction rate given by branching, which leads to lower thermal stability, due to the decrease in strength of the bond closest to the side chain;
- The effect of the functional groups, which either act as electron-withdrawing or electron-donor substituents, the former stabilizing macroradicals as they form, thus reducing the stability of the material.

Furthermore, in accordance with the work of Vasconcelos et al., C. Liu et al. determined experimentally that the beginning of the proper degradation process corresponds to 5% mass loss, at least in the case of cyclic olefins copolymers. Before this value, the main occurring reactions are those involving weak bonds and defects, but not the entire chain. However, this may prove inaccurate in case of simple polyolefins, where the value may also exceed 15% [17].

As a conclusion, it is important to point out what M. C. Celina described as the weak points and limits of thermogravimetric analysis with respect to the prediction of polymer lifetime:

- For many polymers, thermo-oxidative degradation is associated with a weight increase due to incorporation of oxygen. In contrast, TGA forces volatilization of the material and, as such, it represents a process that is often not encountered during polymer aging.
- Thermogravimetry yields values of the activation energy in a high temperature regime that is far from the general temperatures of use. This technique usually delivers values which are much higher than those observed in other studies, such as long-term experiments. Moreover, many polymers show curvature in the Arrhenius plots toward lower activation energies, thus compromising the extrapolation of acceptable data (Figure 11). These occurs both at high and low temperatures, the former bringing about a slower degradation rate as of Eq.2A, while the latter determine a faster one.

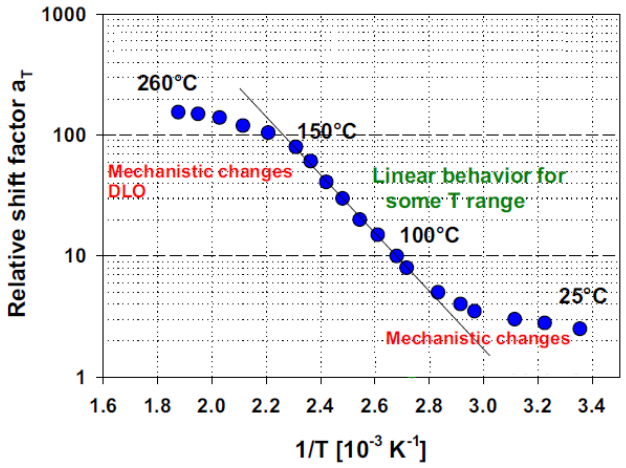

Figure 11 *Sketched graph representing the departure from linearity of a so-called shift factor, more properly a relative degradation rate, thus deviating from the simple Arrhenius behaviour, which are to be expected when working at high temperature*

- Even in case of small samples such as those used in thermogravimetric analyses, diffusion-limited oxidation effects are always present. This method can therefore not easily provide information for overall sample representative oxidation kinetics as it is greatly affected by the permeation of oxygen into the material, and, likewise, the volatile diffusion and desorption from the sample surface.
- Despite the computational power of nowadays instruments, it is difficult to get a proper critical interpretation of the obtained data and to validate the estimation of the material lifetime. Data interpretation is intrinsically complicated or often impossible because polymer degradation rarely proceeds with well resolved individual decomposition steps. Weight loss curves often show multiple parallel degradation steps, and hence the activation energies when 'brute-force' mathematics are applied to weight loss data do not replicate a particular mechanistic step that may govern long-term aging, where limited weight loss is observed [10].

Accordingly, Blanco and several other authors questioned the reliability of activation energies obtained at elevated temperatures when those are much higher than the conventional aging and service ones. To support this statement, the nature of the reaction and degradation kinetics is taken into account as it is not linear across all ranges of temperature. This non-linearity is due to the competition between the degradation mechanism and other competing processes such as the diffusion of oxygen, the different rate at which additives decay, the formation of side products at higher temperatures and the volatility of some degradation products [18].

1.7. Comparison of the two Aging Techniques

Up until now, few works, if any, have tackled the issue of comparing the results obtained from long- and short-term aging. Only recently, a project relating the two procedures in case of unfilled polyamide 6,6 was published as a master's thesis work by Karina Marie Wagner from Washington State University [19].

Firstly, the author suggested that the use of large specimen in a thermogravimetric analysis may affect the results. As a matter of fact, since this

technique consists in heating up the polymer to measure the mass loss, the temperature gradient of the specimen would affect the degradation of the inner portion. This could cause the process to slow down and shift towards higher temperatures (***Figure 12***) as volatile products are unable to escape due to slow diffusion to the surface of a low surface area specimen. Oxygen diffusion plays a key role in oxidation reactions occurring within the material, and a high surface area specimen would produce a more uniform diffusion and more repeatable results from subsequent trials.

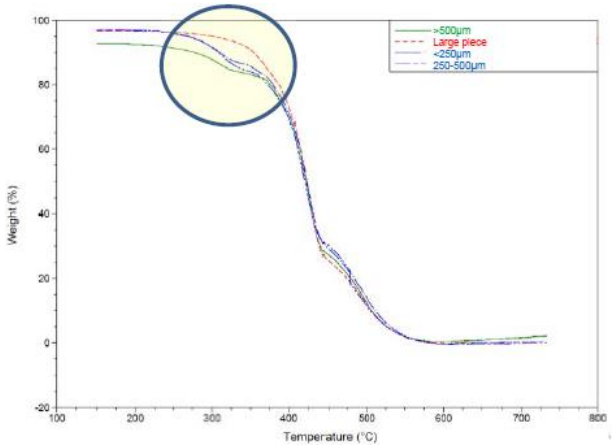

Figure 12 *Comparison of the degradative behaviour of PA 66 as a function of the dimension of the sample in a thermogravimetric analysis performed at 2°C/min*

Furthermore, the author underlined how the difference in activation energies as computed in case of short-term and long-term aging was concerning, even though the thermal indices for such a material were computed within 5°C. As a matter of fact, the latter determined an activation energy equal to 17,2 kJ/mol, while the former gave a value of 68 kJ/mol. On the contrary, the results in terms of thermal index inexplicably turned out to be very similar. To compensate for this difference, a hybrid approach is proposed, where the activation energy of the analytical method is used in coordination with the characteristic temperature and failure times of the physical aging in ovens.

Lastly, the author recorded an initial yellowing of the specimen followed by a sharp blackening due to exposure to elevated temperatures for long periods. However, the core of the material would remain mostly unaffected and therefore white, indicating that the degradation was a surface process. This yellowing is thought to be due to the amino and carbonyl groups reacting to form azeomethines, finally converting to chromomorphic substances that will begin to absorb light at certain wavelengths when their concentration is increased.

CHAPTER TWO
Experimental Details

2. Chapter Content

In this chapter, a presentation of the materials exploited for the project will be provided along with a thorough illustration of the various methods used to evaluate their thermal durability. Moreover, a brief description of the tests employed to assess the mechanical and electrical properties will be given.

2.1. Materials

Throughout this work, two different materials were analysed and studied, namely two specific grades of *Polyamide 6,6* and *Polybutylene Terephthalate*. The base materials are produced by external companies, while compounding and production was carried out directly by LATI S.p.A. Specifically, both polymers are reinforced grades, composed by 70%wt base material and 30%wt filler. These percentages are subject to slight variation because of the presence of processing aids and other additives, such as stabilizers. In both cases, the reinforcement consists of short E-glass chopped strands.

2.1.1. Latamid 66 H2 G/30

Latamid 66 H2 G/30 is LATI S.p.A. trade name for glass fibre reinforced Poly[imino(1,6-dioxohexamethylene) iminohexamethylene] or, more simply, Nylon 6,6. H2 specifies the presence of a thermal stabilizer, while G/30 indicates the type of filler, i.e. glass, and its weight percentage. This semi-crystalline thermoplastic material comes from the polycondensation of two monomers, each containing 6 carbon atoms, namely hexamethylenediamine and adipic acid, hence its name (Figure 13). Its glass transition temperature lies between 50°C and 55°C, while its melting one is around 265°C.

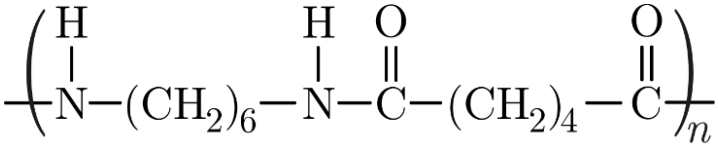

Figure 13 *Latamid 66 repeating unit*

Nylon 6,6 finds its most common application in the textile industry, but it is also much exploited in automotive, let alone guitar manufacturing. In case of a reinforced material,

its most prominent market is that of 3D structural objects, as exemplified in the second aforementioned application. As a matter of fact, it is prone to be compounded in fire-retardant grades to provide a better thermal stabilization. The main properties of this material are: good mechanical, thermal and electrical properties, good wear and chemical resistance and compounding flexibility. The reinforcement is meant to maximize the mechanical properties, especially stiffness and strength [20]. Among all the properties of this specific grade, it is important to underline the previously computed values of relative thermal index, coming from the company yellow cards:

DIELECTRIC STRENGHT	IMPACT RESISTANCE	TENSILE STRENGTH
105	80	105 (3 mm)

2.1.2. **Later 4 G/30**

Later 4 G/30 is LATI S.p.A. trade name for polybutylene terephthalate, a semi-crystalline thermoplastic, filled with 30%wt glass fibre. This polymer is produced by polycondensation of terephthalic acid or dimethyl terephthalate with 1,4–butanediol using suitable catalysts. Its glass transition temperature lies in the range 65°C-70°C, while its melting one is around 225°C (Figure 14).

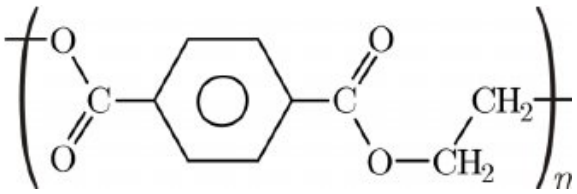

Figure 14 *Later 4 repeating unit*

Its primal uses are in electrical engineering and in automotive construction, although it can also be found processed as thin fibres. Thanks to its chemical resistance, polybutylene terephthalate finds applications in sportswear. This material possesses a good strength and impact resistance, along with a high heat resistance. Moreover, it can be effectively compounded to obtain fire retardant grades, especially when reinforced with glass fibres, and lubricated ones. The values of relative thermal found in the company yellow cards of such a material are:

DIELECTRIC STRENGHT	IMPACT RESISTANCE	TENSILE STRENGTH
140	130	140 (3 mm)

2.2. Injection Moulding

In order to perform mechanical and electrical testing on the material, specimens, whose shape and dimensions will be discussed in the following paragraphs, were obtained by means of *injection moulding* (Figure 15).

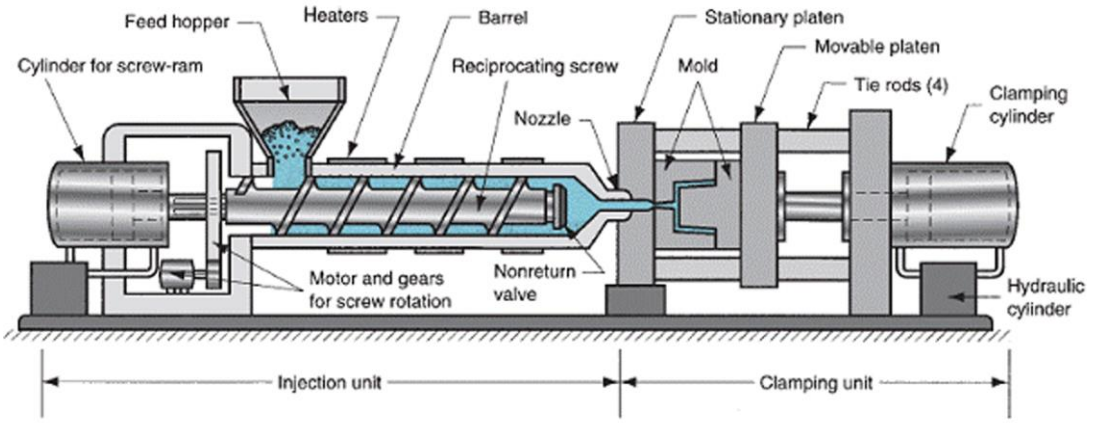

Figure 15 *Injection moulding machine*

The whole process starts with polymer pellets drying for at least 6 hours to remove any absorbed water. Afterwards, they are poured into the feed hopper that leads to extruder, i.e. a barrel with a heated screw, which induces melting both by direct heat and by friction, as the cavity progressively shrinks. Once a homogeneous melt is obtained, the material is injected inside the mould by means of the pressure exerted by the screw, which moves forward to push it through the nozzle. The mould itself is made up of several cavities connected by sprues, runners and gates and the plastic melt flows towards those designed for the application. Once the desired cavity is filled, the mould is left to cool before the ejection of the produced piece, which will generally require some post processing, such as removal of the channels, trimming and refining.

This techniques shows countless advantages, since it is a very repeatable and fast process, producing only a reasonable amount of scrap material. Many parts can be created and produced at the same time by using co-injection moulding and there always is a high production output rate, making it very cost efficient. Moreover, the technique is flexible and can be used for a large amount of materials and applications, provided the required number of specimen to be produced is large, otherwise it would make this method impractical. On the contrary, it also has some cons, namely being the high start-up and tooling costs when modifications to the current mould are required for design

purposes. In addition, not any kind of item can be obtained through this technique, as it may prove unsuitable for asymmetrical parts or complicated ones involving walls with different thicknesses and needing sharply refined edges and corners.

2.3. Long-Term Property Evaluation

This standard UL 746B describes the procedure required to determine the *thermal index* of a material by means of aging in ovens [21]. This quantity is an indication of the material's ability to retain a specific property over time when exposed to elevated temperatures, thus being a measure of the its thermal endurance. Beside an absolute thermal index, a relative one can be established by comparison with a control material of pre-determined service life and field performances. Nevertheless, only the former was considered during this project due to the lack of an appropriate reference.

The thermal-aging characteristics are determined by measuring the changes in certain properties of the material after exposure to predetermined elevated temperature after a selected time. By plotting the log of time to end point against the reciprocal of the absolute temperature, it is possible to fit the so-called life-line of the material by regression. Nonetheless, the behaviour of a material that is subject to thermal aging in air shall never be assumed to be representative of that under service conditions. However, knowledge of its behaviour can be used as the basis for a comparison between different polymers.

The properties which need testing are those which simulate the field-service conditions as closely as possible. Therefore, in the case of polymeric materials, tensile, impact and electrical properties are chosen as representative. Generally, the test consists in studying the changes of properties after aging specimens at up to four different temperatures until an end point is obtained for each. In order to obtain such values, forced-convection ventilated electrically-heated ovens are to be used, in compliance with the standard ASTM D5423 [22]. In the specific case of this project, three "Binder WTC FD-400" ovens were used, each of which was subject to calibration every six months.

It is important to notice that it is assumed that a 50% loss of property due to thermal degradation results in premature risks during service life, which is clearly an

arbitrary choice; however, this choice was not proved unsuitable either. Furthermore, the degradation mechanism is usually a complex combination of effects due to chain scission, oxidation, change in crystallinity, formation of a dense cross-linked skin.

As far as the selection of oven temperatures is concerned, the general guidelines are the following:

- The *lowest oven temperature* is to produce an anticipated end point in no less than 5000 hours;
- The *highest oven temperature* is to produce an anticipated end point in no less than 500 hours;
- Specific aging temperatures cannot be recommended as degradation is a function of the characteristics of each specific polymer;
- The *spread between aging temperatures* is required to be enough to overcome possible measuring issues, besides providing acceptable data for extrapolations; thus, it must be at least 10°C.

While testing the control material, no less than four different temperatures must be exploited, while in case of absolute measures, they can be reduced to three.

The procedure consists in putting a defined quantity of specimen in each oven and in determining a cycle period. The latter is the time lapse between subsequent withdrawals for testing, in which a set of specimen has to be extracted from the oven and left in an environmental chamber at <50% humidity and 23°C ± 2°C for a time at least long enough for cooling. It is commonly required to prepare a large number of specimen inasmuch the materials generally survive more than ten cycles of the test programme. In the specific case of this work, based on literature data and on availability of the ovens, the temperature and time cycles of both materials were chosen as follow:

TEMPERATURE	CYCLE PERIOD	WITHDRAWN SPECIMENS
160°C ± 5°C	**28 days**	**10 for each different property test and thickness**
175°C ± 5°C	**7 days**	
190°C ± 5°C	**3 days**	

As it was pointed out in the previous table, not only does the material itself play an essential role, but also the thicknesses influences the thermal endurance. However, it was proved that the thickness of 3 mm can be held as representative also in case of greater nominal thicknesses. Therefore, in case of tensile testing, both 3 mm thick and 1,5 mm thick specimen were studied.

The aim of the process of thermal aging is to determine the time it takes to reach the end point in each measured property for each temperature, as in the illustrative Figure 16 [21]. As highlighted in the figure, it is possible to plot the property retention percentage as a function of the logarithm of time for each different properties. For each temperature, it is required to compute the time needed for the curves to cross.

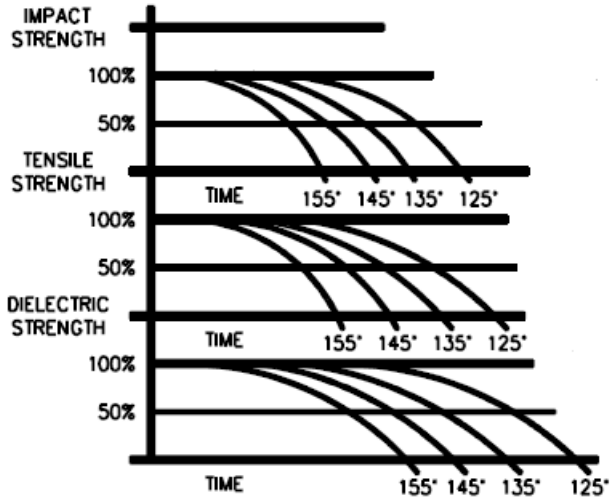

Figure 16 *Expected trend of property degradation as a function of exposure time in case of thermal aging*

The first step to take in order to compute the thermal endurance of the material is to interpolate the data obtained before and after the end point, usually by using a third-order polynomial equation as a function of time. Once this equation has been determined, the time corresponding to 50% of the initial property can be computed. Since the life expectancy can be considered a function of the exposure temperature, the Arrhenius equation (Eq.2A) can be used to estimate the relationship between material lifetime and temperature itself. In this specific case, the equation indicates that the logarithm of the former in hours is a function of the latter in Kelvin, as highlighted in the following (Eq.3).

$$Lifetime = t = A \exp\left(-\frac{E}{RT}\right) \qquad \textbf{(Eq.3A)}$$

$$\ln(t) = -\frac{E}{R}\cdot\frac{1}{T} + \ln(A) \quad \rightarrow \quad y = ax + b \qquad \textbf{(Eq.3B)}$$

$$x = \frac{y-b}{a} \quad \rightarrow \quad T = \frac{-E/R}{\ln(t) - \ln(A)} \qquad \textbf{(Eq.3C)}$$

By making use of the computed time to end point, it is possible to exploit a linear regression analysis to compute the activation energy E of the decay of the property and the pre-exponential factor A which appear in Eq.3A. Once these values are obtained, the temperature corresponding to the selected lifetime can be easily computed by making use of Eq.3C.

This temperature corresponds to the proper thermal index, but a suitable time to failure which can be related to the actual service conditions of the material must be chosen to determine it. Nevertheless, it is important to point out that a proper correlation between this aging programme and the real life of polymers has yet to be established, even though it is generally accepted to define the thermal index for an arbitrary life of $2 \cdot 10^4$, $6 \cdot 10^4$ or 10^5 hours. In the specific instance of this project, the former time was employed for computations. Lastly, for an appropriate assignment of the value, after determining the temperature corresponding to that lifetime, it is recommended to round down to the nearest allowed temperature according to the following increments:

- Every 5°C up to 130°C;
- Every 10°C from 130°C to 210°C including 155°C;

2.4. Properties

To obtain the thermal indices for the various properties as previously described, it is necessary to apply the proper testing methodologies. First of all, each test needs to be carried out in an environmental chamber at the above-described conditions. All of these are quoted in the above-mentioned UL746B standard and the ones employed are issued by ASTM International. All surfaces of the specimen are required to be devoid of flaws, scratches and imperfections and any marking produced on the item must not affect the material being tested. In order to provide an acceptable

result, at least five samples are to be used for each set of aging conditions and type of testing.

2.4.1. **Tensile Properties of Plastics**

The standard ASTM D638 concerns the determination of the tensile properties of plastic materials by means of *dumbbell-shaped* test specimens (Figure 17) [23]. These properties are known to depend on several factors, being the speed and environment of testing and the preparation of the specimen itself. Therefore, the obtained results shall be considered as comparative, but cannot be held as valid should the conditions of application significantly differ from those of testing.

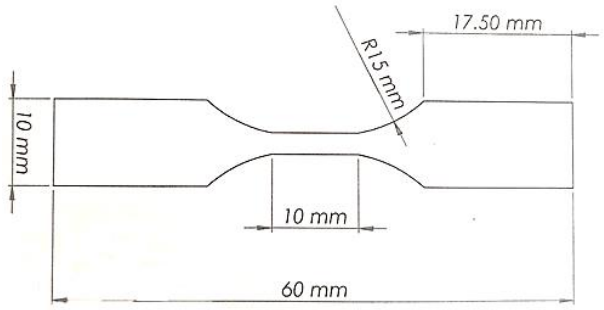

Figure 17 *Specimen exploited for this project, in accordance with ASTM D638, even though dimensions may be prone to small changes because of the process of injection moulding*

Regarding the machine used to perform such testing, it is essentially comprised of two members, one of which is fixed whilst the other is movable and controlled by a drive mechanism, in addition to sets of grips to ensure the clamping of the specimen and its correct orientation, which should avoid any rotary motion, and a suitable load-indicating and crosshead extension-indicating mechanism. Moreover, the use of an instrument designed for determining the distance between two fixed points within the gauge length of the test specimen as the latter is stretched is required. Such item takes the name of extensometer.

The most important parameter in tensile testing is the *speed* of the movable member, which affects the response of the material. As a matter of fact, it determines the time which is left to the molecular chains to rearrange and to react to the imposed stimulus. The faster the upward motion, the more rigid the material will appear, since the test will directly affect the covalent bond of the chains. The effect is the opposite with respect to that of temperature, as the higher the temperature, the softer the

material. The output of tensile testing is the so-called strain-stress curve, an example of which is shown in Figure 18.

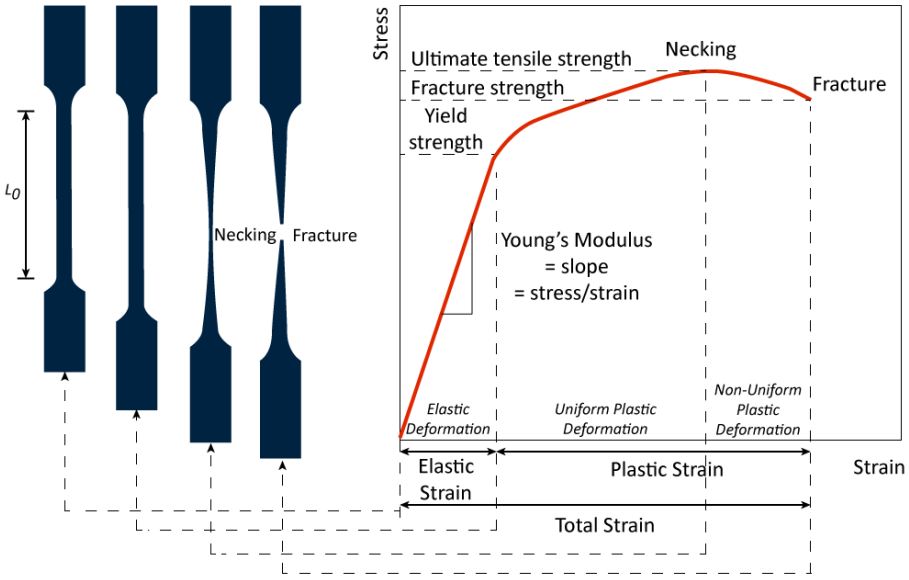

Figure 18 *Typical representation of a stress-strain curve, with key features and respective transformation of the tensile specimen highlighted*

From this plot, the following key properties can be inferred:

- *Ultimate Tensile Strength*, which defines the maximum stress required to pull a specimen up to the point of failure;
- *Percent Elongation at Fracture*, i.e. the change in gage length relative to the original one, expressed as a percent, at the point of failure;
- *Toughness* or *Modulus of Toughness*, which is the energy of mechanical deformation per unit volume prior to fracture, as expressed in Eq.4:

$$Toughness = \int_0^{\epsilon_f} \sigma d\epsilon \qquad \textbf{(Eq.4)}$$

  Therefore, it is the result of the integration of the stress-strain curve.

- *Modulus of Elasticity* or *Young's Modulus*, which is a measure of the stiffness of a material, defining the direct relationship between stress and strain in the linear regime. This property must be evaluated in the region where the material shows an elastic behaviour. Given the fact that this standard does not give a proper indication of which points to consider while computing the elastic modulus, they were chosen in accordance with a different standard, ISO 527

[24]. Specifically, the slope of the curve has to be computed between the elongations of 0,05% and 0,25% as in Eq.5:

$$Elastic\ Modulus = E = \frac{\Delta\sigma}{\Delta\epsilon} = \frac{\sigma_{0,25} - \sigma_{0,05}}{\epsilon_{0,25} - \epsilon_{0,05}} \quad \textbf{(Eq.5)}$$

Yield Strength, namely the stress at which a material exhibits a specified limiting deviation from the linear proportionality between stress and strain
Lastly, this standards provides the rules to make up for the toe region which may generate at the beginning of the test due to take-up of slack and alignment or seating in the specimen. It is important to remind that in such tests, any specimen breaking outside the gauge length must be discarded.

All tensile tests were carried out by means of "Galdabini Sun 2500" dynamometer, equipped with a "Galdabini TCE 2,5t" load cell. The software employed to collect the relative data is "Graphwork 5" and the tests were executed under speed control, with speed of the crosshead fixed at 1 mm/min. As for the extensometer, the type used throughout this project was a non-contact one, specifically a video extensometer, namely a "Mintron digital video camera". This item requires marks on the material to keep track of the deformation and its associated software is "Winext". All instruments are calibrated on a regular basis and the certificates are issued by "S.M.I Misure Ingegneristiche".

2.4.2. **Charpy Impact Resistance**

This standard ASTM D6110 is exploited to determine the resistance of plastic materials to failure by flexural shock generated by a pendulum-type hammer [25]. Most tests require the production of a notch in order to promote a brittle, rather than a ductile, fracture. Nonetheless, during this project, all the specimens were left unnotched since aging produces oxidative species which may alter the geometry of the notch if generated beforehand. Conversely, a later application of the notch might cause the insurgence of defects on the already brittle surface and would expose an unmodified portion of the material.

The machine (Figure 19) is made up of a massive base onto which supports for holding the parallelepiped specimen and a frame to hold the pendulum-type hammer are mounted. The mass of such hammer has to be chosen so that an energy loss of not

more than 85% of its capacity shall be obtained. The striking nose of the latter shall be made of hardened steel and the position of the pendulum holding and releasing mechanism shall lie at a height of 610 mm with respect to the specimen supports. This will give the striking nose a velocity of:

$$v = \sqrt{2gh} \approx 3{,}46\ m/s \qquad \textbf{(Eq.6)}$$

In Eq.6, h stands for the height of fall and g for the local gravitational acceleration. As for the specimen itself, it shall have a width between 3 and 12,7 mm, a thickness of 10 mm and a length between 124,5 and 127 mm.

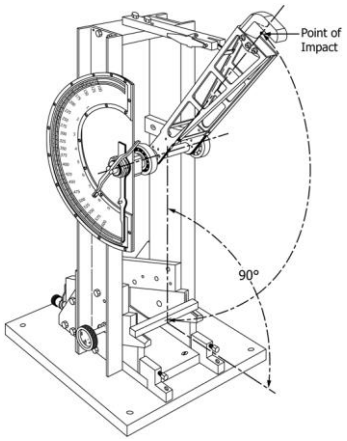

Figure 19 *Simple representation of a Charpy impact machine*

A suitable indicator will provide the energy required to break the specimen, being the sum of the energies of initial fracture, propagation, final breakage and tossing. However, this quantity may comprise friction and vibrational components, thus undermining the reliability of the result. Therefore, suitably designed machine are essential to limit this. The *impact resistance* will be computed by dividing the obtained energy by the transversal area of the specimen.

As for the instrumentation required to carry out this test, a "CEAST® Resil50 Charpy Impactor" equipped with a 6545 hammer was exploited. The machine was calibrated on a regular basis and the certificates are issued by "S.M.I Misure Ingegneristiche". The obtained data was analysed by means of "Microsoft Excel".

2.4.3. **Dielectric Strength of Plastics**

This standard ASTM D149 covers the procedures to determine the dielectric strength of solid insulating materials at commercial power frequencies, generally at 60

Hz, but it is actually suitable in the range from 25 to 800 Hz [26]. By means of electrodes, an increasing voltage is applied to the specimen until dielectric failure occurs, the latter being a sudden increase in conductance, limiting the electric field that can be sustained. Properly, the *dielectric strength* is defined as the voltage gradient at which dielectric failure occurs under the specific test conditions and is obtained by dividing the breakdown voltage by the thickness of the specimen.

The apparatus consists of an alternate voltage source with a well-defined ratio of crest to root-mean-square test voltage, a voltmeter to be used to measure the latter and a series of electrodes, whose surfaces must be kept clean and free from irregularities. In addition, the test chamber must be provided with an insulating medium to prevent flashovers, i.e. disruptive electric discharges. An insulating oil is generally exploited, even though the obtained values cannot be compared with those computed in air.

Lastly, concerning the methods of voltage application (***Figure 20***), it is possible to define the following:

- *Short-Time Test* (a), which consists in applying the voltage uniformly from zero until breakdown occurs, generally at a rate of 500 V/s. This techniques usually takes around 20 s to complete and it's the one which is most commonly exploited.
- *Step-by-Step Test* (b), which starts from 50% of the expected breakdown voltage, to be obtained as quickly as possible, and proceeds with defined jumps.
- *Slow Rate-of-Rise Test* (c), a technique similar to the first one, although it starts at a voltage different from zero and proceeds at a slower rate. The constraint of this technique is that its duration is 120 s at least.

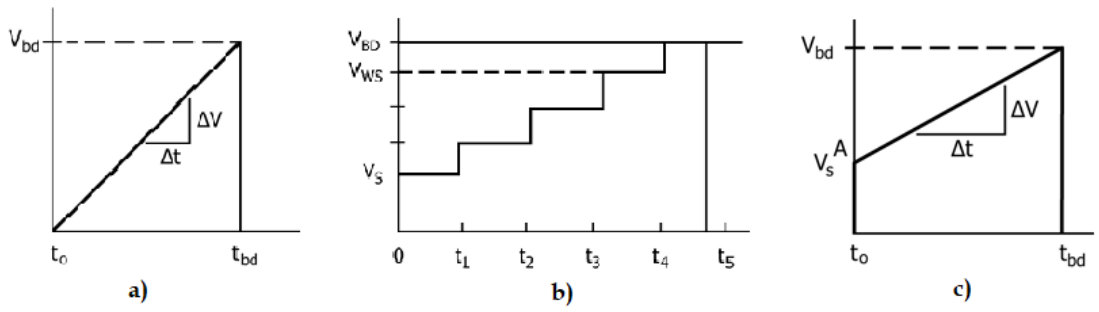

Figure 20 *The three possible pathways for voltage application*

2.5. Thermogravimetry - Procedure

The standards ASTM E2550 and ASTM E2958 [27][28] describe the procedures that shall be followed to perform a correct thermogravimetric analysis, while the computation required to obtain the kinetic parameters will be described in the following chapters. These methods define the assessment of material thermal stability through the determination of the temperature at which the materials start to decompose or react, along with the extent of the mass change. They are suitable and shall be applied only to reactions or decompositions occurring in the range from room temperature to approximately 900°C, either in inert or reactive atmosphere.

Firstly, special focus must be put on the machine itself, called thermogravimetric analyser. It is essentially composed of:

- A *thermo-balance* comprising a furnace able to provide controlled heating up to the desired temperature, a temperature sensor, a continuously recording electro-balance for the mass and a source of purge gas, either pure nitrogen or synthetic air, at a rate of 100 mL/min;
- A *temperature controller* which shall be capable of executing and maintaining the required heating programme;
- A suitable *container*, most likely a titanium crucible, which is basically inert and will be gravimetrically stable throughout the testing;
- A *data collection device* capable of recording and displaying the specimen mass signal as a function of time and temperature.

Concerning the specimens, it is paramount that they are large enough to be considered representative of the material being studied and able to provide an adequate signal. However, the higher the mass, the greatest the chance of hazardous issues during the test, so a compromise shall be found. Generally, a specimen mass between 1 and 10 mg is suggested, even though the range can be extended up to 20 mg. This restriction was respected throughout the project, with an average mass of 18 mg.

The main features which can be spotted in such tests are: the detection of mass change, its extent, the onset temperature and any effect related to the atmosphere (Figure 21). It shall be highlighted that many factors can affect these parameters, the

most prominent being the heating rate because of the intrinsic viscoelasticity of polymers. As a matter of fact, the higher the heating rate, the more shifted towards higher temperatures will be the onset of any reaction, which is also due to the increasing effect of heat transfer limitations.

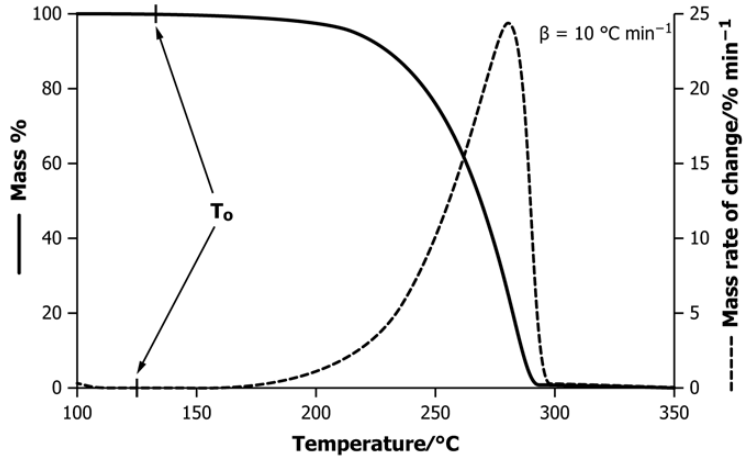

Figure 21 *Typical thermogravimetry (TG curve) and derivative thermogravimetry (DTG curve) plots*

Thermogravimetric analyses can either be performed with a simple ramp from room temperature to the selected end point of the test or with an underlying temperature modulation. Therefore, it is possible to distinguish two techniques, a standard one and a modulated one. The basic steps to follow in either method are:

- Start a calibration of the apparatus in order to have a precise indication of the mass of the specimen throughout the test;
- Place the specimen inside the pan before the closure of the furnace;
- Select the proper temperature programme with constant flow of purge gas at the above-specified rate, according to one of the following paths:
  - Choose a heating rate between 0° and 10°C/min in case of standard thermogravimetry and begin the programme;
  - Start a modulated temperature programme with amplitude of 5°C and a period of 200s with an underlying ramp of 1°C/min in case of modulated thermogravimetry;
- Wait until completion of the degradation process, which in case of this project corresponds to a temperature of 550°C, and start a ramp of 20°C/min up to the temperature of 900°C.

- Cool the furnace up to 80°C before opening, in order to avoid leakage of fumes and other hazardous products.

Once the test comes to an end, kinetic data can be obtained directly from the software and the proper analysis can be carried out according to standards ASTM E1641 and ASTM E1877, which will be examined in the following paragraph. Among all the kinetic parameters, a model-free determination of the Arrhenius activation energy of the decomposition process is feasible. The fact that a proper kinetic model is not required is of the uttermost importance as it makes this technique applicable in any specific case. Nonetheless, the computation of the pre-exponential factor in Eq.2 requires the assumption of a first order kinetic model, thus posing serious limitations on the applicability of the method without more complex and careful studies.

The precision and bias of standard thermogravimetry methods were determined in an interlaboratory test in 2008, to which thirteen laboratories from around the world took part. Nevertheless, further analysis will be conducted by 2020 to determine a more accurate precision and bias statement regarding modulated thermogravimetry and its results.

As for the instrumentation exploited along with this project, a "TA Instruments Q500 thermogravimetric analyser" with built-in results-oriented software was used. TA Instruments itself is in charge of the periodic calibration and control. The sensitivity and the weighing precision of the scale system are 0,1 μg and ± 0,01%, respectively. The machine is equipped with a manual sampler comprising platinum pans and its furnace is provided with Hi-Res control technology, meaning it is able to produce significant improvements over standard linear heating rate TGA in the separation of closely occurring decomposition events.

2.6. **Thermogravimetry – Kinetic Parameters**

The following paragraphs will outline the methods and the calculations required to obtain the desired kinetic parameters from thermogravimetric analyses, be they standard or modulated. ASTM E1641 presents and describes the *Ozawa-Flynn-Wall method* (OFW) to obtain such data, while ASTM E1877 is focused on computing the temperature index and the thermal endurance using those parameters [31][32]. It is

important to underline that both procedures are generally applicable to materials with well-defined decomposition profiles, namely, a smooth, continuous mass change with a single maximum rate.

As for the OFW method [31] described in the first standard, it is based on the general rate equation defined in the previous chapters (Eq.2), which takes the form:

$$\frac{dC}{dt} = \frac{dC}{dT} \cdot \frac{dT}{dt} = \frac{dC}{dT} \cdot \beta = Af(C) \exp\left(-\frac{E}{RT}\right) \quad \textbf{(Eq.7A)}$$

$$f(C) = (n+1)(1-C)^n \quad \textbf{(Eq.7B)}$$

In Eq.7, the constant heating rate β was introduced to obtain a direct relationship between the degree of conversion a and temperature. $f(a)$ was expressed as a function of the order of reaction n. Furthermore, this method offers a procedure to check the order of reaction of the degradation process, by studying Eq.7A in case of *constant temperature*. As a matter of fact, the following estimate for n can be worked out:

$$\frac{d \ln \frac{dC}{dt}}{d \ln(1-C)} = n \quad \textbf{(Eq.8)}$$

By assuming a reaction of the first order, which is generally the case when degradation occurs mostly by random scission, it is possible to obtain the more commonly used Eq.9:

$$\frac{dC}{dT} = A(1-C) \exp\left(-\frac{E}{RT}\right) \cdot \frac{1}{\beta} \quad \textbf{(Eq.9)}$$

In order to directly relate the conversion and the temperature, a resolution of the above-shown differential equation is required. By integration:

$$\int_0^c \frac{dC}{(1-C)} = \frac{A}{\beta} \int_{\tau_0}^{\tau} \exp\left(-\frac{E}{RT}\right) dT \quad \textbf{(Eq.10)}$$

In Eq.10, c stands for the degree of conversion associated to the temperature τ. The integral on the right, however, cannot be solved analytically, as integration by parts leads to the following:

$$\mathrm{F(c)} = \ln(1-c) = \frac{AE}{\beta R}\left[-\frac{e^x}{x} + \int_{-\infty}^{x} \frac{e^X}{X} dX\right] = \frac{AE}{\beta R} p(x) \quad \textbf{(Eq.11)}$$

$$x = -\frac{E}{RT}$$

In Eq.11, the assumption that τ_0 is low enough for the lower limit to be negligible in the integration was made. The polynomial $p(x)$ is the solution of the integral, whose values have been tabulated for limited ranges, and several series expansions and semiempirical approximations exist. One of these is:

$$\log\big(p(x)\big) = -2{,}315 + 0{,}457x \qquad \textbf{(Eq.12)}$$

Eq.12 takes the name of its creator, C.D. Doyle, who broadly studied thermogravimetric analysis.

By taking the logarithm of Eq.11 and by substituting Eq.12, the following equation can be obtained:

$$\log\big(F(c)\big) = \log\frac{AE}{R} - \log(\beta) - 2{,}315 - 0{,}457\frac{E}{RT} \qquad \textbf{(Eq.13)}$$

Thanks to Eq.13, values of the activation energy can be obtained by plotting the logarithm of the heating rate as a function of the reciprocal of temperature for a constant degree of conversion (Figure 22) and by performing a linear regression.

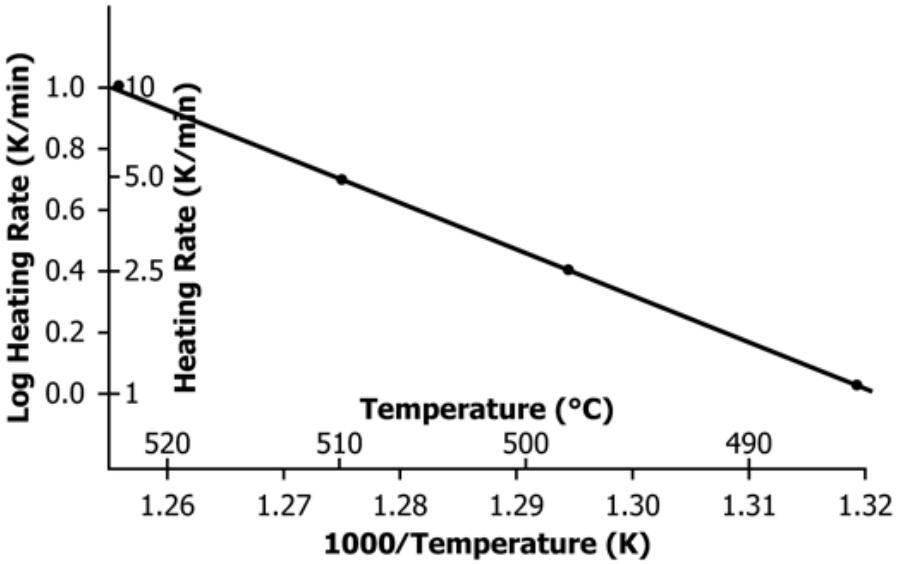

Figure 22 *Exemplificative plot of Eq.12, which can be used for the computation of the activation energy*

As a matter of fact, by rearranging Eq.13 and differentiating, the following is found:

$$\frac{d\log(\beta)}{d\frac{1}{T}} = -0{,}457\frac{E}{R} \qquad \textbf{(Eq.14)}$$

Eq.14 can lead to accurate results provided it is written this way:

$$E = \left(\frac{R}{b}\right)\frac{d\log(\beta)}{d\frac{1}{T}} \qquad \textbf{(Eq.15)}$$

In Eq.15, b is called Doyle's constant.

The procedure consists in performing at least four runs at different heating rates in case of standard thermogravimetry, thus obtaining the respective degradation curves (Figure 23). In general, employing the lowest practicable heating rate will best isolate competing reactions. However, it may occasionally be convenient to raise the heating rate to pick up a high energy reaction that may not be easily discernible under near-isothermal conditions. Therefore, it can be concluded that only methods involving several heating rates can give the correct activation energy. From the curves, the temperatures at which the failure criterion, namely the 5% loss of weight, is met are found for each value of β.

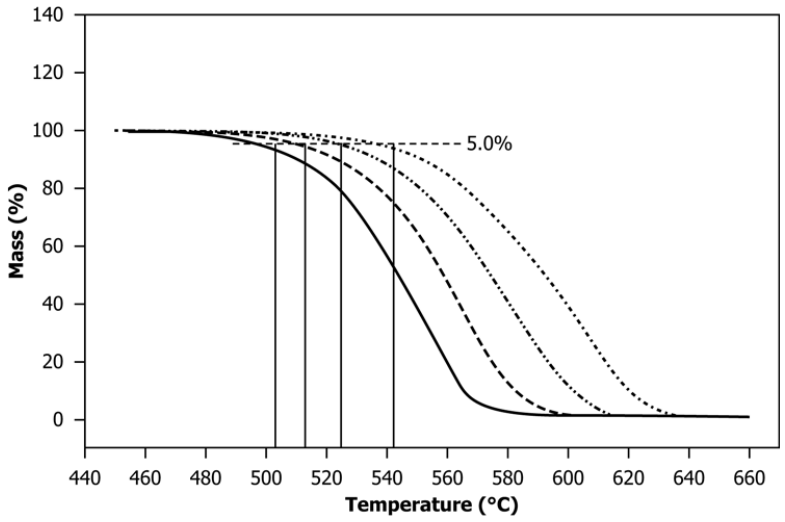

Figure 23 *Generic degradation curves in case of four different heating rates, the lower being that on the left*

During this process, the degradation of the samples was studied in case of five different heating rates, specifically 1 K/min, 2 K/min, 5 K/min, 7 K/min, 10 K/min.

The next step in the procedure is the plotting of the logarithm of the exploited heating rates as a function the freshly found corresponding values of temperature by means of Eq.15 and by setting $b = 0{,}457$. Thus, a first estimate of the activation energy can be obtained by computing the slope of the curve. Nonetheless, this value needs refining

and, firstly, it has to be used to compute a more precise value of b by means of the following table.

E/RT_f	a	b
8	5,3699	0,5398
9	5,898	0,5281
10	6,4157	0,5187
11	6,9276	0,511
12	7,4327	0,505
13	7,9323	0,5
14	8,4273	0,494
15	8,9182	0,491
16	9,4056	0,488
17	9,89	0,484
18	10,3716	0,482
19	10,8507	0,479
20	11,3277	0,477
21	11,8026	0,475
22	12,2757	0,473
23	12,7471	0,471
24	13,217	0,47
25	13,6855	0,469

E/RT_f	a	b
26	14,1527	0,467
27	14,6187	0,466
28	15,0836	0,465
29	15,5474	0,463
30	16,0103	0,4629
31	16,4722	0,462
32	16,9333	0,461
33	17,3936	0,461
34	17,8532	0,459
35	18,312	0,459
36	18,7701	0,458
37	19,2276	0,458
38	19,6845	0,456
39	20,1408	0,456
40	20,5966	0,4558
41	21,0519	0,455
42	21,5066	0,455
43	21,9609	0,454

E/RT_f	a	b
44	22,4148	0,454
45	22,8682	0,453
46	23,3212	0,453
47	23,7738	0,453
48	24,226	0,452
49	24,6779	0,452
50	25,1294	0,4515
51	25,5806	0,4511
52	26,0314	0,4508
53	26,482	0,4506
54	26,9323	0,4503
55	27,3823	0,45
56	27,8319	0,4498
57	28,2814	0,4495
58	28,7305	0,4491
59	29,1794	0,4489
60	29,6281	0,4487

Specifically, the value T_f which is required for this process corresponds to the temperature corresponding to 5% mass loss for the heating rate nearest the midpoint of all heating rates. The process is repeated until following *iterations* lead to a change which is not noticeable anymore, specifically when following activation energies differ by less than 1%. This method was proven to be most generally applicable and reliable.

Different approaches to the computation of the activation energy exist. Kissinger's method is worth noting as it relies on the peak temperature of the rate of weight loss, thus being based on *derivative thermogravimetric analysis* (Figure 24). This procedure consist of a linear regression to fit the following equation, whose slope corresponds to the activation energy:

$$E = R\frac{d\ln\left(\frac{\beta}{T_{peak}^2}\right)}{d\frac{1}{T_{peak}}} \qquad \textbf{(Eq.16)}$$

The derivation of this formula will not be tackled here, but a comparison between the values obtained by means of Eq.15 and Eq.16 will be carried out, in order to show whether they are compliant.

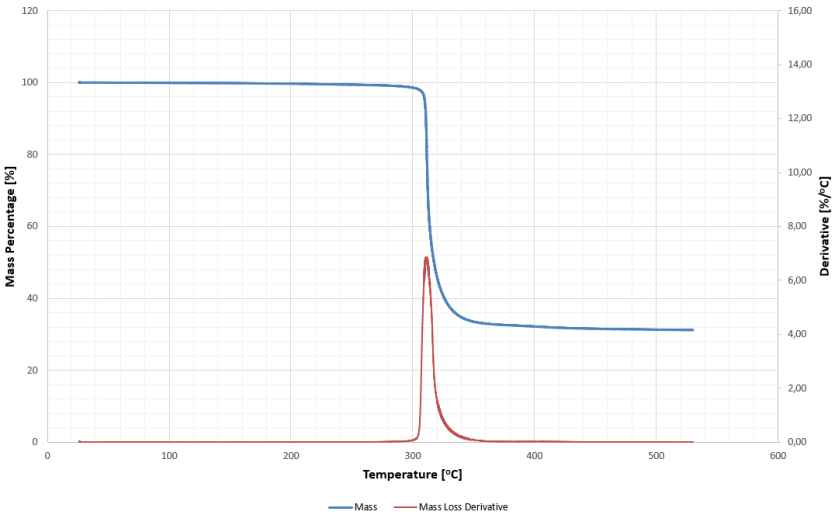

Figure 24 *Plot of a thermogravimetric analysis performed on Polybutylene Terephthalate including both the mass loss and the rate of mass loss as a function of temperature*

Lastly, though not essential for the computation of the temperature index, the value of the pre-exponential factor A can be determined, under the assumption of first-order kinetics. This is done by substitution of the values of activation energy, temperature and heating rate in Eq.13, keeping in mind the definition of $F(c)$ from Eq.11. However, a quicker method exist and it relies on Doyle's approximation and on the constant a, which can be derived from the table above. The method consists in exploiting the following simplified formula, obtaining a value in min^{-1}:

$$A = \left(-\frac{\beta R}{E}\right) \ln(1-c) \cdot 10^{a} \qquad \textbf{(Eq.17)}$$

This formula highlights the direct relationship between a, which is a function of the activation energy and temperature, and $\log(p(x))$. Specifically, the following relationship can be found, even though the numerical values from the table differ slightly, underlying the fact that it is an approximation:

$$a = -\log p(x) = 2{,}315 - 0{,}457x \qquad \textbf{(Eq.18)}$$

On the other hand, as far as modulated thermogravimetry is concerned [28], it is firstly necessary to state that by means of Fourier transforms it is possible to associate a value of heating rate for each variation of temperature, by deconvolution of the

oscillatory response. To put it simple, by just exploiting a single temperature ramp with a superimposed modulation, the same parameters obtained from several runs performed at different heating rates can be found. The proper expression for the activation can be derived from Eq.7 by performing the ratio between the degree of conversion at two close but separate temperatures. Hence, the following is obtained:

$$\frac{\frac{dC_1}{dt}}{\frac{dC_2}{dt}} = \frac{dC_1}{dC_2} = \frac{Af(C_1)\exp\left(-\frac{E}{RT_1}\right)}{Af(C_2)\exp\left(-\frac{E}{RT_2}\right)} \qquad \textbf{(Eq.19)}$$

By assuming that:

$$f(C_1) = f(C_2) \quad \rightarrow \quad \ln\left(\frac{f(C_1)}{f(C_2)}\right) = 0 \qquad \textbf{(Eq.20)}$$

The above is reasonable in case of close temperatures and conversions and allows to get:

$$E = \frac{RT_1T_2\ln\left(\frac{dC_1}{dC_2}\right)}{T_1 - T_2} \qquad \textbf{(Eq.21)}$$

From the sinusoidal temperature programme, it is possible to express the quantity in Eq.19 as:

$$T_1 = T + V \qquad \textbf{(Eq.22A)}$$

$$T_2 = T - V \qquad \textbf{(Eq.22B)}$$

$$\ln\left(\frac{dC_1}{dC_2}\right) = L \qquad \textbf{(Eq.22C)}$$

In Eq.22, V stands for the measured amplitude of the sinusoidal temperature programme and T for the average temperature. All of these values are obtained by deconvolution of the oscillatory temperature programme and the resultant oscillatory rate of weight loss. This is done directly by the software of the thermogravimetric analyser by means of real-time discrete Fourier transforms. The above-defined equations lead to a more compact definition for the activation energy, which can be defined model-free, since it does not depend on knowledge of the kinetic function:

$$E = \frac{R(T^2 - V^2)L}{2V} \qquad \textbf{(Eq.23)}$$

The pre-exponential factor can be found as a function of the average specimen temperature:

$$\ln A = \ln\left(\frac{dC}{1-C}\right) + \frac{E}{RT} \qquad \textbf{(Eq.23)}$$

An interlaboratory test will be conducted by 2020 to develop a detailed precision and bias statement for this procedure, as already stated.

Moving on to the computation of the *temperature index* itself, and therefore to ASTM E1877, it is firstly required to solve the differential equation relating time and conversion as in Eq.7A. All the equations which will be derived in the following paragraphs are valid both in case of standard and modulated thermogravimetry. A complete demonstration shall be provided here by considering that equation and by introducing the weight of the sample instead of the degree of conversion:

$$\frac{dw}{dt} = -Af(w)\exp\left(-\frac{E}{RT}\right) \qquad \textbf{(Eq.24A)}$$

$$\frac{dw}{dT}\beta = -Af(w)\exp\left(-\frac{E}{RT}\right) \qquad \textbf{(Eq.24B)}$$

The minus sign in Eq.24 takes into consideration the decrease of weight as counterposed to the corresponding increase of conversion.

From this couple of differential equation, working by separation of variables, the following can be derived:

$$\int_0^{t_f} dt = Life = -\exp\left(\frac{E}{RT}\right)\int_{w_0}^{w_f} \frac{dw}{Af(w)} \qquad \textbf{(Eq.25A)}$$

$$\int_{w_0}^{w_f} \frac{dw}{Af(w)} = -\frac{1}{\beta}\int_{T_0}^{T_f} \exp\left(\frac{E}{RT}\right) dT \qquad \textbf{(Eq.25B)}$$

The combination of Eq.25A and Eq.25B, yields:

$$Life = \exp\left(\frac{E}{RT}\right)\frac{1}{\beta}\int_{T_0}^{T_f} \exp\left(\frac{E}{RT}\right) dT \qquad \textbf{(Eq.26)}$$

Which cannot be evaluated explicitly, but requires a substitution to allow numerical integration. By recalling the definition of x from Eq.11 and computing its differential $dx = -E/RT^2$ the resulting equation reads:

$$Life = \exp\left(\frac{E}{RT}\right)\frac{E}{R\beta}\int_{x_f}^{x_0} e^{-x}x^{-2}dx \qquad \textbf{(Eq.27)}$$

In Eq.27, it is possible to spot the disappearance of the minus sign because of the inversion of the integral limits.

In order to simplify the problem, by exploiting the linearity of integrals with respect to their limits, it is possible to write:

$$\int_{x_f}^{x_0} e^{-x}x^{-2}dx = \int_{\infty}^{x_0} e^{-x}x^{-2}dx - \int_{\infty}^{x_f} e^{-x}x^{-2}dx \qquad \textbf{(Eq.28)}$$

Since $x \sim 1/T$, it can be shown that the first integral can be neglected as it ranges between 0 and room temperature, where thermo-oxidative degradation is not significant.

The first resolution was proposed by exploiting Doyle's approximation (Eq.12 and Eq.18) and leads to the following definition of the *thermal endurance*, i.e. a plot of the time required to reach 5% of mass loss as a function of temperature:

$$\log(Life) = \frac{E}{2{,}303RT} + \log\left(\frac{E}{R\beta}\right) - a \qquad \textbf{(Eq.29)}$$

By reversing the formula, it is possible to obtain an expression for the *temperature index* of the material as:

$$TI = \frac{E}{2{,}303R\left[\log(Life) - \log\left(\frac{E}{R\beta}\right) + a\right]} \qquad \textbf{(Eq.30)}$$

In Eq.30, $Life$ properly stands for the arbitrary life of the material, i.e. $6 \cdot 10^4$ hours in case of this project.

In order to determine the accuracy of such a method, the relative standard deviations of temperature index and thermal endurance can be estimated according to:

$$\frac{\sigma TI}{TI} = 1{,}2\frac{\sigma E}{E} \qquad \textbf{(Eq.31A)}$$

$$\frac{\sigma Life}{Life} = \left(1 - 0{,}052\frac{E}{RT}\right)\cdot\left(\frac{\sigma E}{E}\right) \qquad \textbf{(Eq.31B)}$$

In both equations, the relative standard deviation of the activation energy can be directly obtained from the previously described regressive and iterative method.

James J. Xu and Christopher A. Kaminski [32] proposed a different and better approach to solving the differential equation by using a least-square fit. This method leads to the following approximation to be used in combination with Eq.27 and Eq.28:

$$\log\left(-\int_{\infty}^{x_f} e^{-x}x^{-2}dx\right) = -\log 100{,}4 - 0{,}463x_f \qquad \textbf{(Eq.32)}$$

The regression, whose result is shown in Eq.32, shows a $R^2 = 0{,}9998$ and does not risk running into sizeable errors, unlike Doyle's approximation, which proves to be slightly less precise. This whole derivation leads to the final estimation of the thermal endurance of the material, which is expressed as:

$$\log(Life) = \frac{E}{2{,}303RT} + \log\left(\frac{E}{100{,}4\beta R}\right) - 0{,}463\frac{E}{RT_f} \qquad \textbf{(Eq.33)}$$

In Eq.33, in case of standard thermogravimetry, β and T_f correspond to the above given definition, namely the heating rate closest to the midpoint of all exploited heating rates and the temperature at which the end-point is reached at such a β, respectively. By reversing this formula, it is possible to finally determine an expression for the temperature index as:

$$TI = \frac{E}{2{,}303R\left[\log(Life) - \log\left(\frac{E}{100{,}4\beta R}\right) + 0{,}463\frac{E}{RT_f}\right]} \qquad \textbf{(Eq.34)}$$

Eq.33 and Eq.34 can be used both in case of standard and in case of modulated thermogravimetry.

Lastly, the authors proposed a different formula for the computation of the accuracy of the above values. However, those are much more complicated and a different approach is suggested, i.e. to perform several experiments, in order to compute more than a single value of thermal endurance and temperature index, thus being able to carry out a statistical analysis on a broader sample. In this work, a presentation of the obtained values will be provided, even though the method by James J. Xu and Christopher A. Kaminski will be exploited in the computations.

2.7. Differential Scanning Calorimetry

Differential Scanning Calorimetry (DSC) is a technique which is exploited to study the thermal transitions of a polymeric material. The difference in the heat required to linearly increase the temperature of a pan containing the sample material and that of a reference one, which is an empty pan, is measured (Figure 25). This means that the graph which is obtained is basically a plot of the heat absorbed by the material [mW/mg] as a function of temperature. This concept is essential, since it means that by means of this technique it is possible to detect phase transitions, in which a certain quantity of heat is released or absorbed, depending on whether the process is *exothermic* or *endothermic*.

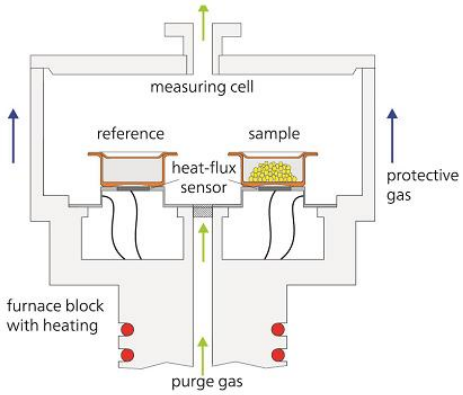

Figure 25 *Schematic representation of a differential scanning calorimeter*

DSC allows the determination of the temperatures at which those transitions occur, namely the glass transition (T_g), the melting (T_m) and the crystallization (T_c) temperatures and the enthalpies related to such processes. As a matter of fact, in correspondence of the two latter events, peaks form, while in case of the former, the curve shifts upwards, highlighting an increase in the heat capacity of the material. It is important to notice that every phase transition occurs over a range of temperature, therefore underlying the intrinsic viscoelasticity of polymers. Moreover, because of the same matter, T_m and T_c will always differ, the former always being higher than the latter.

Before outlining the procedure to follow, it is essential to describe the instrumentation required, which was schematized in Figure 25 and comprises:

- A *furnace* which can provide controlled heating and cooling of both reference and sample pan in the range between -120 and 600°C;

- A *temperature sensor* to deliver an accurate measurement of the temperature with an error equal to ±0,1°C;
- *Differential sensors* to measure the difference in heat flow between reference and sample pan;
- A source of *inert purge gas* to keep the chamber environment controlled;
- A *balance* with capacity greater than 100 mg with sensibility of at least 0.01 mg
- A *software* able to execute specific temperature programmes and recording the heat flow signal as a function of temperature.

The procedures for the execution of the analysis, according to the standard ASTM E793 [33], is the following:

- Weigh up to 20 mg of the specimen into a clean and dry pan, which has to be clamped with a lid in order to minimize the free space;
- Start the inert gas purge;
- Perform a thermal pre-cycle consisting in heating the test chamber at a rate equal to 10°C/min ± 1°C/min up to 20°C ± 5°C beyond the melting temperature and then cooling it back at room temperature with the same rate;
- Start the proper thermal heating scan with the same parameters as the one described above.

Therefore, the whole procedures consists in recording three different runs, the first and the last while heating the chamber and the second while cooling. The aim of this procedure is to get rid of any conditioning of the sample by means of the first two runs, in order to study the material itself in the last one. However, when the focus of the analysis is on the specimen and not on the material itself, it is safe to perform the first run alone, in order to keep track of any modification induced by its history, especially the thermal one. This point is particularly important in case of this project and in general when the crystallinity is to be measured.

Once the plot is obtained, in order to determine the crystallinity of the sample, the enthalpy of fusion [J/g] is to be computed by integrating the melting peak and subtracting the area of the crystallization peak if present:

$$\Delta H = \Delta H_m - \Delta H_c \quad \textbf{(Eq.35)}$$

Once this value is obtained, the following formula is to be used to determine the degree of crystallinity [34]:

$$\%\, Cristallinity = \frac{\Delta H}{\Delta H_{pure} \cdot (1 - \chi)} \cdot 100 \quad \textbf{(Eq.36)}$$

In Eq.36, χ stands for the weight fraction of fibres in the composite material and ΔH_{pure} for the enthalpy of fusion of the 100% crystalline material, which is a theoretical data that can usually be retrieved in literature. As for this project, the following data were used: $\Delta H_{pure}^{PBT} = 145$ J/g and $\Delta H_{pure}^{PA\,6,6} = 226$ J/g [35].

To conclude, regarding the equipment employed during this work, "TA Instruments Q1000 differential scanning calorimeter" was exploited. TA Instruments itself is in charge of the periodic calibration and control. The temperature accuracy of the instrument is ±0,1°C with a temperature range from -180°C to 725°C and calorimetric precision equal to ±0,05%.

2.8. **Viscosimetry**

During this project, three different techniques were exploited to study the viscosity of the polymeric materials being studied. Monitoring of the viscosity of a material is helpful since it allows determining whether or not any change is occurring. For instance, a relationship between the viscosity of a polymeric material and its molecular weight exists, as it can be highlighted by Mark-Houwink equation, which is used in case of solutions:

$$[\eta] = K \cdot M^a \quad \textbf{(Eq.37)}$$

Eq. 37 links the intrinsic viscosity $[\eta]$ of a polymer in a solution with its molecular weight. M. The former is a measure of the solute's contribution to the viscosity of solution, but it won't be examined any further.

Since aging in ovens causes the degradation of material properties because of a decay of the microstructure and therefore a lowering of the molecular mass, this quantity can be used as a control parameter of what is occurring. There are several different ways of keeping track of the viscosity of a substance and, during this project,

three were performed: *Melt Flow Index* measurement, *Viscosity Number* determination and *Zero-shear viscosity* individuation by means of parallel plates rheological testing in a Dynamic Mechanical Analysis (DMA) machine. As for the latter, a relation similar to Mark-Houwink equation exists between zero-shear viscosity η_0 and molecular weight, with the value a generally equal to 3,4. The behaviour emerges after a certain critical molecular weight for entanglements to become effective has been exceeded.

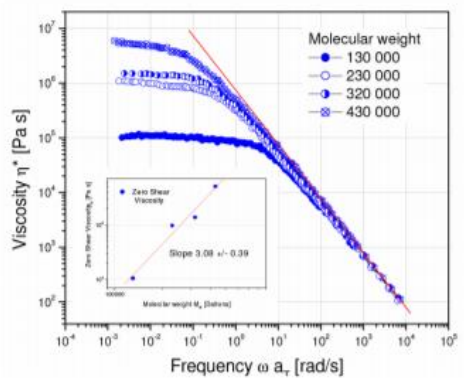

Figure 26 *Graph depicting the behaviour of the logarithm of viscosity as a function of frequency and therefore shear rate. By extrapolating viscosity at zero shear, the smaller graph representing the linear relationship of the logarithm of such value as a function of molecular weight was obtained.*

The analysis of the employed techniques together with the relevant standards follows.

2.8.1. **Melt Flow Index**

The *Melt Flow Index* (MFI) or *Melt Mass Flow rate* is not a proper measure of the viscosity of a polymeric material, but it is just an indication of the ease of flow of the melt. This is an indication of the viscosity and molecular mass of the polymer melt, with greater flow values corresponding to low molecular weights. It is defined as the mass, in grams, flowing out of a standardized die at the end of a heated vertical cylinder over 10 minutes, under the pressure generated by the gravimetric weight. Therefore, this technique is to be intended merely as a comparative practice between grades of the same family. The basic apparatus required to perform such a test is an extrusion plastometer operating at a fixed temperature.

Such a machine is constituted by the following elements (Figure 27):

- A *vertical cylinder* with a length between 115 and 180 mm and an internal diameter of 9,550 ± 0,007 mm, made of a material resistant to wear and corrosion up to the maximum temperature of the heating system;

- A *piston* at least as long as the cylinder with a head of 6,35 ± 0,10 mm in length, capable of sustaining weights, and a diameter of 9,474 ± 0,007 mm, with two thin reference marks inscribed, made of a material having the same properties of that used for the cylinder, but with lower hardness for ease of maintenance;
- A *heating system* and a *temperature-control system* with maximum deviation of ±1°C at a distance of 10 ± 1 mm above the die and ±2,5°C elsewhere;
- A *die* made of either tungsten carbide or hardened steel, with a length of 8,000 ± 0,025 mm and a diameter of 2,095 ± 0,005 mm, which shall be checked regularly with a go/no-go gauge;
- A *set of removable loads* with a permissible error in weight equal to ±0,5%;
- External *timer* and *balance* with respective accuracy of ±1% the measured interval and ±1 mg.

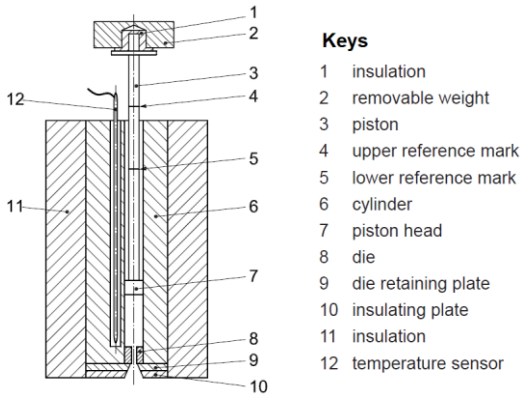

Figure 27 *Representation of the main elements constituting an extrusion plastometer*

The samples to be used for such a practice may be of any form and dimension that can fit the cylinder and shall be conditioned in a dry oven before testing.

As for the procedure itself, the guidelines from the standard ISO 1133 [36], with conditioning, heating temperatures and load depending on the specific material:

- Charge the cylinder with 3 to 8 mg of the conditioned sample and pack it so that no air bubbles form;
- Put the piston inside the cylinder, either loaded or unloaded depending on the ongoing flow of material;
- Heat the sample as the specified temperature for 5 min;

- Load the piston if unloaded and allow the material to flow until a bubble-free filament is extruded;
- When the lower reference mark on the piston has reached the top edge of the cylinder, start the timer and simultaneously cut off the extrudate with the cutting tool and discard;
- Collect cut-offs for a given time interval so that the extrudate is not less than 10 mm;
- Weigh the extrudate and express the MFI in grams of polymer per 10 minutes, according to the formula:

$$MFI = 600 \cdot \frac{m}{t} \qquad \textbf{(Eq.38)}$$

In Eq.37, m stands for the mass extruded in the time interval t.

Precision of this method is expected to be equal to $\pm 5\%$ in intra-laboratory tests, but it is required to pay attention to factors such as cross-linking and thermal degradation which could be induced by long exposure to testing conditions. Therefore, more than one measure is to be carried out in order for the obtained value to be considered acceptable.

As for this project, a "Zwick/Roell Mflow" extrusion plastometer with built-in results-oriented software was exploited. The machine is equipped with a precision piston transducer which ensures accurate measurement of piston stroke and the device is subject to periodic calibration and control. As for the testing conditions of Later 4 G/30, which underwent such testing, the conditioning temperature and time were respectively 110°C and at least 2 hours, while the proper test temperature and load were equal to 250°C and 2,16 kg.

2.8.2. **Dynamic Mechanical Analysis**

Dynamic Mechanical Analysis (DMA) is a technique used to determine various properties of polymeric materials over a spectrum of either temperature, time or frequency, depending on the testing geometry and conditions. It is especially useful for studying the viscoelastic behaviour of plastics, which are non-Newtonian fluids. An

example of its application is the computation of the complex modulus by applying a sinusoidal stress and measuring the response in strain and its delay.

Actually, the machine can also be exploited as a *parallel plates rheometer* to determine the viscosity of a polymer melt at constant temperature by varying the shear rate to which it is subject. As a matter of fact, the relationship between shear stress τ and shear rate $\dot{\gamma}$ can be expressed by means of the viscosity η as:

$$\tau = \eta\dot{\gamma} \qquad \textbf{(Eq.39A)}$$

$$\bar{\bar{\tau}} = \eta\bar{\bar{\Delta}} \qquad \textbf{(Eq.39B)}$$

Eq.39B refers to the three-dimensional non-isotropic case, where shear stress and shear rate need to be considered as tensors, in order to take into account all possible directions. $\bar{\bar{\Delta}}$ is called the *rate of deformation* tensor. Moreover, in case of non-Newtonian fluids, the viscosity is intrinsically a function of the shear rate, more specifically of the second invariant of its tensor, which is defined below as:

$$I_2 = \frac{1}{2}\left[\left(t_r\bar{\bar{\Delta}}\right)^2 + t_r\left(\bar{\bar{\Delta}}^2\right)\right] = \frac{1}{2}\left[\left(\sum_{i=j}\Delta_{ij}\right)^2 + \sum_{i=j}\Delta_{ij}^2\right] \qquad \textbf{(Eq.40)}$$

Yielding:

$$\eta = \eta\left(II_{\bar{\bar{\Delta}}}\right) \qquad \textbf{(Eq.41)}$$

In case of simple shear, such as that between two parallel plates, it is possible to show how this relationship reduces to:

$$\eta = \eta(\dot{\gamma}) \qquad \textbf{(Eq.42)}$$

Since:

$$\bar{\bar{\Delta}} = \begin{bmatrix} 0 & \dot{\gamma} & 0 \\ \dot{\gamma} & 0 & 0 \\ 0 & 0 & 0 \end{bmatrix} \qquad \textbf{(Eq.43)}$$

An in-depth demonstration of all these notions will not be provided as it is not central for the development of the project [37].

Depending on the proper relationship between viscosity and shear rate, several behaviours can be identified. Polymers are shear-thinning or pseudo-plastic materials, meaning their viscosity decreases with increasing shear rate, as also exemplified by

honey being stirred into a jar. The most important relationships between τ, η and $\dot{\gamma}$ are highlighted in the graphs below (Figure 28):

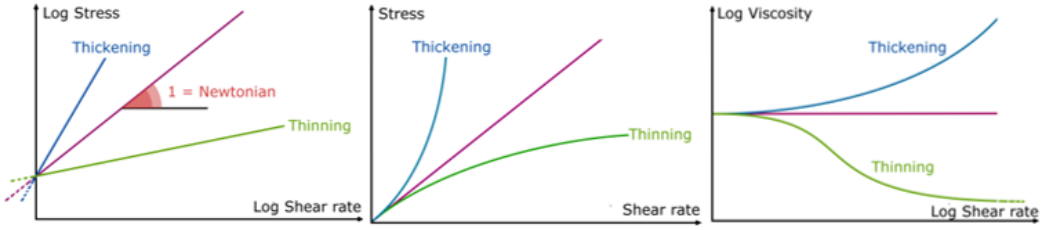

Figure 28 *Exemplificative plots of the relationships between shear stress, shear rate and viscosity in case of Newtonian, Shear Thinning and Shear Thickening materials*

Coming back to the specific testing which can be performed by means of dynamic mechanical analysis, rate sweep tests at constant temperature in parallel plates setting allow plotting of the graph on the right in Figure 28. The test consists in assessing the shear stress response of a polymer melt subject to a set of frequencies generated by the rotating lower plate, thus being able to determine the viscosity over a spectrum of shear rates (Figure 29).

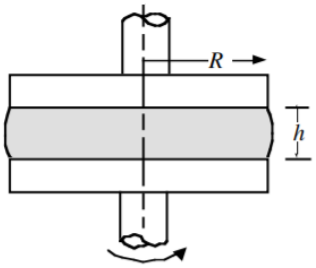

Figure 29 *Exemplification of the parallel plates configuration exploited in rate sweep tests*

The general dynamic mechanical analyser comprises the following parts:

- A *furnace*, which is the proper sealed test chamber, is equipped with thermocouples and inlet for the purge gas and must provide a heating precision of ±1°C;
- A *cooling system*, generally a liquid nitrogen one;
- A *clamping system*, which can be substituted with a set of *parallel plates* and a *ring* to allocate the specimen, either solid in case of the former or to be melted as in the latter, and which is equipped with a thermocouple;
- A system to provide *oscillatory stress* or *strain* and a *detector*, capable of determining the dependent and independent experimental parameters;

- A *software* capable of running suitable programmes, collecting data and determining dependent variables;
- A *caliper* or *micrometer* to determine dimension with a precision of ±0,01 mm.

As for the procedure itself, based on the standard ASTM E1640 [38], a custom-made one was exploited in case of Later 4 G/30

- Weigh 4 ± 0,5 g of polymer, taken from the samples produced with injection moulding;
- Heat the furnace up to the testing temperature, which corresponds to 250°C;
- Lower the upper plate so that it come almost in contact with the lower one and set this distance as the zero with the micrometer;
- Open the furnace, lift the upper plate, put the weighed material inside the parallel plates and close them with a metallic ring;
- Allow the material up to 10 minutes to melt, remove the metallic ring and pull the plates closer until a force is detected by the machine;
- Take notice of the distance between the plates in order to use it to set a rate sweep analysis at constant temperature and start the programme, recording the viscosity as a function single growing values of the shear rate.

As for the apparatus employed during this process, a "Rheometric Scientific Dynamic Analyzer RDA II" was used in the frequency range between 0,01 s^{-1} and 1250 s^{-1}. This machine was subject to many maintenance controls by competent personnel during this project because of its age and since it hadn't been used for a long time.

2.8.3. **Determination of Viscosity Number**

A unique way to study the viscosity of a material is to dissolve it in a proper solvent and to measure its time of flow in a viscosimeter, specifically down a capillary tube. By direct comparison between the times of flow of the solution and of the solvent alone, an index can be obtained. This value, properly called *viscosity number*, is commercially important in the case of polyamides, as it constitutes a simple and quick comparison between different grades. When studying Latamid 66 H2 G/30, the

standard ISO 307 requires the use of sulfuric acid with 96% w/w concentration, along with other solvents which are of no interest in this work.

The principle of this procedure is to compare the times of flow as described above, using a concentration of polyamide equal to 0,005 g/ml in the solvent at a fixed temperature of 25°C ± 0,05°C. In case a volumetric flask of capacity 25 mL is being used, as in this project, the following mass of material is to be weighed:

$$m = \frac{125}{1 - \frac{w}{100}} \pm 0{,}1 = 178{,}57 \pm 0{,}1\ mg \qquad \textbf{(Eq.44)}$$

In Eq.44 w corresponds to the weight fraction of additives in the polyamide and the mass m is expressed in milligrams. Once the material has been prepared, a quantity of about 20 mL of sulfuric acid is to be added to the flask, which is then subject to magnetic stirring. Such a process may take up to several hours for a complete dissolution of the polymeric material and it is usually followed by centrifugation and vacuum filtering before the solution can be poured in the viscosimeter itself.

The main components of the machine itself are the following:

- A *thermostatic bath* capable of being maintained at 25°C ± 0,05°C and controlled by a total immersion thermometer;
- A *time device* for measurements of accuracy of 0,1 s;
- A *Ubbelohde type viscosimeter* (Figure 30), a u-shaped piece of glassware with a measured reservoir on one side and a measuring bulb with a capillary on the other, in addition to a third arm extending from the end of the capillary and open to the atmosphere.

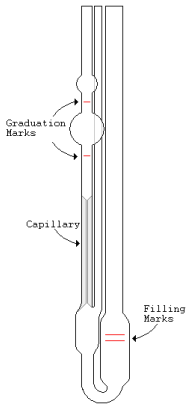

Figure 30 *Representation of a Ubbelohde type viscosimeter*

As for the procedure itself, determined from the standard ISO 307 [39], a liquid is introduced into the reservoir and then sucked through the capillary and measuring bulb. Afterwards, the liquid is released and the time it takes for it to pass through two calibrated marks is measured. Such a measurement is repeated until two following times do not differ by more than 0,5%. The mean value is considered to be the flow time of the solution and can be used to compute the viscosity number VN in millilitres per gram as:

$$VN = \left(\frac{\eta_{solution}}{\eta_{solvent}} - 1\right) \cdot \frac{1}{C} = \left(\frac{t_{solution} - t_c}{t_{solvent} - t_{0c}} - 1\right) \cdot \frac{1}{C} \qquad \textbf{(Eq.45)}$$

In Eq. 45 t_c and t_{0c} refer to correction factors for the flow time of the solution and of the solvent respectively and are applied by directly by the software. The relationship between the flow times and the viscosity can be demonstrated, but will not be carried out here. In Eq.45, the concentration C of the polymer in grams per millilitre can be obtained according to the formula:

$$C = \frac{m}{1000 \cdot 25 \cdot \left(\frac{100}{100 - w}\right)} = 0{,}005\ g/mL \qquad \textbf{(Eq.46)}$$

The machine used during this project was a "Rheotek RPV-1 Polymer Viscosimeter", which is a two-position system calibrated according to ISO 17025 and subject to periodic maintenance and control.

CHAPTER THREE
Experimental Results

3. Chapter Content

In the following chapter, the outcome of both aging programme will be provided. This section of the work is only aimed at showing the obtained data, while an analysis of these results will be delivered in chapter 4.

3.1. Long-Term Aging

3.1.1. Preparation

All samples were obtained by injection moulding. Specifically, for each material, the following quantities were produced:

TYPE OF SPECIMEN	QUANTITY
3 mm Dumbbell-shaped	400
1,5 mm Dumbbell-shaped	400
Charpy Impact	400
Dielectric Strength Discs	320

The precise shape and dimension of such pieces was already described in the previous chapters. The difference in numerosity in case of the specimens for dielectric-rigidity testing is due to fact that LATI S.p.A. does not own the proper instrumentation to carry out the tests. Therefore, a collaboration with the "*Università degli Studi di Genova*" was established and the specimens were sent there, thus requiring a lower number.

Before placing the samples inside the ovens, an analysis of data regarding a similar programme, which had been carried out by the company, was performed in order to determine which were the most suitable temperatures. During such a work, which only involved Later 4 G/30, four different temperatures had been chosen and the following results were obtained in case of tensile properties:

TEMPERATURE	TIME TO FAILURE [hours]
150°C	4761
160°C	2984
170°C	1689
180°C	895

By plotting the logarithm of time to failure as a function of the reciprocal of temperature expressed in Kelvin, it was possible to perform a regression of these data as of Eq.3A, thus obtaining:

$$Lifetime = 5{,}39758 \cdot 10^{-8} \exp \frac{10687{,}93190}{T} \qquad \textbf{(Eq.47)}$$

The determined coefficient of determination R^2 for Eq.47 was found to be equal to 0,9915. By means of such an equation, it was possible to get an estimation of the times to failure in a broader range of temperature, under the assumption that Eq.47 holds in a certain range of temperatures. The latter may prove incorrect because the activation energy of a degradation progress may be subject to changes over broad ranges of temperature, as described in the previous chapter.

Given the fact that only three ovens were available at the beginning of the programme, the chosen temperatures and the respective predicted time to failure were:

TEMPERATURE	PREDICTED TIME TO FAILURE
160°C	2984 hours = 125 days
175°C	1229 hours = 52 days
190°C	568 hours = 24 days

Nevertheless, it is important to underline that the materials tested during this work were formulated in order to provide better environmental resistance in comparison with those that had been studied in the project the company carried out beforehand. Therefore, an improvement of the endurance was expected.

From this data, an ideal cycle period, i.e. the time between subsequent withdrawals from the ovens, was determined, so that at least ten withdrawals and subsequent testing would be performed. Hence, this period was selected to be equal to one tenth of the predicted time to failure, rounded down, so as to match the following table:

TEMPERATURE	PREDICTED TIME TO FAILURE
160°C	30 days
175°C	10 days
190°C	5 days

Nevertheless, these cycle periods are to be intended as an approximation of when the withdrawals occurred. After this designing phase, one hundred specimen for each

property test were placed inside each ovens, with the exception of samples for dielectric strength, in which case only eighty were used. The remaining ones were stored in an environmental chamber so that they could be used to measure the properties at time zero, to perform other analysis and in case of any need.

3.1.2. **Results**

After the start of the programme, monitoring of the properties of both materials proceeded according to the withdrawal schedule highlighted in the previous paragraph. First of all, the values at time zero were measured on the specimens kept in the environmental chamber, where both conditioning and testing occurred. The results in case of tensile strength and Charpy impact resistance of unnotched samples were the following:

PROPERTY	LATAMID 66 H2 G/30	LATER 4 G/30
Tensile Strength 3 mm	161,3 MPa	120,28 Mpa
Tensile Strength 1,5 mm	166,55 MPa	119,94 MPa
Charpy Impact Resistance	68,98 kJ/m^2	59,21 kJ/m^2

It can be noticed that the tensile strength of the 3 mm specimen turns out to be greater than that of the 1,5 mm one in case of Latamid 66 H2 G/30, while in case of Later 4 G/30 the values are almost equal. In case of injection-moulded polymers, an increase in mechanical properties is to be expected with decreasing thickness. This can be explained in terms of higher degree of orientation for thinner specimens, which leads to a rise in crystallinity, an effect which is magnified in case if composite materials [40].

As for the dielectric strength, tests were carried out at the Electrical Engineering laboratories of Genova's university. Using short-time tests, as described in the previous chapter, five measurements were performed per aging condition and the mean starting values were found to be equal to:

PROPERTY	LATAMID 66 H2 G/30	LATER 4 G/30
Dielectric Strength	24,4 kV/mm	25,27 kV/mm

3.1.2.1. **Latamid 66 H2 G/30**

In this paragraph, the values describing the evolution of the selected properties will be reported, in case of Latamid 66 H2 G/30. All the values will be presented as percentages in accordance with UL 746B, starting from the *tensile strength*:

160°C – TENSILE STRENGTH		
Time [hours]	1,5 mm	3 mm
0	100 %	100 %
188,5	94,85 %	95,53 %
381,5	88,86 %	93,82 %
696	80,91 %	90,12 %
1224	79,37 %	83,21 %
1965	77,09 %	69,82 %
2520	63,3 %	59,29 %
3360	51,41 %	45,66 %
3960	45,88 %	39,36 %

175°C - TENSILE STRENGTH		
Time [hours]	1,5 mm	3 mm
0	100 %	100 %
336	93,5 %	95,35 %
504	86,55 %	89,35 %
720	80,94 %	79,31 %
1056	72,32 %	67,81 %
1224	72,3 %	65,56 %
1440	63,88 %	54,6 %
1656	59,09 %	46,44 %
1824	50,25 %	42,28 %
2064	49,95 %	40,63 %

190°C - TENSILE STRENGTH		
Time [hours]	1,5 mm	3 mm
0	100 %	100 %
96	99,35 %	101,27 %
216	91,74 %	93,63 %
360	87,77 %	89,14 %
504	77,31 %	82,17 %
720	76,08 %	75,76 %
888	66,04 %	62,37 %
1056	52,46 %	52,27 %
1200	50,77 %	41,38 %
1416	38,33 %	31,92 %

These trends can better be represented by plotting the property retention percentage as a function of the logarithm of time, as shown in Figure 4:

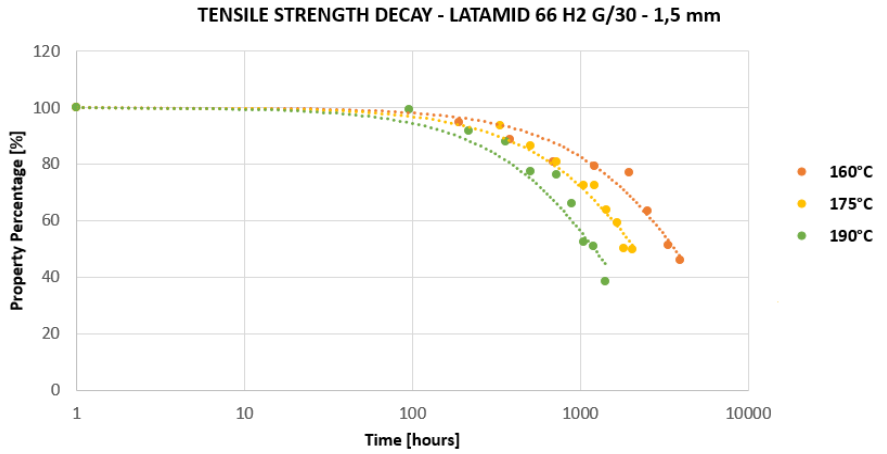

Figure 31 *Plot of the evolution of the tensile strength of Latamid 66 H2 G/30 1,5 mm for the three aging temperatures*

In Figure 31, the dotted lines represent an exponential fitting which is only meant to underline the typical behaviour of the property decay. As for the thickness of 3 mm, a similar graph can be determined starting from the obtained data. Once more, a fitting will be shown to display the trend (Figure 32).

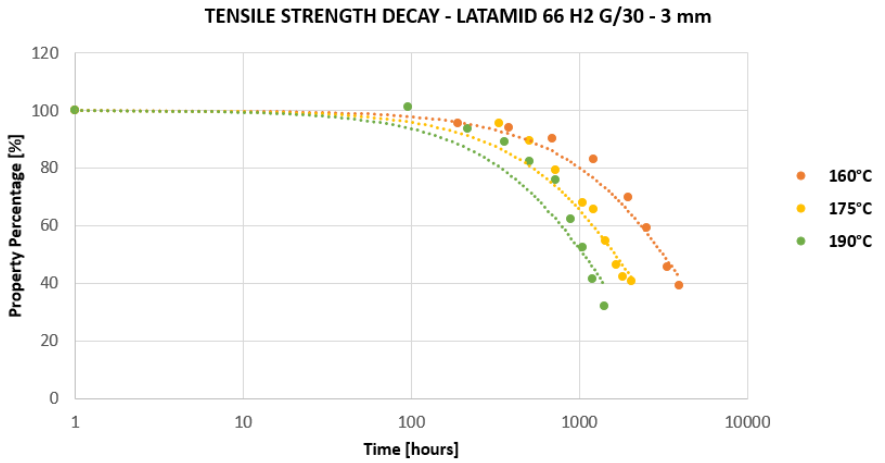

Figure 32 *Plot of the evolution of the tensile strength of Latamid 66 H2 G/30 3 mm for the three aging temperatures with respective exponential fitting*

The evolution of such a property can also be displayed using a stress-strain plot at various times of aging for a given temperature, which highlights a progressive embrittlement. For the sake of simplicity and brevity, only the percentage of retention for a temperature of 175°C is shown (Figure 33) for materials.

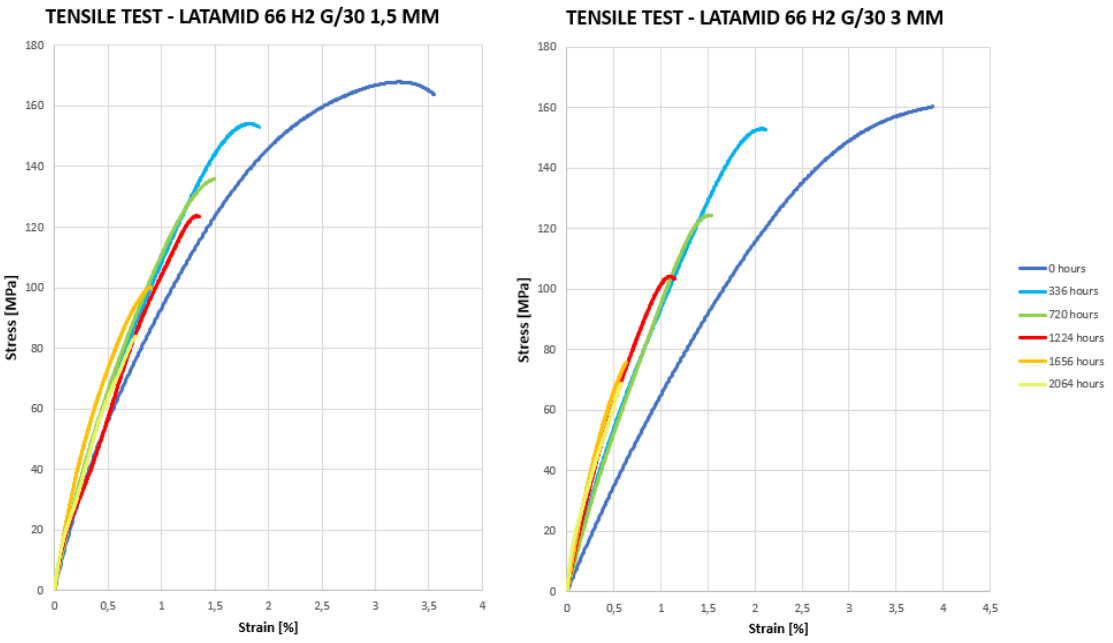

Figure 33 *Stress-strain plot of Latamid 66 H2 G/30 highlighting the evolution of the curve in case of subsequent times of aging in ovens at 175°C*

The evolution of the Charpy impact resistance for unnotched specimens is the following:

160°C – CHARPY IMPACT RESISTANCE	
Time [hours]	Value
0	100 %
188,5	69,41 %
381,5	56,69 %
696	46,19 %
1224	40,8 %

175°C - CHARPY IMPACT RESISTANCE	
Time [hours]	Value
0	100 %
96	63,09 %
336	45,89 %
504	42,58 %
720	32,54 %

190°C - CHARPY IMPACT RESISTANCE	
Time [hours]	Value
0	100 %
44,5	63,99 %
96	56,49 %
216	47,65 %
360	36,19 %

The trends as a function of the logarithm of time are shown in Figure 34:

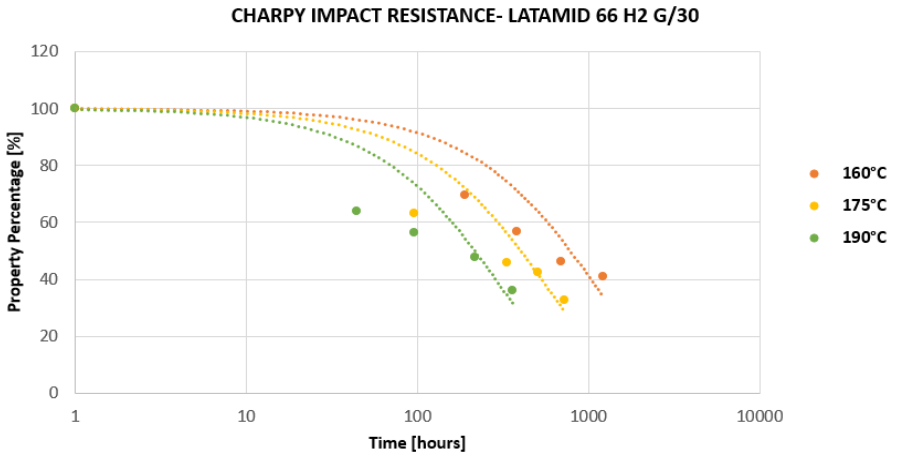

Figure 34 *Plot of the evolution of the Charpy impact resistance of Latamid 66 H2 G/30 for the three aging temperatures with respective exponential fitting*

Figure 34 clearly shows that the evolution of the Charpy impact resistance is much more abrupt in the beginning, with a plot shifted towards shorter times with respect to the previously presented properties. The significant reduction in impact toughness can be ascribed to polyamide being semi-crystalline in nature. At elevated temperatures, during the decomposition of the polymer chain, the molecular weight of the molecule was reduced, microcracks were formed after time, crystallization was enhanced (as described by [19]), leading to brittle behaviour and severely affecting the impact

strength. As molecular weight is reduced, the large entangled macromolecules became shorter and were no longer able to retain their resistance to deformation as they could slide past each other more readily under less force. Moreover, a more brittle behaviour can be expected since the oxidation of the surface of the specimen has a serious influence on impact resistance. Therefore, the presence of a defect from where failure may start is more likely to occur than in the case of other properties.

A similar study was carried out in case of dielectric strength and all experiments were carried out in an oil bath by means of spherical electrodes. These electrodes were preferred over flat ones as they prevent the creation of an interface between the electrode itself and the surface of the specimen. As a matter of fact, the latter is influenced by thermal stresses which can cause the specimen to bend. As for the experimental method, short-time tests with a rate equal to 1 KV/s were exploited.

The following results were obtained in terms of property retention, expressed as a percentage:

160°C - DIELECTRIC STRENGTH	
Time [hours]	Value
1	100 %
382	101,37 %
1965	90,71 %
2520	74,04 %
3360	69,4 %

175°C - DIELECTRIC STRENGTH	
Time [hours]	Value
1	100 %
504	96,99 %
1050	92,9 %
1656	72,95 %
2064	66,42 %

190°C - DIELECTRIC STRENGTH	
Time [hours]	Value
1	100 %
360	98,91 %
720	95,36 %
1056	78,42 %
1416	60,66 %

The retention of such a property is substantially better than the tensile strength and the Charpy impact resistance. However, no samples were available to perform further measures and the time corresponding to a property loss equal to 50% could not be determined experimentally.

The plot representing the loss of property in case of dielectric strength is shown in Figure 35. Even though the failure criterion was not met, the usual degradative trend can be distinguished. Therefore, it can be assumed that an extrapolation of the obtained data could lead to acceptable values, which will then be used for the determination of the thermal index.

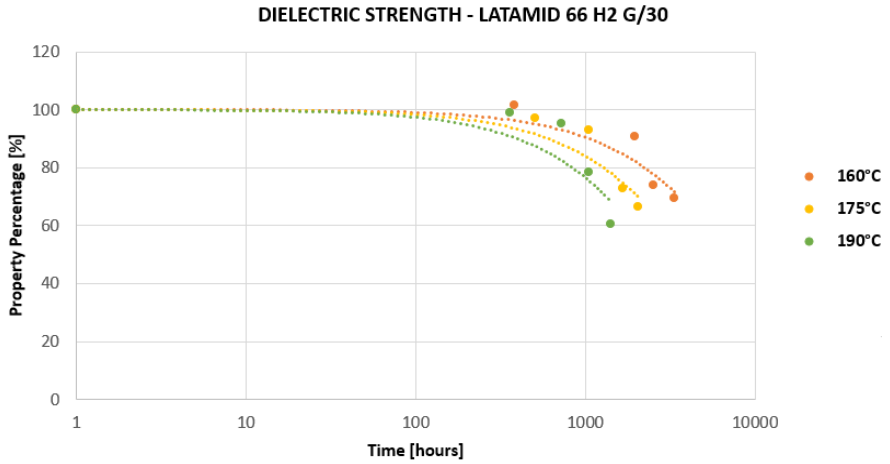

Figure 35 *Plot of the evolution of the dielectric strength of Latamid 66 H2 G/30 for the three aging temperatures with respective exponential fitting*

3.1.2.2. Later 4 G/30

In this paragraph, as in the previous one, the evolution of the selected properties as percentages will be shown. As previously done for Latamid 66 H2 G/30, the evolution of the tensile strength over the aging time will be presented first, followed by the Charpy impact resistance and by the dielectric strength:

160°C - TENSILE STRENGTH		
Time [hours]	1,5 mm	3 mm
0	100 %	100 %
381,5	117,57 %	112,96 %
696	116,6 %	113,05 %
1224	114,88 %	111,91 %
1965	113,28 %	109,91 %
2520	113,02 %	109,18 %
3360	104,59 %	95,94 %
3960	87,4 %	82,74 %
4824	81,32 %	79,25 %
6264	72,74 %	70,18 %
8644	60,49 %	59,21 %
10104	54,03 %	51,9 %
11564	48,25 %	42,89 %

175°C - TENSILE STRENGTH		
Time [hours]	1,5 mm	3 mm
0	100 %	100 %
96	115,54 %	111,95 %
336	124,53 %	117,49 %
504	118,22 %	112,23 %
720	117,59 %	111,81 %
1056	110,21 %	110,62 %
1224	108,59 %	106,05 %
1440	105,49 %	101,18 %
1656	92,81 %	86,33 %
1824	83,58 %	73,16 %
2064	79,21 %	71,63 %
2544	70,76 %	68,11 %
3054	65,44 %	61,89 %
3628	58,46 %	55,4 %
4120	53,07 %	50,39 %
4676	47,57 %	45,27 %

190°C - TENSILE STRENGTH		
Time [hours]	1,5 mm	3 mm
0	100 %	100 %
44,5	114,8 %	110,34 %
96	115,94 %	112,25 %
216	120,33 %	115,6 %
360	123,7 %	119,03 %
504	112,15 %	104,17 %
720	98,79 %	104,09 %
888	84,78 %	87,44 %
1056	77,69 %	77,67 %
1200	68,21 %	75,15 %
1416	57,49 %	67,37 %
1536	54,08 %	61,26 %
1750	52 %	58,19 %
1944	49,06 %	53,2 %
2256	44,9 %	49,79 %
2448	42,54 %	47,01 %

The final results in case of 160°C were extrapolated because it was unfeasible to reach those times in the timeframe of this project. The plots representing of property retention percentage as a function of the logarithm of time for these trends are the following, starting with the 1,5 mm thick specimens (Figure 36):

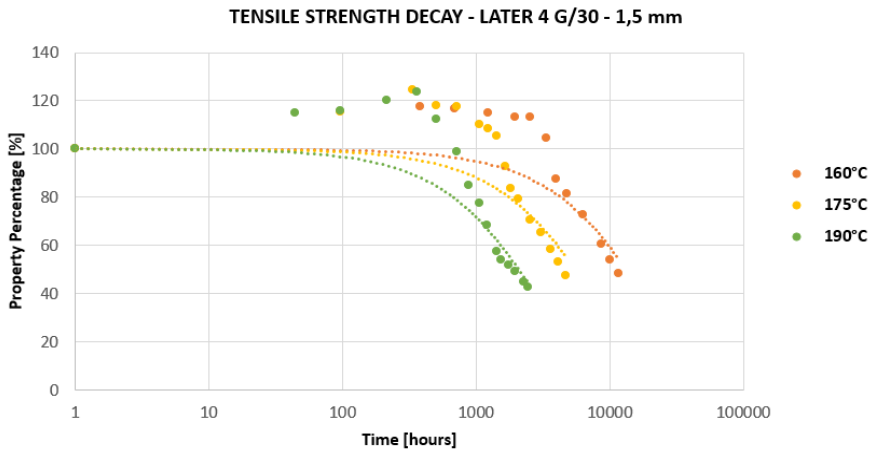

Figure 36 *Plot of the evolution of the tensile strength of Later 4 G/30 1,5 mm for the three aging temperatures*

One features emerges from this graph, that is to say the increase in property value at low times. This occurred for all temperatures, thus requiring further investigation to determine its causes. Among the most likely, a possible increase in crystallinity, molecular mass or even crosslinking would be compliant with an increase in the tensile strength. The behaviour was further confirmed by the degradative trend of the 3 mm thick specimens (Figure 37):

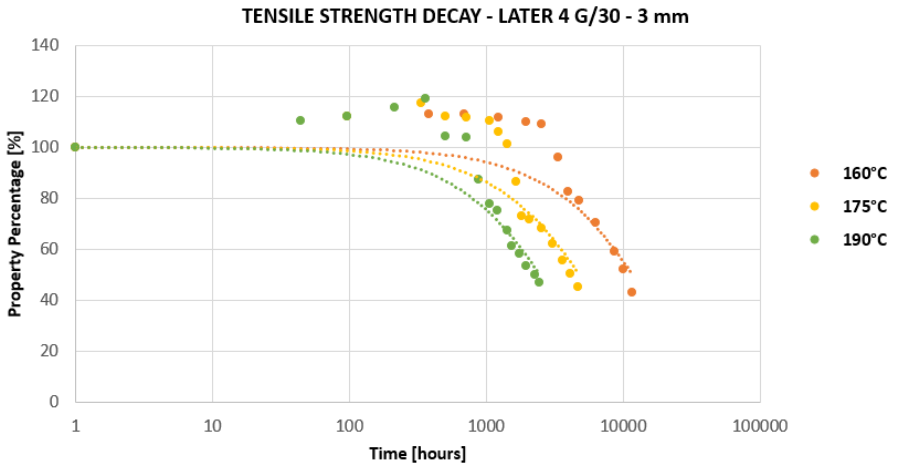

Figure 37 *Plot of the evolution of the tensile strength of Later 4 G/30 3 mm for the three aging temperatures*

An attempt at determining the origin of such a phenomena will be presented in a later chapter. Figure 38 shows the trend at 175°C in a stress-strain plot, highlighting the fact that the increase in tensile strength is generally related to a decrease in strain at break:

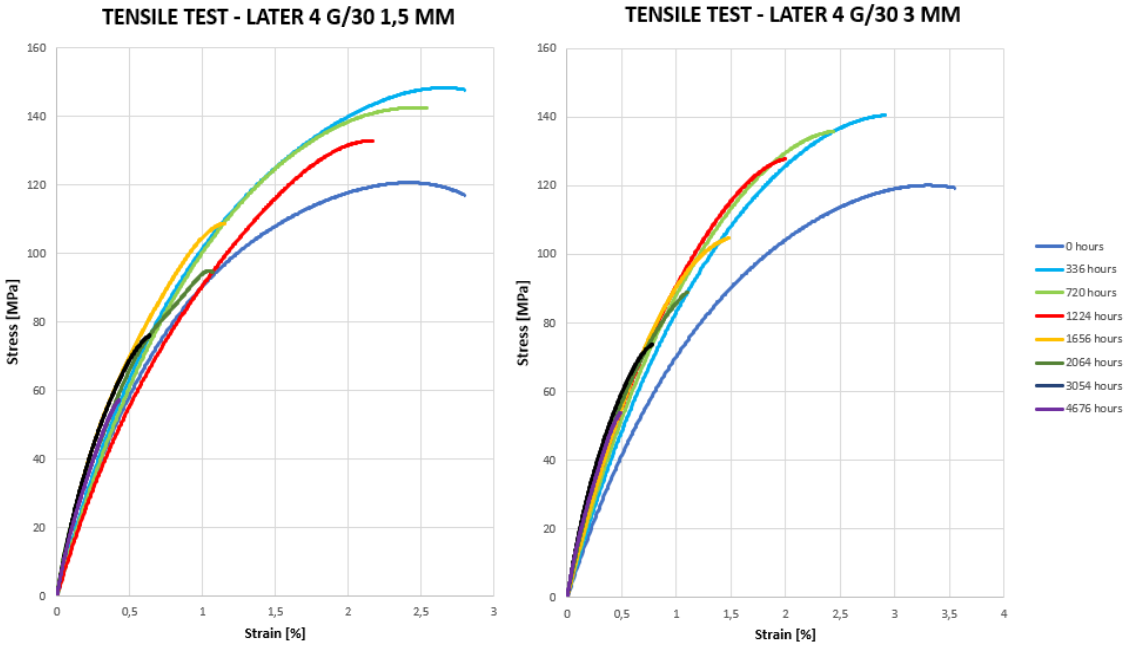

Figure 38 *Stress-strain plot of Later 4 G/30 highlighting the evolution of the curve in case of subsequent times of aging in ovens at 175°C*

As for the Charpy impact resistance of the unnotched specimens, the following results were obtained:

160°C – CHARPY IMPACT RESISTANCE	
Time [hours]	Value
0	100 %
381,5	86,69 %
696	78,42 %
1224	75,73 %
1965	72,61 %
2520	68,96 %
3360	57,64 %
3960	45,35 %

175°C – CHARPY IMPACT RESISTANCE	
Time [hours]	Value
0	100 %
96	87,17 %
336	82,09 %
504	75,12 %
720	69,82 %
1056	65,85 %
1224	55,49 %
1440	46,96 %

190°C – CHARPY IMPACT RESISTANCE	
Time [hours]	Value
0	100 %
44,5	77,05 %
96	70,42 %
216	66,21 %
360	61,77 %
504	45,41 %
720	42,32 %
888	40,54 %

These data can be represented as a function of the logarithm of time, similarly to what has been done before (Figure 39).

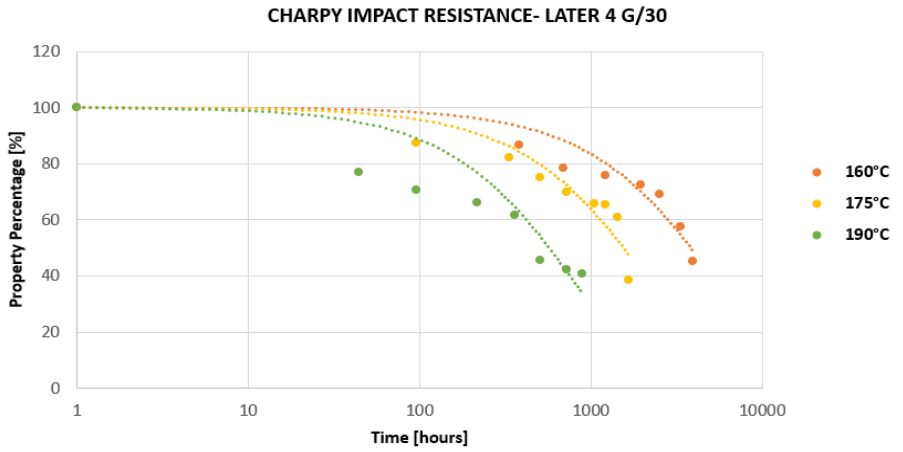

Figure 39 *Plot of the evolution of the Charpy impact resistance of Later 4 G/30 for the three aging temperatures with respective exponential fitting*

To conclude the paragraph regarding long-term aging of Later 4 G/30, the evolution of dielectric strength is now presented:

160°C - DIELECTRIC STRENGTH	
Time [hours]	Value
1	100 %
382	98,73 %
3360	94,55 %
4824	92,35 %
6264	92,08 %

175°C - DIELECTRIC STRENGTH	
Time [hours]	Value
1	100 %
504	98,33 %
1050	97,85 %
2064	92,88 %

190°C - DIELECTRIC STRENGTH	
Time [hours]	Value
1	100 %
1200	99,47 %
1750	68,07 %
2448	51,98 %

By plotting these values as a function of the logarithm of time, the following is obtained (Figure 40):

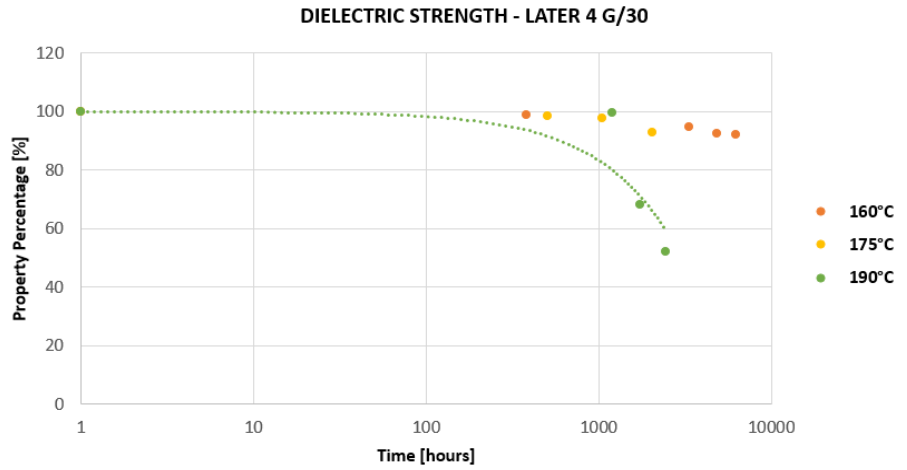

Figure 40 *Plot of the evolution of the dielectric strength of Later 4 G/30 for the three aging temperatures with respective exponential fitting*

As it appears from the tables and the graph, in case of Later 4 G/30, the dielectric strength seems not to be influenced by thermal aging, at least at the to lower temperatures. As a matter of fact, even for the longest aging times, the values of such a property do not show a significant decrease. Therefore, the only reasonable extrapolation might be that for the highest temperature, i.e. 190°C, which does not allow for the determination of the thermal index.

3.2. Thermogravimetric Analysis

3.2.1. Preparation

In order to obtain samples suitable for thermogravimetric analysis, pieces were cut off from unaged tensile specimens with a weight ranging from 18 to 22 mg. This was done out of simplicity and because of unavailability of further polymer pellet after the process of injection moulding. After the calibration of the scale, the material underwent the following thermal programme, which was already shown in detail:

- Start of the gas flow and of data acquisition;
- Temperature ramp equal to 1.00 °C/min up to 550.00 °C with undergoing temperature modulation of ± 5.00 °C for 200 s, using Hi-Res sensitivity;
- Stop of data acquisition and start of pure air flow;
- Temperature ramp of 50.00 °C/min up to 900.00 °C;
- Temperature equilibration at 80.00 °C.

3.2.2. Results

The most interesting features which were obtained from such a programme are the degradation curve and its derivative, the activation energy plot, the temperature corresponding to 5% the total mass loss and the temperature corresponding to a maximum in the derivative. The temperature corresponding to the start of the degradation process is not objective and was not exploited. The results of the modulated thermogravimetric programme will be presented, starting from Latamid 66 H2 G/30.

3.2.2.1. Latamid 66 H2 G/30

The thermogravimetric analysis of such a material led to a set of results similar to those shown in Figure 41. The peculiar shape of the curve pinpointed the fact that more than one reaction occurred in the same range of temperatures. This means that the kinetics of degradation was not smooth and continuous, therefore, that such a technique should not suitable for this material, at least for this specific grade. As a matter of fact, such a

result was not confirmed by any literature data, suggesting that it may be due to specific additives present in this material.

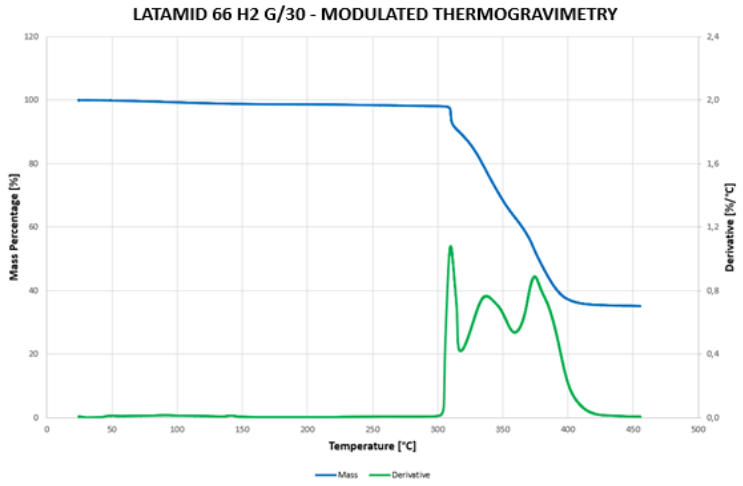

Figure 41 *Plot of a modulated thermogravimetric run performed on Latamid 66 H2 G/30 in inert atmosphere, showing both the percentage mass loss and its derivative*

Therefore, different strategies of analysis were employed to tackle such an issue. The first try was to perform separate standard thermogravimetric runs at different heating rates according to Ozawa-Flynn-Wall method (ASTM E1641) and presented in chapter 2. Specifically, the heating rates which were used were equal to 20°C/min, 15°C/min, 10°C/min, 5°C/min, 2,5°C/min and 1°C/min. Furthermore, all the specimens were subject to drying in salts for at least 48 hours before starting the procedure, in order to eliminate any contribution due to absorbed water. An example of the obtained degradation curves is given below (Figure 42) for a heating rate equal to 1°C/min:

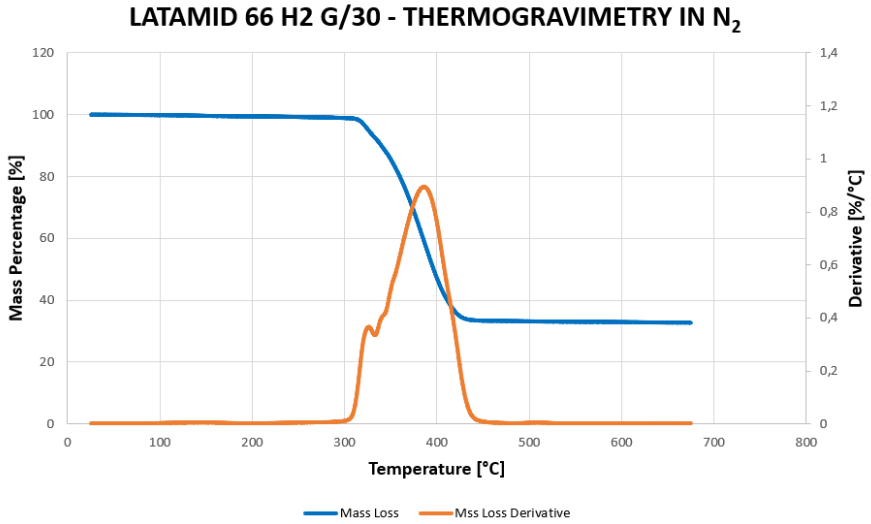

Figure 42 *Plot of a standard thermogravimetric run performed on Latamid 66 H2 G/30 in nitrogen at a heating rate equal to 1°C/min, showing both the percentage mass loss and its derivative*

As Figure 42 highlights, the degradation process is not a simple one, but comprises many simultaneous features. Presumably, this implies the presence of an underlying decay of some additives, which makes it a non-smooth mass change with multiple maximum rates. Therefore, such a process would still not be suitable for the simplified treatment proposed in chapter 2, at least not for the computation of the pre-exponential factor, as confirmed by the computation of the order of reaction according to Eq.8, yielding:

$$n = \frac{d \ln \frac{dC}{dt}}{d \ln(1 - C)} = 2{,}159 \qquad \textbf{(Eq.48)}$$

Such a result implies the need for a more complex thermogravimetric analysis. Even though the activation energy can still be obtained since the Flynn-Ozawa-Wall method is a model-free one, which doesn't imply knowledge of the reaction order, the final focus of this project is on the temperature index. Therefore, such a computation will not be carried out and another procedure will be sought after.

For the sake of obtaining a first-order kinetics of degradation, a new procedure was developed in collaboration with Stefano Tagliabue, a PhD student in materials engineering at Politecnico di Milano. This was done in order to isolate and cancel the contribution which had caused a peak in the mass loss derivative at lower temperatures. Such a thermogravimetric programme comprised:

- An initial temperature ramp at a rate equal to 10°C/min up to 300°C;
- An hour-long isothermal programme at 300°C to get rid of the additive contribution;
- An equilibration to the temperature of 200°C to stabilize the reaction of degradation;
- A new temperature ramp at a rate equal to the desired heating rate (10°C/min, 7°C/min, 5°C/min, 2,5°C/min and 1°C/min) up to 600°C/min;
- A final temperature ramp of 20°C/min up to 900°C followed by equilibration at 80°C.

Such a technique yielded the following result (Figure 43):

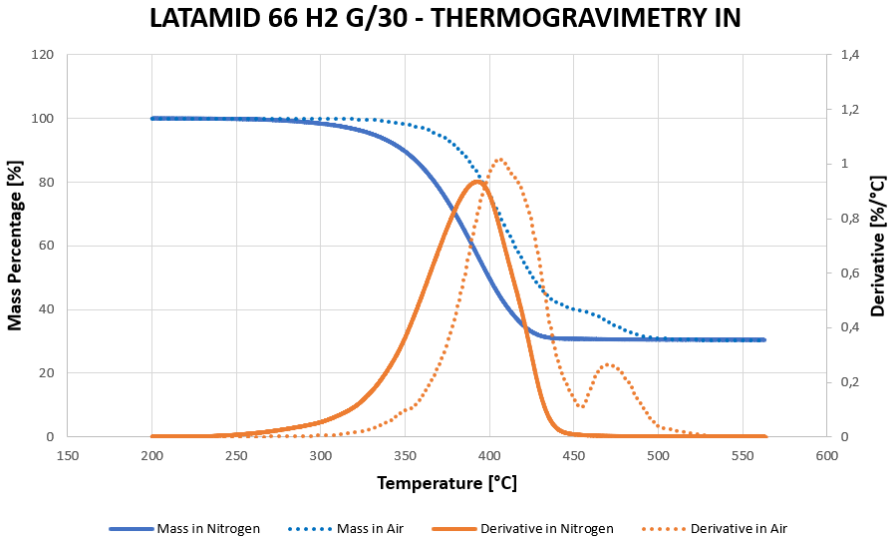

Figure 43 *Plot of a standard thermogravimetric run performed on Latamid 66 H2 G/30 in both nitrogen and air at a heating rate equal to 1°C/min, showing the percentage mass loss and its derivative*

The curve obtained from the thermogravimetry in air shows a dump corresponding to the carbonization stage, i.e. the degradation of char and other products of the oxidative reaction at high temperatures. It is important to notice a direct correlation between the peak in the mass loss derivative between these results (Figure 43) and the ones obtained with the normal procedure (Figure 42). The resulting plot shows an opposing trend with respect to Later 4 G/30, for which the curve of the run performed in air was more shifted towards the left. This behaviour is compliant with what described by Wagner [19] and a possible explanation will be presented in the following chapters.

3.2.2.2. Later 4 G/30

In case of this material, the thermogravimetric analysis led to better results, since a behaviour similar to that of Latamid 66 H2 G/30 was not observed. On the contrary, the degradative behaviour was smooth and compliant with literature, thus making it possible to use the procedures explained in chapter 2 to compute the temperature index and obtain a plot of the thermal endurance.

The features described above will now be presented, along with a sample graph of the degradation curve and its derivative and of the activation energy which

was directly computed by the software during the analysis. The results will be shown both in case of an inert environment, specifically nitrogen, and of air (Figure 44).

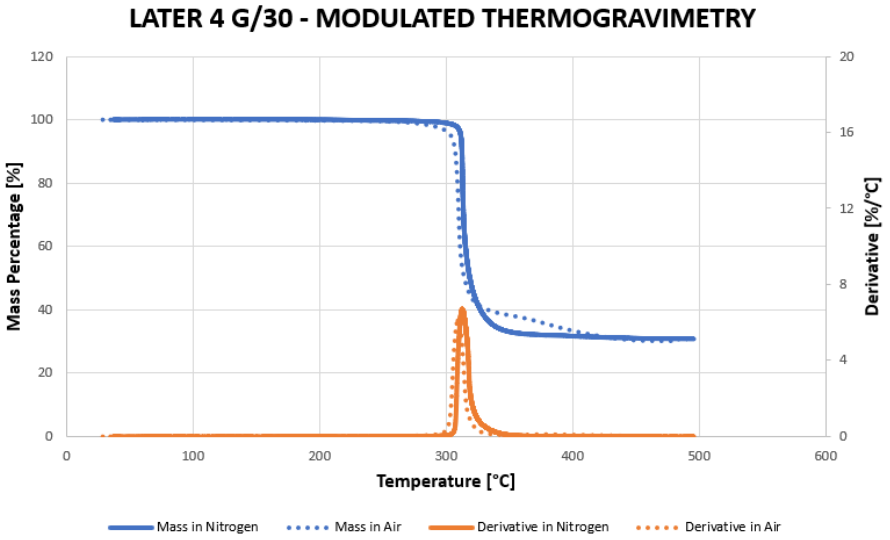

Figure 44 *Plot of a modulated thermogravimetric run performed on Later 4 G/30, both in nitrogen and air as a comparison, showing both the percentage mass loss and its derivative*

This analysis shows that the transition between the mass plateaux was smooth both in case of inert and reactive environment and the plot of the derivative better enhanced this fact, as a single peak is present. This makes both cases compliant with what described by the standards and therefore suitable for computation. It is important to notice that the degradative behaviour in case of the two atmospheres is slightly different since in the case of air, the presence of oxygen causes the reaction to occur earlier. Moreover, the end of the reaction is characterised by a different slope in the latter case, which can be ascribed to the late burning of char and other oxidation products.

As for the plot of the activation energy determined by the software, the typical U-shaped curve can be detected and it is more pronounced in case of air as the environment. this underlines the fact that the reaction in air is essentially longer, but also clearly shows how the activation energy throughout the degradation process is mostly constant, only rising at the end. On the other hand, in case of nitrogen as an environment, the reaction is consumed in a shorter temperature range, even though the nominal values of activation energy for both cases are similar during the degradative process itself (Figure 45). Furthermore, it is important to highlight a perfect superposition between the temperature corresponding to the maximum in the mass loss derivative and that corresponding to the lowest value of activation energy.

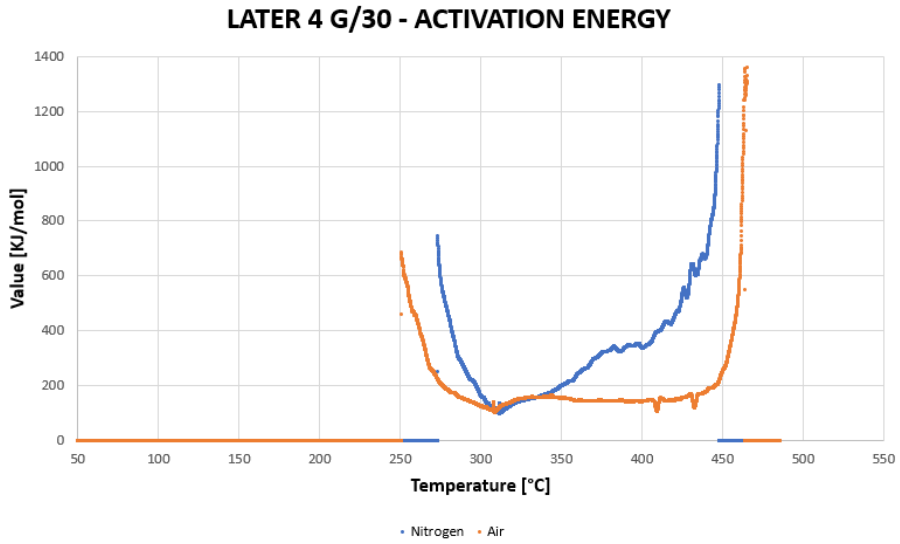

Figure 45 *Plot of the activation energy as obtained by means of modulated thermogravimetric analysis in case of Later 4 G/30 in nitrogen and air*

As for the features of interest, the following table provides a summary of the values of the temperatures corresponding to 5% mass loss and to the maximum of mass derivative obtained from the various modulated thermogravimetry runs, starting from those performed in inert atmosphere:

RUN	MASS [g]	5% TEMPERATURE [°C]	MAX DERIVATIVE TEMP [°C]
1	15,3	308,98	312,19
2	15,47	310,65	312,77
3	22,23	311,7	313,52
4	16,21	309,97	311,74
5	17,54	309	311,26
6	18,91	302,85	304,31
AVERAGE	17,61	308,86	310,97
REL. ST. DEV.	15,01%	1,01 %	1,08 %

As it appears from the table, the relevant temperatures show a dependence on the mass of the specimen, even though the values are not dispersed much. As a matter of fact, higher masses generally shift the degradative curves to the right and this is generally also true for molecular weights, although this trend is not absolutely true. The matching values of activation energy, computed according to Eq.23 were found to be:

RUN	5% ACT EN [kJ/mol]	MAX DERIVATIVE ACT EN [kJ/mol]
1	103,36	89,71
2	121,2	97,54
3	109,26	95,08
4	115,95	113,53
5	97,44	101,61
6	109,75	92,69
AVERAGE	109,49	98,36
REL. ST. DEV.	7,77 %	8,62 %

Unlike the values of temperature, the oscillation in activation energy was far greater due to the irregularities of the respective plot (as of Figure 45), at least in case of inert environment. This is perfectly highlighted by the higher values of relative standard deviation in percentage. Given the high dispersion and the poor significance of the pre-exponential factor in the computation required in this project, this quantity won't be presented here. The trends of the values of activation energy can be better represented by means of the following graph (Figure 46):

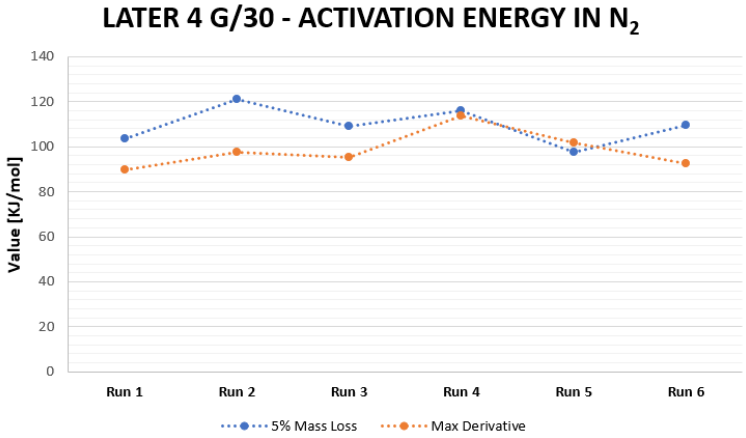

Figure 46 *Representation of the trends of activativation energy determined in inert atmosphere along the various runs*

In case of reactive atmosphere, the obtained data are the following:

RUN	MASS [g]	5% TEMPERATURE [°C]	MAX DERIVATIVE TEMP [°C]
1	19,38	299,56	309,32
2	19,46	299,93	309,49
3	17,13	296,62	300,65
4	17,53	297,42	301,33
5	16,1	296,77	301,09
AVERAGE	17,92	298,06	304,376
REL. ST. DEV.	8,18 %	0,53 %	1,51 %

Once more, a trend exists between the increase in specimen mass and the shift of the temperatures towards higher values. As for the corresponding values of activation energy, the following ones were found:

RUN	5% ACT EN [kJ/mol]	MAX DERIVATIVE ACT EN [kJ/mol]
1	126,14	104,52
2	109,65	99,31
3	125,48	104,86
4	127,73	99,71
5	126,07	109,12
AVERAGE	123,014	103,504
REL. ST. DEV.	6,11 %	3,94 %

Apart from the value determined from Run 2, the activation energy determined in case of a reactive atmosphere for a mass loss corresponding to 5% is mostly constant, thus highlighting the high repeatability of such a technique. This trend can be better stressed out by means of the following plot (Figure 47):

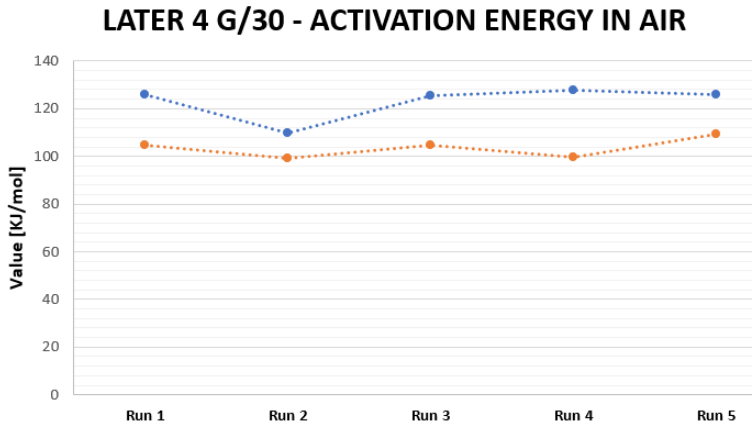

Figure 47 *Representation of the trends of activativation energy determined in reactive atmosphere along the various runs*

The computation of the thermal and temperature indices starting from these values will be carried out in the following chapter.

CHAPTER FOUR
Analysis

4. Chapter Content

In this chapter, a mathematical analysis of the previously found data will be performed with the aim of obtaining the value of thermal index, both in case of long-term aging and short-term one. At the end, a table summarizing the obtained results in terms of thermal indices will be provided for both materials.

4.1. Latamid 66 H2 G/30

The first data to be analysed are those regarding Latamid 66 H2 G/30, starting from the aging in ovens followed by thermogravimetry.

4.1.1. Tensile Strength

As far as the computation of the *thermal index* itself is concerned, it was firstly required to evaluate the time at which the failure criterion had been met for each combination of temperature and thickness. Abiding by the rules described in paragraph 2.3., the obtained data was interpolated using a third-degree polynomial and the following results for a property loss equal to 50% were found:

TEMPERATURE	TIME TO FAILURE (1,5 mm)	TIME TO FAILURE (3 mm)
160°C	3501,53 hours	3061,71 hours
175°C	2064,86 hours	1532,77 hours
190°C	1250,55 hours	1085,91 hours

These values are not completely in accordance with what was suggested by UL 746B, since the time required to meet the failure criterion in case of the lowest temperature is lower than 5000 hours. This fact shall be considered when analysing the final results, especially the activation energy, whose trend might not be constant for any temperature range. Employing a lower aging temperature for Latamid 66 H2 G/30 might have led to more precise results. This however was unfeasible due to the number of available ovens.

By taking the natural logarithm of the times to failure and plotting them as a function of the reciprocal of temperature in Kelvin, it was possible to perform a linear

regression as explained in Eq.3A and Eq.3B, which takes the name of Arrhenius plot (Figure 48):

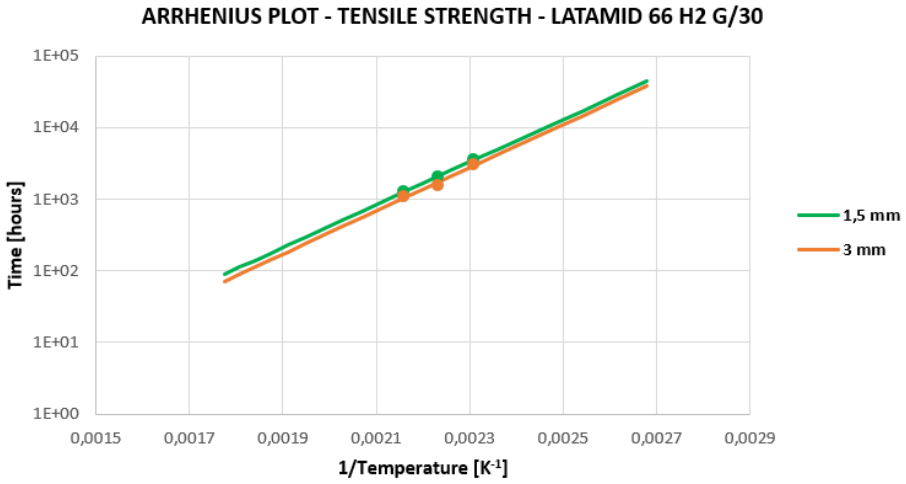

Figure 48 *Arrhenius plot of the time to failure as a function of the reciprocal of temperature, with dots representing the actual data, in case of tensile strength of different thicknesses of Latamid 66 H2 G/30*

Specifically, the following relationships were determined according to the standard UL 746B:

1,5 mm $$\ln t = 6884{,}564 \cdot \frac{1}{T} - 7{,}732$$ **(Eq.49A)**

3 mm $$\ln t = 6954{,}899 \cdot \frac{1}{T} - 8{,}080$$ **(Eq.49B)**

Corrected correlation factors R^2 equal to 0,99996 in case of 1,5 mm thickness and to 0,94159 in case of 3 mm thickness were determined. Eq.49 led to the determination of the activation energy E for the aging process and to the pre-exponential factor A:

1,5 mm $$E = 6884{,}564 \cdot R = 57{,}24\ kJ \cdot mol^{-1}$$ **(Eq.50A)**

$$A = \exp(-7{,}732) = 4{,}39 \cdot 10^{-4}\ hours$$ **(Eq.50B)**

3 mm $$E = 6954{,}899 \cdot R = 57{,}82\ kJ \cdot mol^{-1}$$ **(Eq.50C)**

$$A = \exp(-8{,}080) = 3{,}10 \cdot 10^{-4}\ hours$$ **(Eq.50D)**

Eq.50A and Eq.50C show that the values of activation energy for different thicknesses only differ by approximately 1%, which underlines how the mechanism of property loss is the same and only depends on the material and on the property being measured. The reason why these values are negative is that the regression was that the Arrhenius relationship links time and the reciprocal of temperature, while in case of Eq.7A, used

for thermogravimetry, the heating rate is used. Since the latter is the inverse of a time, the activation energy will be expressed as positive in the following chapters.

By exploiting Eq.33, it is also possible to build a graph of thermal endurance, where the lifetime is expressed as a function of temperature (Figure 49):

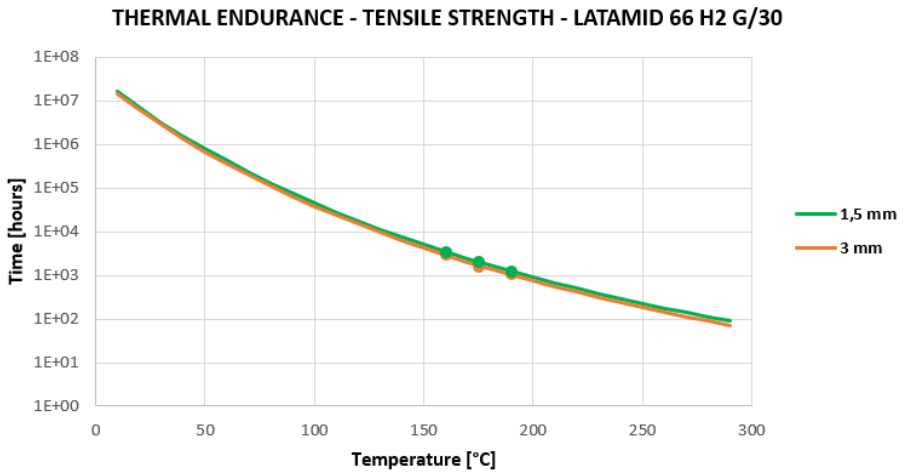

Figure 49 *Thermal endurance plot with dots representing the actual data in case of tensile strength of different thicknesses of Latamid 66 H2 G/30*

Hence, determination of the temperature corresponding to a lifetime of $6 \cdot 10^5$ hours for the tensile strength was feasible by using Eq.3C:

1,5 mm
$$T = \frac{57{,}24 \cdot 10^3/R}{\ln(60000) + 7{,}732} = 94{,}34°\text{C} \qquad \textbf{(Eq.51A)}$$

3 mm
$$T = \frac{57{,}82 \cdot 10^3/R}{\ln(60000) + 8{,}080} = 91{,}32°\text{C} \qquad \textbf{(Eq.51B)}$$

In terms of thermal index, these values both correspond to a TI equal to 90, lower of 15 points compared to the value presented in chapter 2, a feature which could be caused by the higher temperatures which were examined in this project. Nevertheless, it must be noted that those results were not absolute ones but represent a relative thermal index, i.e. one which is tuned according to the value of a reference material, which was not considered in this analysis.

4.1.2. **Charpy Impact Resistance**

The interpolation of the obtained data led to the determination of the values of time corresponding to a property loss equal to 50%, as explained previously:

TEMPERATURE	TIME TO FAILURE
160°C	600,47 hours
175°C	287,93 hours
190°C	173,47 hours

However, these times to failure do not respect the restrictions imposed by UL 746B, both for the highest and for the lowest temperatures. This shall be considered in the final discussion. Nevertheless, by means of these values, the Arrhenius plot (Figure 50) and its corresponding equation were determined:

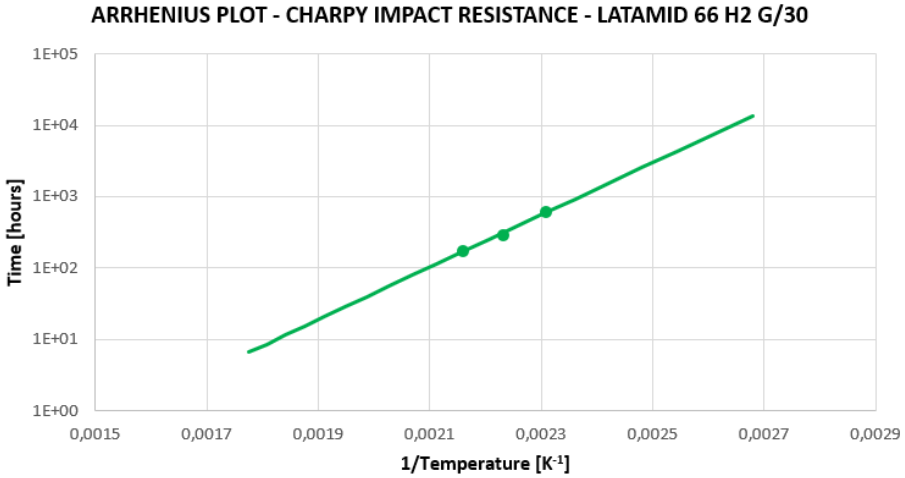

Figure 50 *Arrhenius plot of the time to failure as a function of the reciprocal of temperature, with dots representing the actual data in case of Charpy impact resistance of Latamid 66 H2 G/30*

Yielding the relationship:

$$\ln t = 8452{,}514 \cdot \frac{1}{T} - 13{,}129 \qquad \textbf{(Eq.52)}$$

A corrected correlation factor R^2 equal to 0,98245 was determined. As for the activation energy and pre-exponential factor, the following values were determined:

$$E = 8452{,}514 \cdot R = 70{,}27\ kJ \cdot mol^{-1} \qquad \textbf{(Eq.53A)}$$

$$A = \exp(-13{,}129) = 1{,}99 \cdot 10^{-6}\ hours \qquad \textbf{(Eq.53B)}$$

These values significantly differ from those of Eq.50, highlighting the fact that thermal degradation has a different influence on each property.

Lastly, by means of the acquired data, a plot of the thermal endurance (Figure 51) and the value of thermal index can be determined:

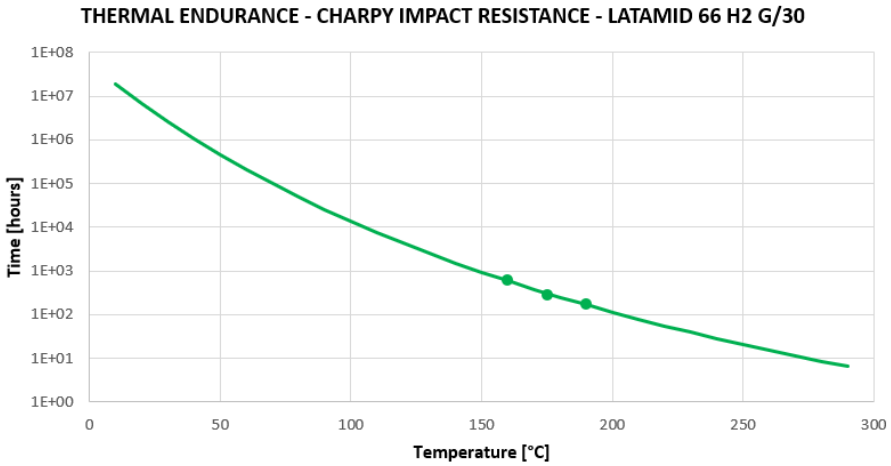

Figure 51 *Thermal endurance plot with dots representing the actual data in case of Charpy impact resistance of Latamid 66 H2 G/30*

Hence, the temperature corresponding to a lifetime of $6 \cdot 10^4$ hours in case of Charpy impact resistance can be found as:

$$T = \frac{70{,}27 \cdot 10^3 / R}{\ln(60000) + 13{,}129} = 77{,}12°\text{C} \qquad \textbf{(Eq.54)}$$

Leading to a value of thermal index equal to 75, which is way smaller than that obtained in case of tensile strength and than the corresponding literature data. Compared to the value determined in the previous study, this one turns out to be slightly lower (5 points), highlighting how the influence of higher temperatures on the Charpy impact resistance is higher than that on tensile strength.

4.1.3. **Dielectric Strength**

An extrapolation of the obtained values of dielectric strength was performed in order to obtain the expected times corresponding to a property loss equal to 50%. The values of corrected R^2 were found to be equal to 0,94258 for the lowest temperature, 0,81268 for the middle one and 0,89490 for the highest one. Therefore, these were considered as an acceptable approximation for the following computations. The obtained values of time to failure were the following:

TEMPERATURE	TIME TO FAILURE
160°C	6655,91 hours
175°C	4019,30 hours
190°C	1927,56 hours

By means of these data, it is possible to build the Arrhenius plot (Figure 52) and find its defining equation:

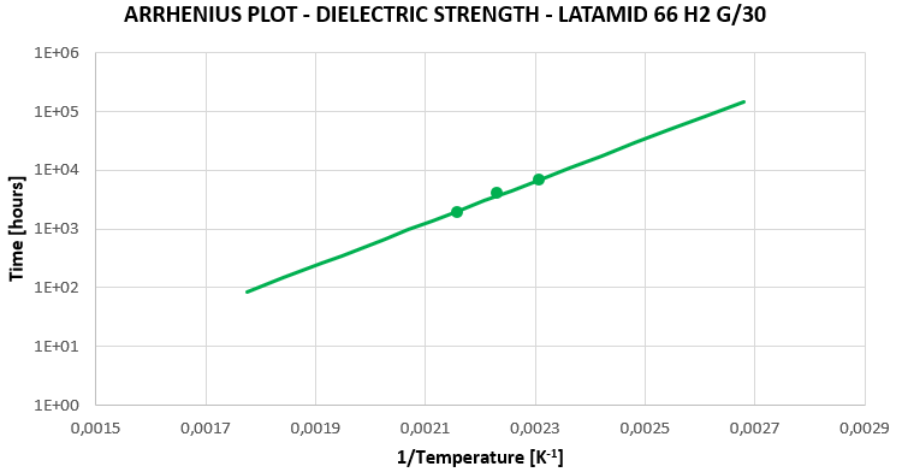

Figure 52 *Arrhenius plot of the time to failure as a function of the reciprocal of temperature, with dots representing the actual data in case of dielectric strength of Latamid 66 H2 G/30*

The corresponding equation, yielding a corrected R^2 equal to 0,96827 is:

$$\ln t = 8266{,}740 \cdot \frac{1}{T} - 10{,}238 \qquad \textbf{(Eq.55)}$$

Starting from this equation, the values of activation energy and pre-exponential factor are the following:

$$E = 8266{,}740 \cdot R = 68{,}73\ kJ \cdot mol^{-1} \qquad \textbf{(Eq.56A)}$$

$$A = \exp(-10{,}238) = 3{,}58 \cdot 10^{-5}\ hours \qquad \textbf{(Eq.56B)}$$

Leading to the thermal endurance plot (Figure 53):

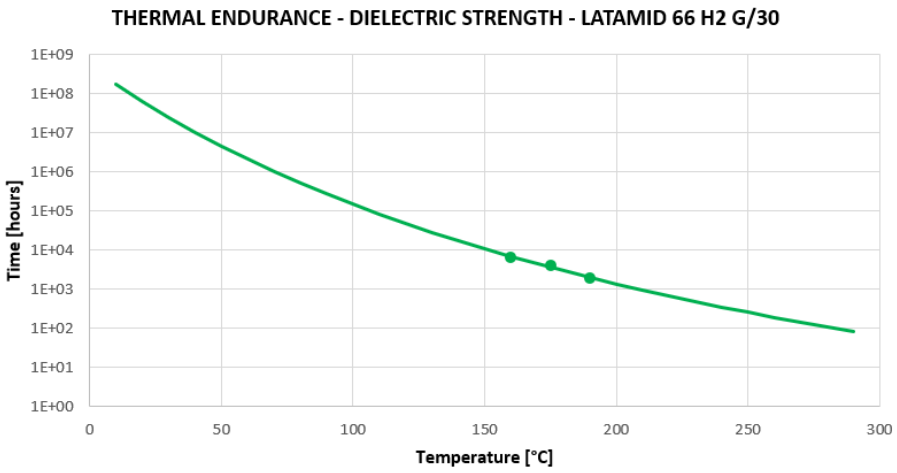

Figure 53 *Thermal endurance plot with dots representing the actual data in case of dielectric strength of Latamid 66 H2 G/30*

The temperature corresponding to the failure criterion was found to be equal to:

$$T = \frac{68{,}73 \cdot 10^3/R}{\ln(60000) + 10{,}238} = 116{,}05°\text{C} \qquad \textbf{(Eq.57)}$$

This value corresponds to an absolute thermal index equal to 115, way higher than those found in case of the other properties and 10 points greater than those corresponding to the values of the yellow cards. The dielectric strength of this insulating material is its prominent properties as it was found to be more resistant to thermal degradation.

4.1.4. **Thermogravimetric Analysis**

Starting from selected procedure, the following orders of reaction were computed in case of the programme performed in inert and reactive atmosphere:

$$n_{NITROGEN} = \frac{d\ln\frac{dC}{dt}}{d\ln(1-C)} = 1{,}169 \qquad \textbf{(Eq.58A)}$$

$$n_{AIR} = \frac{d\ln\frac{dC}{dt}}{d\ln(1-C)} = 1{,}131 \qquad \textbf{(Eq.58B)}$$

These values highlights an improvement in the analysis, which can now be most safely carried out in its most simple form, i.e. as though the order of reaction were equal to one.

Following the test method described in chapter 2, the temperatures corresponding to a mass loss equal to 5% were determined for each heating rate and both in case of inert and reactive environment:

HEATING RATE	N_2 ATMOSPHERE	SYNTHETIC AIR
10°C/min	366,26°C	400,5°C
7°C/min	361,2°C	394,25°C
5°C/min	353,91°C	386,28°C
2°C/min	327,95°C	371,17°C
1°C/min	321,26°C	363,11°C

Afterwards, by plotting the logarithm of the heating rate as a function of the reciprocal of temperature for this constant degree of conversion (Figure 54), it was possible to obtain a first estimated value of the activation energy by exploiting Eq.15. This was done

both for the values of temperature corresponding to the selected mass loss and those related to the peak of the mass loss derivative, used for the Kissinger's analysis.

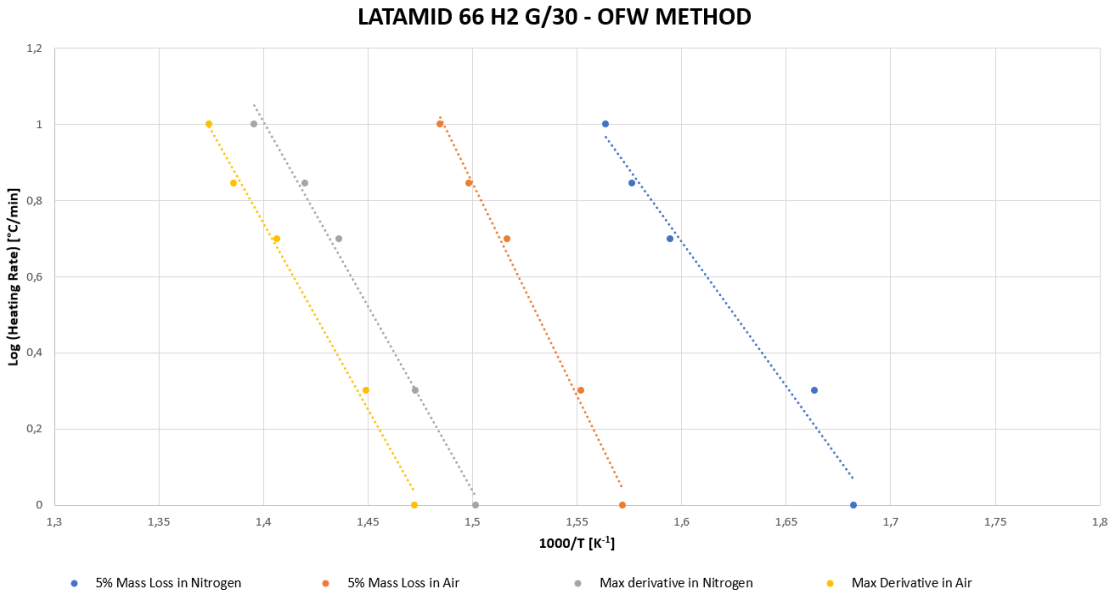

Figure 54 *Plot of the heating rate as a function of the reciprocal of temperature for a constant degree of conversion, used for the determination of the activation enegrgy according to Ozawa-Flynn-Wall method*

Subsequent iterations of the value of the coefficient b led to the determination of the following values for E and corrected R^2 at 5% mass loss:

ATMOSPHERE	ACTIVATION ENERGY	CORRECTED R^2
Nitrogen	137,98 kJ/mol	0,96869
Synthetic Air	203,28 kJ/mol	0,98924

Such values differ greatly even though the material is the same in both cases and only the surrounding environment changes. A different estimation of the activation energy was obtained by using Kissinger's equation (Eq.16) and the temperatures corresponding to the peak of the mass loss derivative:

ATMOSPHERE	ACTIVATION ENERGY	CORRECTED R^2
Nitrogen	174,60 kJ/mol	0,98623
Synthetic Air	175,10 kJ/mol	0,98718

As for the values of pre-exponential factors, given the fact that they are not actually required for the computation of the temperature index, they will only be reported as computed by means of Eq.17. No further comment about their magnitude will be

provided, even though the obtain values are consistent with examples found in literature.

ATMOSPHERE	5% MASS LOSS	MAX DERIVATIVE
Nitrogen	$2{,}41 \cdot 10^{11}\ min^{-1}$	$1{,}91 \cdot 10^{11}\ min^{-1}$
Synthetic Air	$1{,}29 \cdot 10^{16}\ min^{-1}$	$1{,}48 \cdot 10^{16}\ min^{-1}$

In order to use the obtained data to compute the temperature index by means of Eq.33, a reference temperature was selected as the one corresponding to a loss equal to a mass loss of 5% in case of the midpoint heating rate (5°C/min). This led to the determination of the following values:

ATMOSPHERE	5% MASS LOSS		MAX DERIVATIVE	
	TEMPERATURE	TI	TEMPERATURE	TI
Nitrogen	143,61°C	140	172,59°C	170
Synthetic Air	208,64°C	200	190,57°C	190

Nevertheless, apart from the first temperature index, these values are not comparable with any data found in literature, being considerably higher.

Given the dissimilar use of the Arrhenius equation in case of long-term aging and in case of thermogravimetry, exploited according to Eq.7A and not Eq.3A in the case of the latter, such a graph will not be presented. As a matter of fact, the plot of thermal endurance is believed to bear a higher significance (Figure 55):

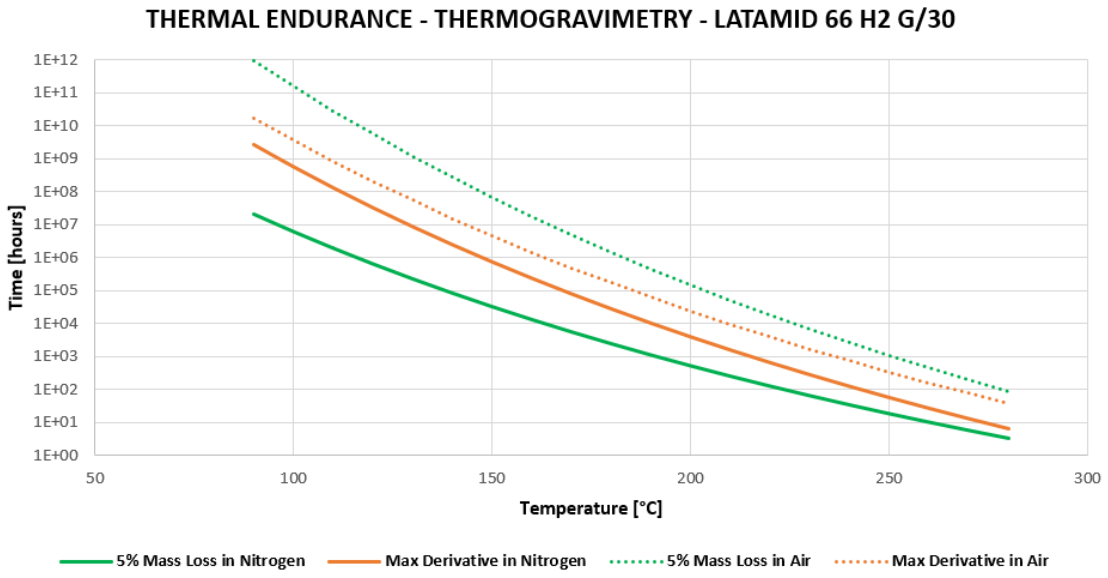

Figure 55 *Thermal endurance plot of Latamid 66 H2 G/30 obtained thanks to the data found by means of different runs of thermogravimetry*

4.2. Later 4 G/30

In the following paragraphs, the computation of thermal index in case of Later 4 G/30 will be carried out, starting from the data obtained by means of long-term aging to move on to those obtained by means of thermogravimetry.

4.2.1. Tensile Strength

The same procedure as for Latamid 66 H2 G/30 was performed, starting with the interpolation meant to obtain the times corresponding to a property loss equal to 50%, which led to:

TEMPERATURE	TIME TO FAILURE (1,5 mm)	TIME TO FAILURE (3 mm)
160°C	11104,10 hours	10620,47 hours
175°C	4422,83 hours	4160, 16 hours
190°C	1905,96 hours	2227,83 hours

Starting from these data, the determination of the Arrhenius plot (Figure 56) and of its corresponding equation was carried out:

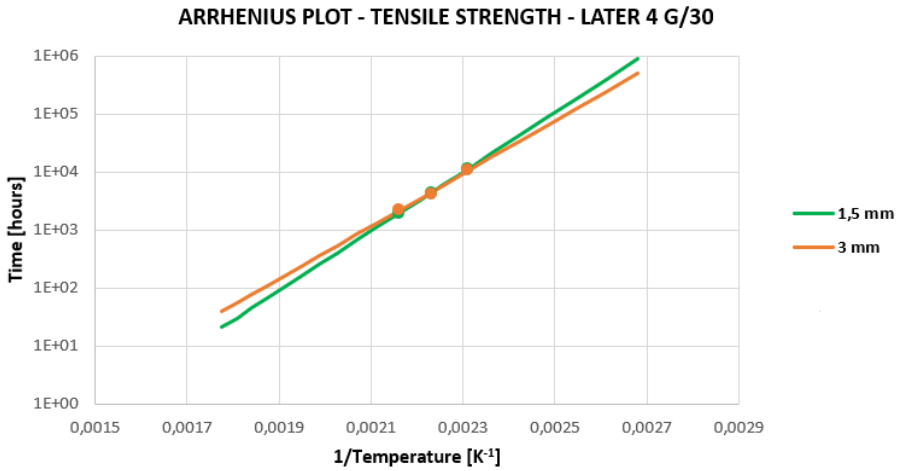

Figure 56 *Arrhenius plot of the time to failure as a function of the reciprocal of temperature, with dots representing the actual data in case of tensile strength of different thicknesses of Later 4 G/30*

Yielding:

1,5 mm $$\ln t = 11786{,}377 \cdot \frac{1}{T} - 17{,}899$$ **(Eq.59A)**

3 mm $$\ln t = 10463{,}655 \cdot \frac{1}{T} - 14{,}928$$ **(Eq.59B)**

Corrected correlation factors equal to 0,99991 in case of 1,5 mm thickness and to 0,99528 in case of 3 mm thickness were determined. The following values of activation energy E and pre-exponential factor A were computed:

1,5 mm $$E = 11786{,}377 \cdot R = 97{,}99\ kJ \cdot mol^{-1}$$ **(Eq.60A)**

$$A = \exp(-17{,}899) = 1{,}69 \cdot 10^{-8}\ hours$$ **(Eq.60B)**

3 mm $$E = 10463{,}655 \cdot R = 86{,}99\ kJ \cdot mol^{-1}$$ **(Eq.60C)**

$$A = \exp(-14{,}928) = 3{,}29 \cdot 10^{-7}\ hours$$ **(Eq.60D)**

In case of this material, the fitting and the computed data show how the thickness of the specimens has a clear impact on the performances of the material.

As for the thermal endurance, the following plot was determined (Figure 57):

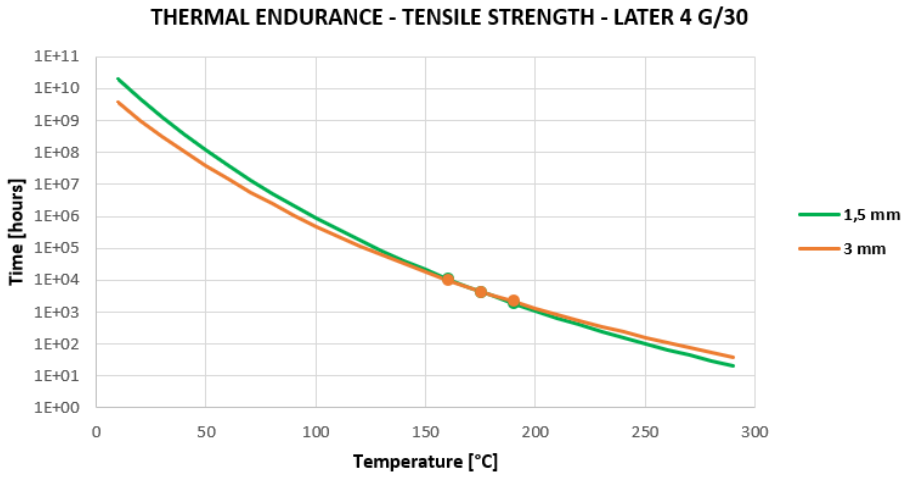

Figure 57 *Thermal endurance plot with dots representing the actual data in case of tensile strength of different thicknesses of Later 4 G/30*

Starting from the computed data, the temperature corresponding to a lifetime of $6 \cdot 10^4$ hours in case of tensile strength for Later 4 G/30 was found to be:

1,5 mm $$T = \frac{97{,}99 \cdot 10^3 / R}{\ln(60000) + 17{,}899} = 134{,}67°C$$ **(Eq.61A)**

3 mm $$T = \frac{86{,}99 \cdot 10^3 / R}{\ln(60000) + 14{,}928} = 130{,}38°C$$ **(Eq.61B)**

Notwithstanding the considerable difference in activation energy, the indices turned out to be both equal to 130 and not too far from the already presented ones, which may be due to the higher temperatures employed in this project.

4.2.2. **Charpy Impact Resistance**

By performing an interpolation, it was possible to estimate the time corresponding to a property value loss equal to 50% for all three aging temperatures:

TEMPERATURE	TIME TO FAILURE
160°C	3751,24 hours
175°C	1364,72 hours
190°C	445,39 hours

Hence, the corresponding Arrhenius plot (Figure 58) and its equation were determined:

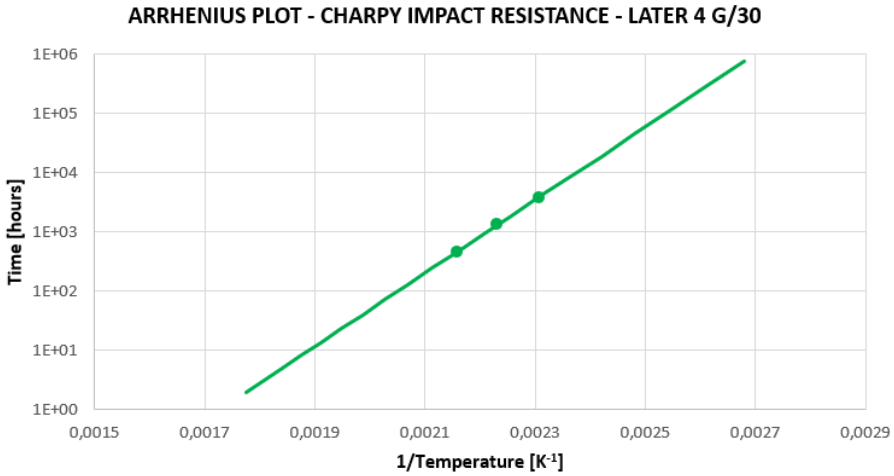

Figure 58 *Arrhenius plot of the time to failure as a function of the reciprocal of temperature, with dots representing the actual data in case of Charpy impact resistance of Later 4 G/30*

Yielding:

$$\ln t = 14235{,}981 \cdot \frac{1}{T} - 24{,}607 \qquad \textbf{(Eq.62)}$$

Whose corrected coefficient of correlation R^2 was found to be equal to 0,99525 after a statistical analysis. The latter was relatively higher than the one found in case of Latamid 66 H2 G/30, meaning that the results are slightly less dispersed. Regarding the activation energy and pre-exponential factor, the following values were found:

$$E = 9638{,}218 \cdot R = 118{,}36\ kJ \cdot mol^{-1} \qquad \textbf{(Eq.63A)}$$

$$A = \exp(-24{,}607) = 2{,}06 \cdot 10^{-11}\ hours \qquad \textbf{(Eq.63B)}$$

Finally, by means of all the acquired data regarding the Charpy impact resistance of Later 4 G/30, it was possible to build the thermal endurance plot (Figure 59):

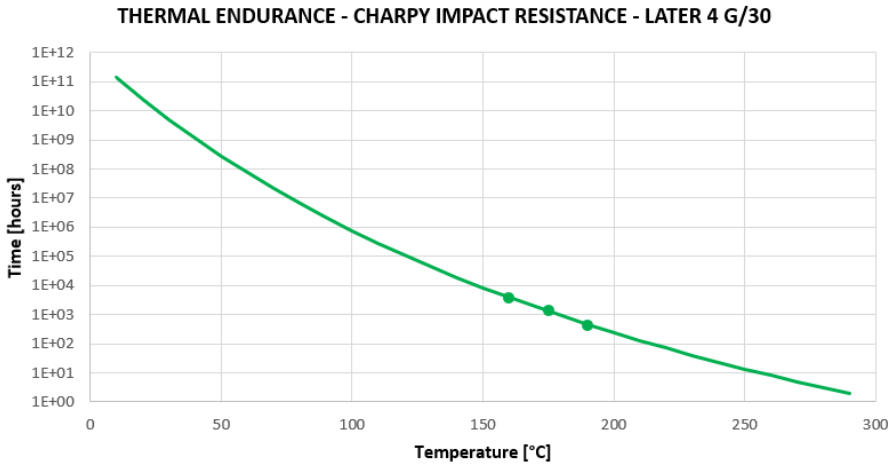

Figure 59 *Thermal endurance plot in case of Charpy impact resistance of Later 4 G/30*

Therefore, the temperature corresponding to a lifetime of $6 \cdot 10^4$ hours in case of Charpy impact resistance is computed as:

$$T = \frac{118{,}36 \cdot 10^3 \ /R}{\ln(60000) + 24{,}607} = 126{,}64°\text{C} \qquad \textbf{(Eq.64)}$$

Which corresponds to a thermal index equal to 125°C. As compared to the data expressed in chapter 2 and coming from a previous study, this value is only 5 points lower, making it compliant.

4.2.3. **Dielectric Strength**

Starting from the results obtained in the analysis performed in collaboration with the Electrical Engineering laboratories of *Università degli Studi di Genova*, it was not possible to determine the thermal endurance. As a matter of fact, the dielectric strength did not show any sign of decaying for the tested aging times. The only datum which could be obtained was that regarding the time to failure in case of the highest temperature, which was found to be equal to 3189,04 hours.

4.2.4. **Thermogravimetric Analysis**

The data obtained in the previous chapter were used for the computation of the temperature index abiding to both Eq.30 and Eq.34, even though the second one represents the most recent approximation, which will be presented and exploited for the plot of the thermal endurance. Once more, an Arrhenius plot was derived, even

though, in this case, it was developed starting from the value of activation energy and not with the objective to determine it, given the different methodology of this analysis. Furthermore, because of the differences between Eq.2A and Eq.3A, the pre-exponential factor derived by means of Eq.17 shall not be compared with that derived from long-term aging.

By using Eq.34, it was possible to obtain the following values of temperature index starting from the data obtained in the previous chapter. The values corresponding to the maximum derivative of mass loss were determined so as to have a comparison with the Kissinger method of standard thermogravimetry. Specifically, the following table summarizes what was found in case of inert environment and adds the rounding down which was typical of the thermal index:

RUN	5% MASS LOSS		MAX DERIVATIVE	
	TEMPERATURE	TI	TEMPERATURE	TI
1	103,43°C	100	87,24°C	85
2	123,69°C	120	99,58°C	95
3	111,42°C	110	95,58°C	95
4	117,9°C	115	116,27°C	115
5	95,98°C	95	101,25°C	100
6	107,98°C	105	88,7°C	85
AVERAGE	110,07°C	110	98,1°C	95
REL. ST. DEV.	9,68 %		11,09 %	

The following plot represents the trends in temperature index as computed in case of 5% mass loss and maximum derivative of the mass loss (Figure 60):

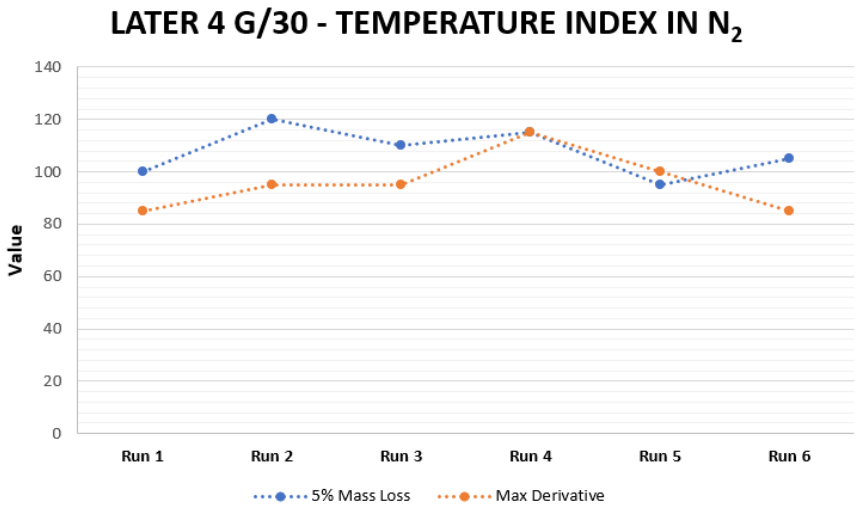

Figure 60 *Plot representing the trends of Temperature Index for Later 4 G/30 in inert environment*

It is important to stress out that different values are found for each run, making the process unsuitable, if not properly honed, for the determination of the temperature index in a single run. Furthermore, this plot clearly puts an emphasis on the fact that the data obtained in case of the maximum derivative of the mass loss generally predict a lower lifetime for the material.

As for the case of a reactive atmosphere, the following values of temperature index were obtained:

RUN	5% MASS LOSS		MAX DERIVATIVE	
	TEMPERATURE	TI	TEMPERATURE	TI
1	123,22°C	120	106,66°C	105
2	108,20°C	105	99,12°C	95
3	122,52°C	120	104,86°C	100
4	123,35°C	120	97,77°C	95
5	123,14°C	120	107,74°C	105
AVERAGE	120,14°C	120	103,23	100
REL. ST. DEV.	5,54 %		4,37 %	

Which can be visually represented as (Figure 61):

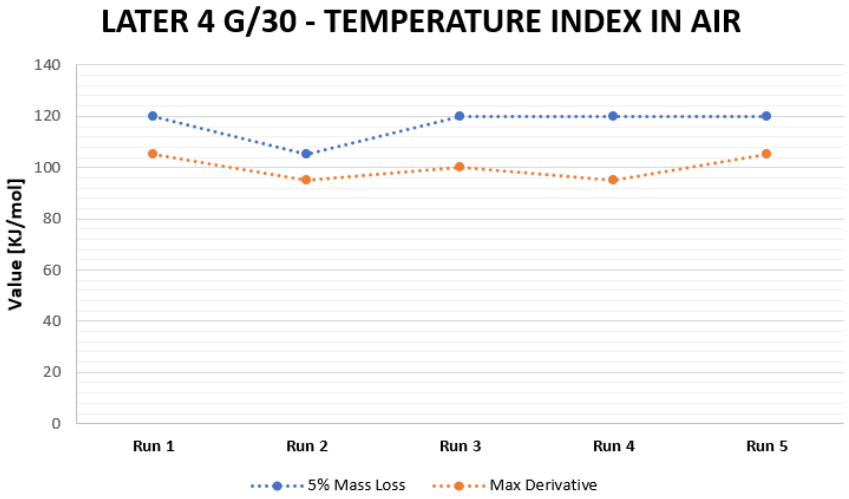

Figure 61 *Plot representing the trends of Temperature Index for Later 4 G/30 in inert environment*

These values show smaller dispersion if compared with those obtained in an inert atmosphere. A comparison between these activation energies and those obtained by means of long-term aging will be performed in the following chapter.

Lastly, as for the graphs representing the thermal endurance, obtained by using Eq.33, only one run in nitrogen will be shown, for the sake of brevity (Figure 62):

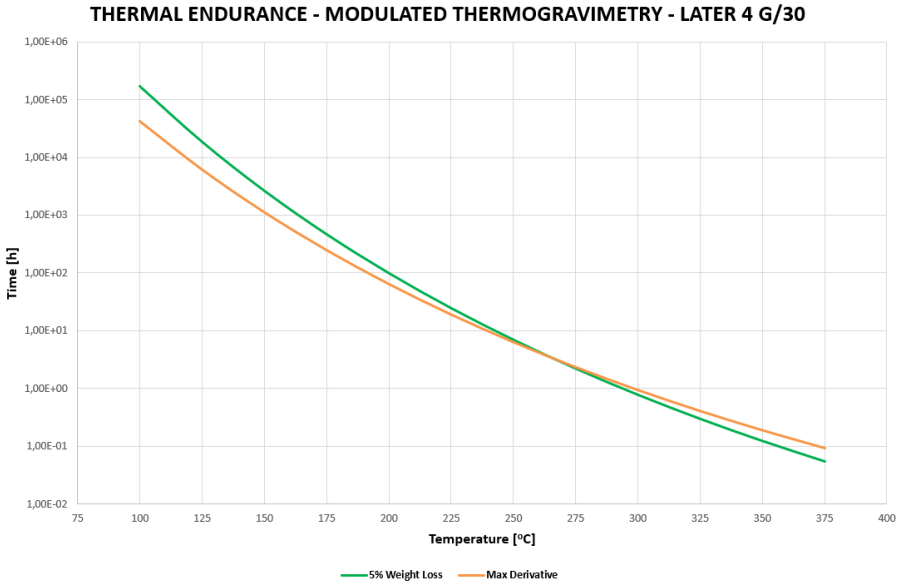

Figure 62 *Thermal endurance plot of run 3 of Later 4 G/30 in inert atmosphere, as obtained from modulated thermogravimetry*

CHAPTER FIVE
Discussion and Further Analyses

5. Chapter Content

This chapter will offer a comparison between the data of thermal and temperature index as well as some further analysis which was performed in order to investigate specific features which emerged from long-term aging.

5.1. Foreword

The main aim of this work was to determine whether a correlation between short-term and long-term aging could be established, so as to be able to obtain all the valuable data concerning decay of properties in a shorter time and with a lower expense. Nevertheless, it is necessary to start by making some observation regarding the employed procedures.

First of all, an analysis of Eq.3A and Eq.7A, which are the equations exploited for the derivations of the models, is mandatory, both in case of long-term and short-term procedures. The formula are reported here for clarity:

Long-term $$Lifetime = t = A \exp\left(-\frac{E}{RT}\right) \quad \textbf{(Eq.3A)}$$

Short-term $$\frac{dC}{dt} = Af(C) \exp\left(-\frac{E}{RT}\right) \quad \textbf{(Eq.7A)}$$

From these equations, it is clear that the activation energy is related to time in two different ways. As a matter of fact, by following the procedures described in the standard UL 746B for long-term aging in ovens, negative values of the activation energy would be obtained , since $\exp(-\mathrm{ax}^{-1})$ is a monotonically increasing function for each $a > 0$. Since $R > 0$, the activation energy is required to be negative. However, such a value was always presented as positive. The dissimilarity between the two methods is further highlighted when the lifetime is obtained from Eq.7A by rearranging Eq.33:

$$Lifetime = 10^{\frac{E}{2{,}303RT}+\log\left(\frac{E}{100{,}4\beta R}\right)-0{,}463\frac{E}{RT_f}} \propto A \exp\left(\frac{E}{RT}\right) \quad \textbf{(Eq.33)}$$

Which requires the activation energy to be positive. All of this is due to the fact that the Arrhenius equation was not exploited correctly as it should always be used to relate a rate constant to the reciprocal of temperature. In case of time, it would be safer to adopt a relationship similar to Eq.33, which can be obtained by taking the reciprocal of the

right side of Eq.3A. After this consideration, given the relationship between the unity of measurements of time and of rate constant, it can be assumed that it is possible to try to establish a relationship between the opposite of the activation energy obtained in long-term experiments and that found in case of short-term procedures.

Secondly, it is necessary to underline that the environment to which the materials are subject while aging in ovens is an oxidative atmosphere. Therefore, it is expected that thermogravimetric analysis performed in synthetic air should lead to comparable results, as the material should be subject to thermo-oxidative degradation as in ovens. For the sake of comparison, however, the short-term analysis was also carried out in an inert atmosphere, so as to be able to grasp any difference regarding the two methods.

From a general perspective, the two techniques are indeed completely different since short-term aging monitors the loss of weight in case of a heating ramp, while long-term aging studies the decay of properties for specimens held at constant temperature. Moreover, when studying how the various properties evolve in case of aging in ovens, different behaviours are to be expected for each one of the three and for each thickness. This could also lead to the need of using different aging temperatures according to the property under investigation. Lastly, the time of exposure is a significant factor as it affects which reaction may occur during the test. Therefore, the fact that comparable results can be obtained seemed highly unlikely at the beginning of this project.

5.2. Comparison of the Results

In the following table, the obtained results are presented, both in terms of activation energy and indices. Some results retrieved in literature will also be presented so as to have a comparison with other works.

Firstly, it is worth noting that the values of activation energy obtained in case of thermogravimetric analysis are usually higher than those coming from long-term aging. Nonetheless, this does not necessarily imply higher temperature index, since the computation pathway of such a quantity is different for short-term and long-term techniques. As a matter of fact, for the former the reference temperatures play a key role and can cause the index to vary greatly.

The obtained values in case of Latamid 66 H2 G/30 were the following:

LATAMID 66 H2 G/30			
DIELECTRIC STRENGHT	IMPACT RESISTANCE	TENSILE STRENGTH	THERMOGRAVIMETRY 5% MASS LOSS
68,730 kJ/mol	70,274 kJ/mol	57,24 kJ/mol (1,5 mm) 57,82 kJ/mol (3 mm)	137,99 kJ/mol (N_2) 203,28 kJ/mol (Air)

LATAMID 66 H2 G/30			
DIELECTRIC STRENGHT	IMPACT RESISTANCE	TENSILE STRENGTH	THERMOGRAVIMETRY 5% MASS LOSS
115	75	90 (1,5 mm) 90 (3 mm)	140 (N_2) 200 (Air)

Even though this values were lower than the yellow cards ones, although not tuned with respect to a reference material, it must be noted that the requirements of the standard UL 746B were not met, since the failure time corresponding to the lower and higher aging temperature were lower than 500 hours and 5000 hours. Such a result highlights the need to adopt different aging conditions even for the same material. Speaking with hindsight, a better choice would have been to exploit the temperature of 160°C as the highest one for the study of the dielectric strength, which, however, was unfeasible since only three ovens were available during this project. As far as the the literature values are concerned, Rammo and Mahdi provided a compendium collection of activation energies coming from thermogravimetric analysis of polyamide 6,6, derived according to different kinetic models. The obtained values are generally broadly dispersed, varying from 101 to 200 kJ/mol for a conversion of 5%, and vary according to the exploited technique. Even though the results of this analysis fall into the specified limits, such an extensive range does not bear great significance [41]. As a matter of fact, for the computation of the temperature index, another required parameter is the reference temperature, which greatly influences the final result.

As for Later 4 G/30, the following results were obtained:

LATER 4 G/30			
DIELECTRIC STRENGHT	IMPACT RESISTANCE	TENSILE STRENGTH	THERMOGRAVIMETRY 5% MASS LOSS
/	118,358 kJ/mol	97,99 kJ/mol (1,5 mm) 86,99 kJ/mol (3 mm)	109,49 kJ/mol (N_2) 123,01 kJ/mol (Air)

LATER 4 G/30			
DIELECTRIC STRENGHT	IMPACT RESISTANCE	TENSILE STRENGTH	THERMOGRAVIMETRY 5% MASS LOSS
/	100	130 (1,5 mm) 130 (3 mm)	110 (N_2) 120 (Air)

Once more, the determined times to failure in case of impact resistance do not meet the requirements imposed by UL 746B, although this only occurs in case of the lowest temperature. In order to obtain a more precise result, a set of four temperatures should have been chosen in case of this property, with the lowest one being lower than 160°C. A brief research showed that the activation energy of polybutylene terephthalate coming from thermogravimetric analysis are not greatly influenced by the atmosphere, generally displaying similar results for nitrogen and synthetic air. In particular, the most common values for a conversion of 5% fall in the range between 150 and 190 kJ/mol, which are slightly higher than those determined during this project [42][43].

As for the values of activation energy and temperature index derived by means of the Kissinger's procedures, these values were lower than the ones computed by means of the temperature corresponding to 5% mass loss in all cases. Such a behaviour should have been expected since they are relative to an advanced degradation state. Therefore, they won't be considered any further.

5.3. **Specimen Appearance and Viscosity**

A simple visual inspection can give a better idea of the differences between the oxidative behaviour of Latamid 66 H2 G/30 and Later 4 G/30 (Figure 63).

Figure 63 *Effect of oxidation after exposure to the temperature of 190°C for 1416 hours, both in case of Later 4 G/30 (left) and Latamid 66 H2 G/30 (right)*

Not only is the colour of the specimen affected in case of the former, but also the surface roughness is completely changed. Oxidation brings about a loss of smoothness and causes the polyamide specimen to look granulated and microcracked, with the rising of glass fibres to the surface, thus providing proof for the worse mechanical behaviour of Latamid 66 H2 G/30 with respect to Later 4 G/30. This behaviour is consistent with what suggested by Wagner [19], who described the transition from white to yellow to black as a reaction between amino and carbonyl groups. Specifically, it has been found that the main route of thermal degradation of this polyamide is the elimination of the main organic product cyclopentanone and also some hydrocarbons, nitriles and vinyl groups [41]. Moreover, glass fibres tend to rise to the surface during degradation of the polyamide, while this phenomenon does not occur in case of polybutylene terephthalate, whose surface remains smooth.

A simple analysis of the evolution of the viscosity number of Latamid 66 H2 G/30 highlighted a progressive reduction. This can be directly linked to a decrease in molecular weight, which is due to the degradation of the molecular chains in a thermo-oxidative atmosphere, as one would imagine. However, for short times, an increase can be pointed out and this can be associated to a sort of annealing with polycondensation at the solid state. Nevertheless, such a behaviour did not affect the properties of the material. The trend of the values of viscosity number as obtained after aging at 190°C can be seen below:

Time [h]	Value [mL/g]
1	145,95
360	158,37
888	90,15
1200	57,09

The starting values states that the studied polyamide belongs to the class of medium-viscosity polyamides, which ranges from a viscosity value of 140 to a value of 155.

As for LATER 4 G/30, melt flow index measures were carried out to obtain an estimation of its viscosity. Specifically, the average values computed for a virgin specimen and one which underwent aging at 190°C after 360 hours were the following:

Virgin	Aged
30,4	8,3

Such a reduction could be linked to a significant increase in viscosity and thus molecular weight. In order to establish the real behaviour of the material, a similar procedure was carried out for the unfilled material, therefore not loaded with fibres. As a matter of fact, an interaction with the fibres could lead to chain extension and crosslinking because of the intrinsic reactivity of primer and surfactants. The following average MFI's were determined over a series of experiments:

Virgin	Aged
50,4	26

The ratio between these values is 1,94, while in case of the filled material it corresponded to 3,66. Therefore, it can be assumed that such a behaviour is partly due to the reactivity of the fibres and partly to the material itself, maybe because of a phenomenon of polycondensation at the solid state as reported in [44], a process which occurs in case of annealing at temperatures slightly lower than the melting. A better examination of this behaviour will be provided in the following paragraphs.

5.4. Evolution of Crystallinity

Generally speaking, the differences between the values of activation energy and thermal indexes computed in case of dielectric strength, Charpy impact resistance and tensile strength is not puzzling at all, since it is legitimate to assume that oxidation due to continuous exposure to a reactive environment at elevated temperatures may affect each property differently. A simple explanation to this behaviour can be given by considering that oxidation mainly affect the surface of the specimen, at least in the beginning. Consequently, depending on the role played by the surface in the determination of a specific property, the values may vary. For instance, in case of impact resistance, a broader area of the specimen is interested and any defect or weak zone of the outermost layers of material may cause cracks to start to propagate more easily and in a quicker way. Such a behaviour can also be explained by taking into account an increase of the crystallinity of the specimen, leading to a more brittle behaviour, but also to an increase in other properties such as the tensile strength.

An evaluation of such phenomenon was performed by means of differential scanning calorimetry of a specimen after aging in oven at a fixed temperature of 190°C.

Each run was performed at a heating rate equal to 1°C/min. This was possible by exploiting Eq.36, which considers the heat released during fusion of the crystals, for different aging times. The following plot (Figure 64) was obtained for the initial stages of aging and it shows that the trend of the experimental data can be described by means of logarithmic curves, thus highlighting how the rate of increase of crystallinity decreases over time.

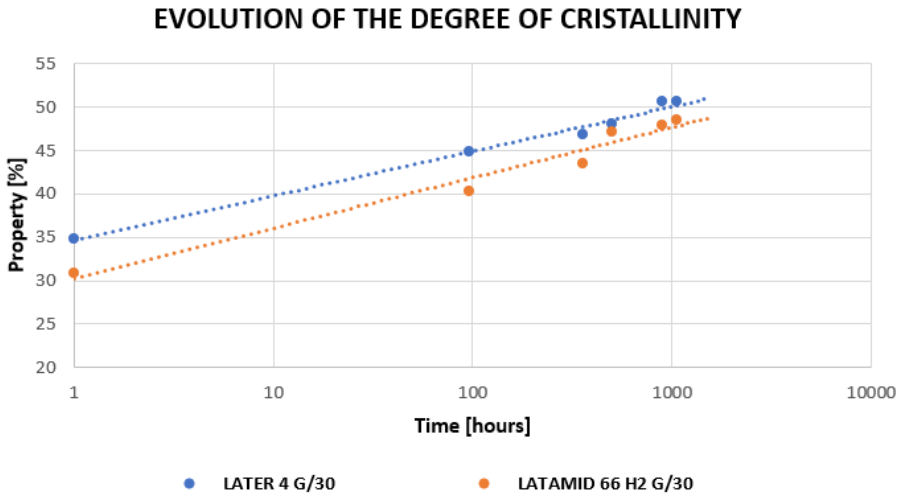

Figure 64 *Graphical representation of the increase of crystallinity over aging at 190°C, as computed from the enthalpy of fusion*

By examining the DSC plots more carefully, the insurgence of a second peak over aging time can be noticed (Figure 65) in case of Later 4 G/30:

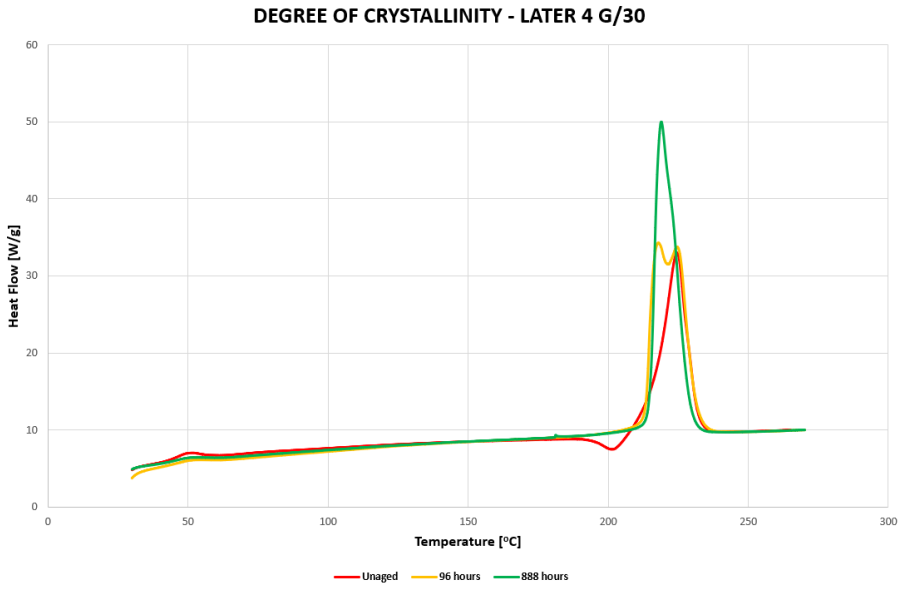

Figure 65 *Differential Scanning Calorimetry performed on Later 4 G/30 at different aging times*

A change of the peaks in the melting curve can be observed with different ageing times, both in terms of peak temperatures and number of maxima. A literature analysis revealed the existence of a complex fusion behaviour [45][46] and of two crystalline phases (α and β) for this material, a coarser one (β), which is dominant in case of materials coming from injection moulding and subject to stretching, and a more refined one (α), which can be obtained by tempering [44]. It is safe to assume that the initial crystalline structure, coming from injection moulding, where cooling is very quick, corresponds to the coarse one. Due to exposure to high temperatures, an initial annealing is favoured, thus leading to a progressive transition between the two phases. This kind of heat treatment causes an increase of degree of crystallinity, which can be reflected by a rise in strength and hardening over time and by an embrittlement in the later period of ageing [47]. As for the exothermic drop in heat of fusion which can be observed in case of the unaged specimen, it is to be attributed to variations in spherulitic morphology after primary crystallization [48].

As for Latamid 66 H2 G/30, a similar but more complex behaviour was highlighted (Figure 66):

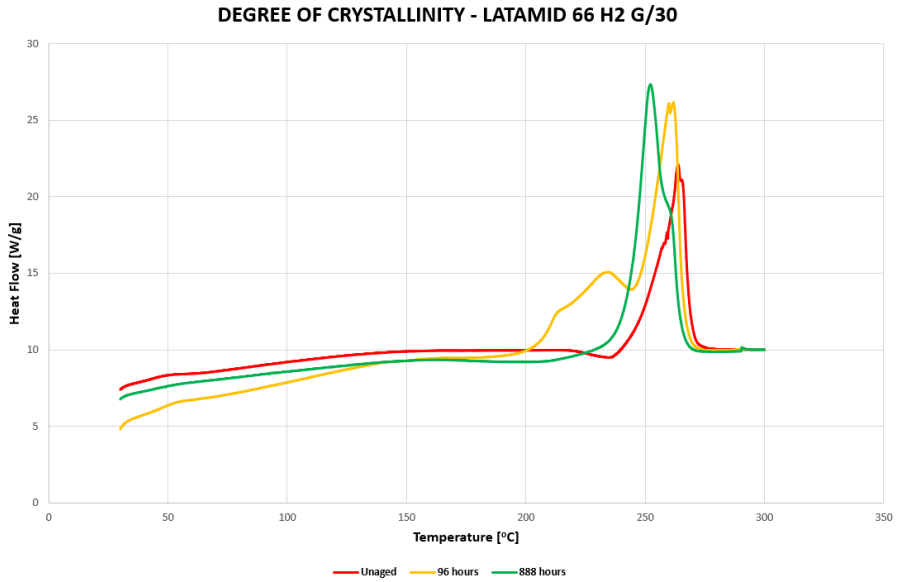

Figure 66 *Differential Scanning Calorimetry performed on Latamid 66 H2 G/30 at different aging times*

Such a result can be ascribed to similar causes since polyamide 6,6 is known to have more than one crystalline phase and a transition between them is to be expected upon aging. Nevertheless, no further analysis was carried out for this material as the main focus of the analysis was to determine an increase in crystallinity alone.

Once more, for both material, unfilled grades were also examined. The resulting curves, which will not be displayed, were mostly equal to the already-presented ones, the only difference being the lower initial degree of crystallinity. This can be explained by considering that the fibres can act as nucleating agents.

To conclude, the combination of thermal oxidation and the increase of crystallinity explains the reduced impact behaviour of both materials. For longer aging times, the differential scanning calorimetry curves of both materials showed earlier melting temperatures and a separation of the peaks, which can be ascribed to the fusion of lower molecular weight products, a symptom of thermal degradation.

5.5. Latamid 66 H2 G/30

5.5.1. Modulated Thermogravimetry

The first observation in case of Latamid 66 H2 G/30 is that this material did not show a simple degradative path, but three peaks were highlighted in its derivative. This complex behaviour was attributed to some specific additive, since no similar cases were found in literature. In order to confirm this supposition, the additive, namely Irganox® 1098, a sterically hindered phenol, was subject to a modulated thermogravimetric analysis to emphasize the features of its decay. The following plot (Figure 67) shows a comparison between the two mass loss derivatives:

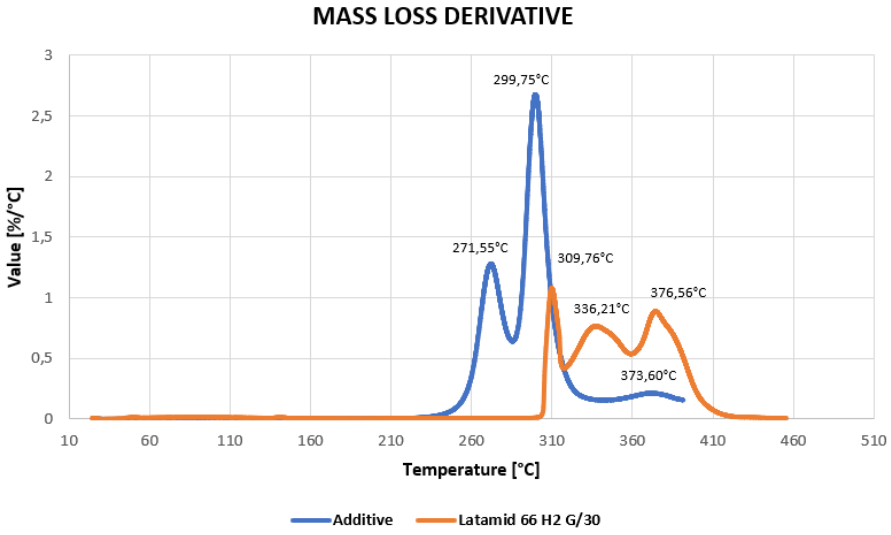

Figure 67 *Mass loss derivative plot in case of a modulated thermograimetry of Latamid 66 H2 G/30 and the additive Irganox® 1908*

In spite of the shift between the two curves which can be due to the specimen, being a powder in case of the additive and therefore prone to quicker degradation, it can be noticed that the temperature corresponding to the ignition of the decomposition of the additive is close to that of the start of the degradation of the polymer. This comes directly from the nature of anti-oxidant of the additive. Therefore, it could be reasonably supposed that the peaks can be related and that the additive is the main reason why a modulated approach cannot be exploited for the computation of the temperature index.

5.5.2. **Standard Thermogravimetry**

By comparing the activation energies and the thermal and temperature indices in case of Latamid 66 H2 G/30, it is evident that the two procedures do not give compliant results. Specifically, the results coming from the thermogravimetric analysis are way too high even when compared with the ones available in yellow cards. Nevertheless, this can be ascribed to the method of analysis. As a matter of fact, modulated thermogravimetry was not applicable due to the presence of simultaneous side reactions which undermined the thermal degradation of the material itself, making it not suitable for the analysis dictated by the standards. As for the substitutive technique which was developed using the Flynn-Ozawa-Wall method, the results in terms of order of reaction suggested that the complete method could be applied (reaction of the first order). However, by comparing a standard thermogravimetric run and the newly employed one, a shift toward the right could be evidenced (Figure 68):

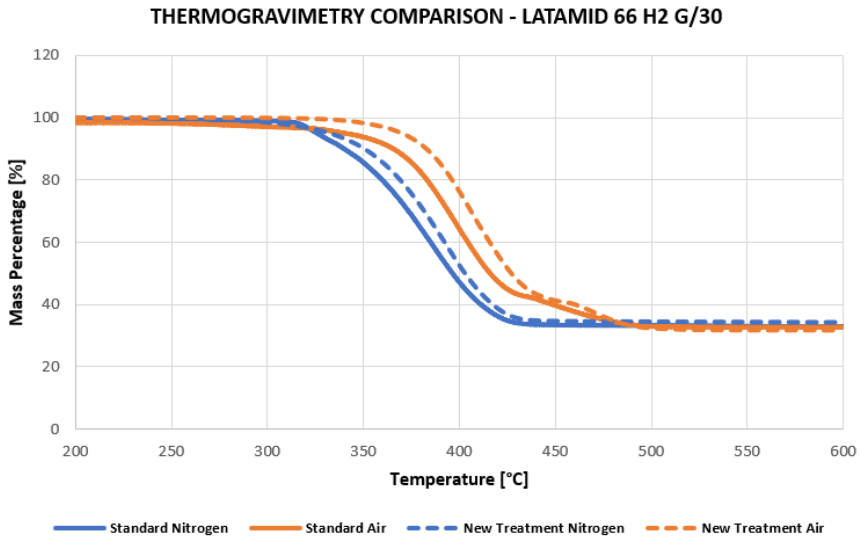

Figure 68 *Comparative plot of the differences between the standard and the adopted thermogravimetric programme*

Firstly, it is possible to notice a shift toward the right of the runs performed in air with respect to those performed in nitrogen, a feature which can be associated to the action of the additive as described above. However, this fact alone would not be a hindrance toward the computation of the thermal index, as it is a characteristic of the material itself. The real issue comes from the isothermal programme of the new procedure, which, despite making the degradation follow a first-order kinetics, causes a further shift to the right equal to approximately 20°C in case of reactive environment. Moreover, the translation between the run performed in nitrogen and that in air is further enhanced by this.

5.5.3. **Temperature Shift**

The main issue about the shifting of the curve toward the right is the need of a reference temperature in the computation of the temperature index (Eq.34). As a matter of fact, by making the numerical computation in Eq.34, it is possible to establish the influence of the reference temperature with respect to the activation energy:

$$TI = \frac{E}{194{,}857 - \frac{19{,}147 \cdot \ln(E)}{\ln(10)} + 1{,}066 \cdot \frac{E}{T_f}} \qquad \textbf{(Eq.65)}$$

In order to compare how the two variables influence the thermal index, it is required to take partial derivative. Nevertheless, this approach does not consider that a relationship between the reference temperature and the activation energy exists, the former being the temperature corresponding to 5% mass loss for the medium heating rate. It is assumed that a variation of the former would not affect the latter greatly, which could find an evidence by examining a common activation energy plot obtained from modulated thermogravimetry in air (Figure 45). This shows that the variation in activation energy is generally not significant along the temperatures were degradation occurs. Nevertheless, the relationship between this datum and reference temperature cannot be quantified easily, as it comes from a complex kinetic analysis, the following results can be considered indicative of the dependence of the thermal index on the two variables.

$$\left(\frac{\partial TI}{\partial E}\right)_{T_f} = \frac{T_f^2 \cdot (178{,}793 - 7{,}318 \cdot \ln(E))}{\left(E + 182{,}793 \cdot T_f - 7{,}801 \cdot T_f \cdot \ln(E)\right)^2} \qquad \textbf{(Eq.66A)}$$

$$\left(\frac{\partial TI}{\partial T_f}\right)_E = \frac{0{,}938 \cdot E^2}{\left(E + 182{,}793 \cdot T_f - 7{,}801 \cdot T_f \cdot \ln(E)\right)^2} \qquad \textbf{(Eq.66B)}$$

The following image (Figure 69) shows a depiction of the function and its derivative in the range of energies from $1 \cdot 10^2$ kJ/mol to $2 \cdot 10^2$ kJ/mol and temperatures from 600 K to 700 K, which is assumed to be representative of this study.

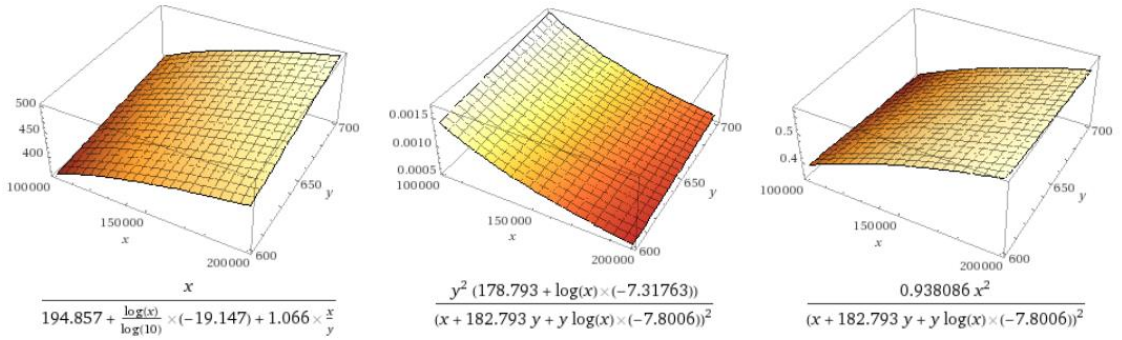

Figure 69 *Plot of the function of thermal index, its partial derivative with respect to activation energy (x) and its partial derivative with respect to the reference temperature (y) , respectively*

By examining the values on the vertical axis in case of the two derivatives, a correspondence between a variation of activation energy and reference temperature can be estimated. As a matter of fact, by considering the other variable as constant, the effect of a shift of 1 K in temperature can be associated to a variation of activation energy equal to approximately 350 J/mol. Furthermore, the first plot highlights the effect of a variation of the reference temperature on the temperature index itself.

Therefore, despite meeting all the requirements in terms of smoothness of the curve a first-order reaction, such a procedure doesn't offer a correct analysis of the material and should not be exploited. Nor is further tuning of this technique an interesting field of research, since it is complex to determine which shall be the optimum and correct solution from the point of view of the results.

In case of LATAMID 66 H2 G/30, this analysis led to the conclusion that the proposed techniques were not suitable. As a matter of fact:

- The modulated thermogravimetry gave a complex degradative pathway which calls for a more complex analysis, thus requiring a different approach;
- A standard multiple-run thermogravimetry showed the same issue as the modulated one;

- The proposed multiple-run analysis, comprising the isotherm at 300°C, caused a shifting of the curves towards the right, thus making resulting unsuitable for a correct computation of the kinetic parameters.

The reasons for such a behaviour of the material were examined firstly by visual inspection and then by studying the available literature. In order to proceed with the former, a standard thermogravimetric analysis was stopped before reaching 300°C and the specimen was removed from the furnace. The following photograph (Figure 70) shows a comparison between the unaged specimen and the extracted one:

Figure 70 *Comparison between an unaged Latamid 66 H2 G/30 sample and one subject to a heat ramp up to 300°C in a thermogravimetric furnace*

This revealed the creation of an oxidized shell along with a swelling of the sample. The latter can be ascribed to an imperfect drying of the specimen prior to the thermogravimetric analysis, while the former is a symptom of the tendency of polyamide to quickly oxidize.

Gijsman et al. suggest that oxygen permeation can affect the spatially dependent degradation rate of polymers, which is the case when the oxygen consumption rate is higher than its permeation rate, resulting in the so-called diffusion-limited oxidation (DLO) conditions. The oxidation will therefore be heterogeneous and an oxidation profile over the material thickness will develop, being more relevant the thicker the specimen. The effect of temperature was also measured and permeation profiles were obtained. These showed that the core of the sample is only affected by permeation to a lower extent, as the outer layer act as a sort of barrier [49].

This reasoning explains the shift of the degradation curve towards the right during non-isothermal analysis, since the bulk of the specimen is preserved for longer time [19]. Such a behaviour could have been avoided by using a powder, whose surface area to volume ratio is higher. However, given the lack of proper grinding machines during this project, it was unfeasible to follow such a path.

5.6. Later 4 G/30

5.6.1. Analysis of the results

As for Later 4 G/30, the values of thermal and temperature index are closer and the procedures may be considered equivalent, at least in terms of mere numbers. On the contrary, the computed activation energies show a greater variability. As a matter of fact, the value coming from thermogravimetric analysis in air is almost equal to that derived from the decay of the dielectric strength, while the other are substantially lower. Nevertheless, it is important to notice that the requirements imposed by UL 746B in terms of aging time for the lowest temperature were not met in case of this property. It is essential to remember that the difference in activation energy is not related to a difference in thermal and temperature index since the computations are significantly different.

As it can be noticed from Figure 44, Later 4 G/30 shows a different behaviour from that of Latamid 66 H2 G/30 under thermogravimetric analysis. As a matter of fact, there is no shift between the curve obtained in air and nitrogen and the effect of carbonization is greatly reduced. This stems from the fact that this material was not compounded with Irganox® 1098 and, therefore, is not subject to the formation of a sort of protective shell.

Moreover, for the sake of comparison, a non-modulated analysis of Later 4 G/30 was carried out. This was done in order to check whether the results stemming from a modulation procedure and a multi-run one could be considered equivalent. A procedure compliant with ASTM E1641 was exploited by using the usual heating rates, that is to say 10°C/min, 7°C/min, 5°C/min, 2°C/min, 1°C/min. A comparison between the runs in inert and reactive atmosphere at 1°C/min is provided below (Figure 71):

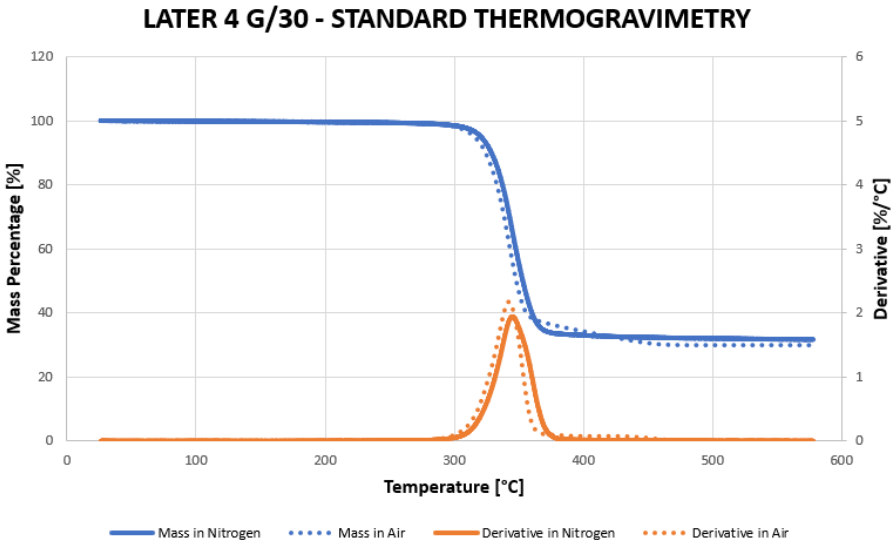

Figure 71 *Plot of a standard thermogravimetric run performed on Later 4 G/30 at a rate of 1°C/min, both in nitrogen and air, showing the percentage mass loss and its derivative*

As compared to Figure 44, this plot shows a small shift towards the right due to the absence of modulation and a less steep transition between the two plateaux. A procedure similar to that described in the previous chapters was adopted and the following results were obtained in terms of activation energy and temperature index:

ATMOSPHERE	ACTIVATION ENERGY	TEMPERATURE INDEX	CORRECTED R^2
Nitrogen	118,38 kJ/mol	120	0,99317
Synthetic Air	148,73 kJ/mol	140	0,99873

In accordance with what stated above, these values are higher than the respective ones obtained by means of modulated thermogravimetry. Specifically, the temperature index obtained in case of reactive atmosphere is equal to the datum derived from the yellow cards in chapter 2, both for dielectric and tensile strength. Nonetheless, it is still higher than the values obtained during this project by means of long-term analysis (100 and 130 for impact resistance and tensile strength, respectively).

In order to evaluate whether the results coming from short-term procedures and long-term ones are in good accordance, a comparison of the plots of thermal endurance will now be presented. As a matter of fact, such a graph portrays the predicted lifetime of the material over a broad range of temperatures, thus being not limited to a single value of time and its related temperature. The following plots compare the thermal endurance coming from modulated and standard thermogravimetry with that computed from the decay of tensile strength. Specifically,

the values computed for the 1,5 mm thick specimens were used, since the samples for all thermogravimetric analyses were taken from them. For the same of comparison, both atmospheres were studied.

In case of reactive environment, which should be more representative of the oven conditions, the following plot was obtained (Figure 72):

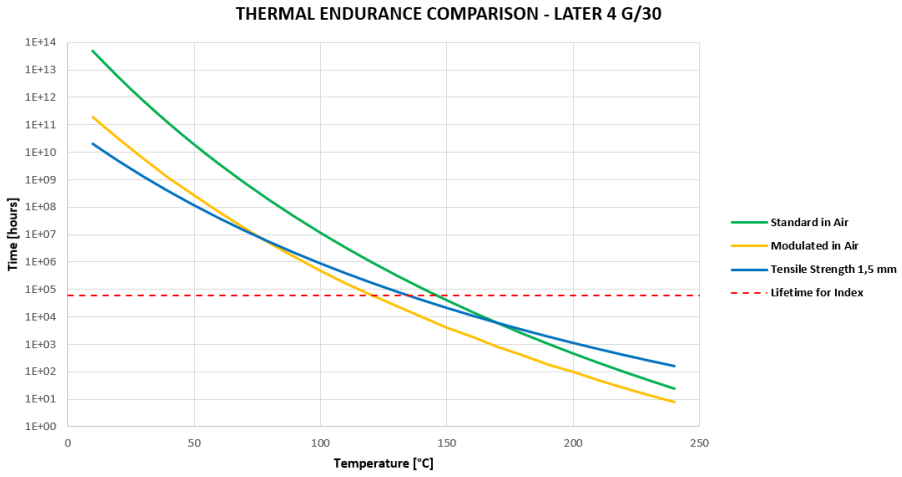

Figure 72 *Comparative plot of thermal endurances from modulated thermogravimetry and long-term aging for the tensile strength*

While for the inert one (Figure 73):

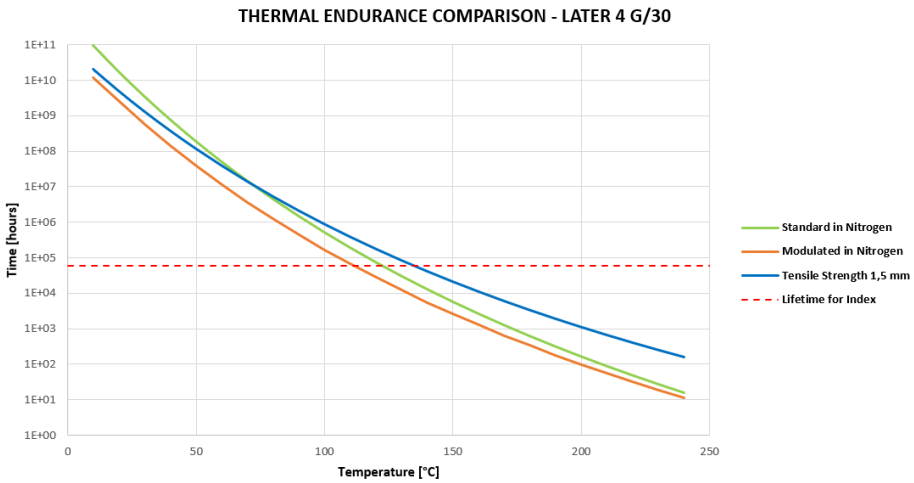

Figure 73 *Comparative plot of thermal endurances from standard thermogravimetry and long-term aging for the tensile strength*

It is clear from these plots that none of the method of analysis offers a good approximation across every range of temperature. The worst one corresponds to the standard thermogravimetry performed in air, while the more conservative one is represented by the modulated analysis in nitrogen. Compared to the thermal endurance

derived from long-term aging, the other two plots are conservative only after 75°C approximately. From this point of view, it would be safe to consider them as acceptable approximations, especially the modulated thermogravimetry in air, for the sake of this project.

5.6.2. **Evolution of the Viscosity**

By examining the results of the melt index analysis and by inspecting Figure 38, an increase of viscosity can be identified in correspondence with an improvement of the tensile performance of Later 4 G/30. An interpretation of such a behaviour could be given by considering an increase of the molecular weight in the material. As a matter of fact, such a phenomenon is known to be linked to a rise in tensile strength, as described in [50][51]. Moreover, as already described, an increase of crystallinity was also evidenced and this can be linked to the evident higher stiffness of the material in those stages of aging. Therefore, it seems legitimate to assume that the interaction of these factors led to an improvement of the tensile behaviour of this material, which was also less influenced by thermal oxidation and therefore premature degradation. All in all, aging in ovens can be interpreted as an annealing process at its initial stages.

In order to confirm the increase of molecular weight, a rheological analysis was performed with a parallel-plates setup, thus allowing a measure of the viscosity at different strain rates (or frequencies). As a matter of fact, a relationship between zero-shear viscosity and molecular weight exists, as pointed out in chapter 2. Higher molecular weights would cause a higher plateau viscosity and an earlier transition from Newtonian to non-Newtonian behaviour [52]. The following table shows the extrapolated values of zero-shear viscosity for the case of aging at 190°C at various times:

Time [hours]	η_0 [Pa*s]	η_0 Ratio	Trans Freq [s^{-1}]
0	370,50	1	15,62
96	3601,56	9,72	8,59
360	3626,57	9,79	9,24
720	1062,66	2,87	11,56
1056	601,99	1,62	12,42
1416	316,42	0,85	18,39

A relevant increase in viscosity alongside a shifting of the transition frequency towards the left can be spotted, being a symptom of an increase of molecular weight.

Besides, the case of the same base polymer, but unfilled, was examined, so as to have a comparison:

Time [hours]	η_0 [Pa*s]	η_0 Ratio	Trans Freq [s^{-1}]
0	127,56	1	47,38
168	303,13	2,38	33,51
336	179,25	1,41	39,56
672	89,48	0,70	46,36
840	61,54	0,48	65,72

A similar behaviour to that presented before is highlighted, both in terms of viscosity and transition frequency. Nonetheless, the variation is greatly reduced, which is an indication of the extent of the effect of the fibres on such a process. A display of the rheological curves that were obtained is shown below in case of the filled grade (Figure 74):

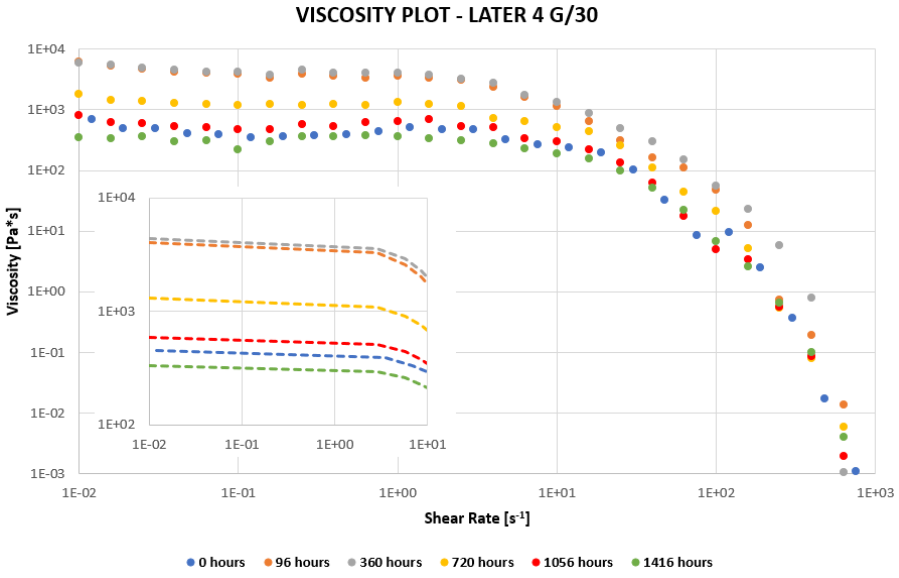

Figure 74 *Plot representing the evolution of the viscosity of Later 4 G/30 upon aging in ovens, with zooming of the extrapolations at early frequencies*

This analysis is meant to underline that holding the material at high temperature for long times brought about an initial increase of molecular weight, which is due to a process of polycondensation at the solid state along with one driven by the interactions with the fibre, which the provider of the glass fibres confirmed as possible.

In order to check whether a crosslinking of the material or a mere phenomenon of chain-extension had occurred, a sample of Later 4 was dissolved in a solution 0.005 g/ml phenol/1.2-dicholoro benzene (1:1) after aging. The solution was then filtered in order to separate the dissolved fraction from the undissolved one, since the latter was believed to comprise any possible crosslinked residue. Nevertheless, a thermogravimetric analysis of this deposit showed no trace of organic fraction if not for residues of the filter. All of the measured mass was attributed to glass fibres. Such a simple analysis cannot be held as a proof of the fact that no crosslinking had occurred and a more detailed one should be carried out to check on that.

CHAPTER SIX
Conclusions

Nowadays, polymers and composite materials have widespread applications in everyday life because of their versatility, cost-effectiveness and tailored production. However, their properties and characteristics show a strong dependence on time and temperature and a prediction of the durability of these materials is of the uttermost importance in the industrial sector. The usually-employed techniques of analysis require a strict monitoring of their behaviour over prolonged periods of aging at different temperatures, in order to determine the activation energy of the degradative process and a quantity called thermal index itself. This value expresses the maximum temperature at which a specific material can retain its mechanical or electric properties for a set lifetime, generally $6 \cdot 10^5$ or $1 \cdot 10^6$ hours. The computation of this quantity is both time and money consuming as it exploits isothermal programmes at elevated temperatures which could last up to years.

Therefore, to shorten the times and costs of such a process, a short-term analytical method comprises various thermogravimetric analyses was studied as an alternative way to predict the durability of polymeric materials, in accordance with ASTM standards. A comparison between these accelerated methods was performed for two different composite materials, namely a polyamide 6,6 (Latamid 66 H2 G/30) and a polybutylene terephthalate (Later 4 G/30) with 30%w glass fibres.

The results of long-term aging in oven evidenced a general reduction of molecular weight due to thermo-oxidative degradation. Nevertheless, in its early stages, this treatment also resulted in an annealing of the second material, whose tensile properties considerably improved. This phenomenon was associated to an increase of crystallinity and molecular weight due to the interaction with fibres at elevated temperatures, but a similar effect was not spotted in the other material. Furthermore, it was noted that the obtained values of time to failure did not meet the requirements of UL 746B in case of Charpy impact resistance. Speaking with hindsight, a separate range of lower temperatures should have been chosen for the monitoring of this property.

On the other hand, the thermogravimetric analysis proved to be unsuitable for the polyamide due to the presence of a specific additive, namely an antioxidant. As a matter of fact, it brought about the creation of an oxidized shell which hindered the penetration of oxygen in the bulk of the material, thus causing a delay in the degradation. Such a behaviour was noticed both in case of modulated and standard

thermogravimetry and implied the impossibility to adopt this technique for a simple computation of the thermal index of this material. A novel technique was developed by exploiting an isothermal programme at 300°C to cancel the contribution of the additive. However, this caused the degradative curve to shift to the right, thus making the computation inaccurate. The usage of fine granulated powders instead of small pieces of material would have been a better choice to prevent this behaviour. Conversely, this issue was not registered in case of polybutylene terephthalate, whose kinetics of degradation were of the first-order. Therefore, it can be assumed that by using an unfilled material, free of anti-oxidant additives, results in accordance with those coming from long-term aging could have probably been obtained also in case of polyamide 6,6.

A direct comparison between the two techniques was not possible for Latamid 66 H2 G/30, but could be performed in case of Later 4 G/30. The results showed reasonable agreement in terms of thermal index, but the activation energy for the degradative process showed significant differences, thus resulting in dissimilar curves of thermal endurance. This is thought to be due to the intrinsically different processes being monitored, namely the loss of mechanical or electric properties due to isothermal programmes and the loss of mass due to a heating ramp. The plots of thermal endurance can be used to provide a better comparison between the techniques than the thermal index alone, since they predict the lifetime of the material over a broader range of temperatures.

The conclusion of this work is that short-term analytical methods implying the usage of thermogravimetry can't substitute long-term aging in the prediction of the durability of all kinds of material, even though this technique can be safely exploited in case of substances with a simple kinetics of degradation. However, it is important to underline that this procedure should not replace long-term aging until a real connection has been established between these two predictive techniques and they have been proven to provide equal results.

Since the use of short-term analytical methods for the computation of the thermal index is still in its embryonic stages of development, the room for further development is huge. First of all, the relationship between short-term and long-term techniques shall be sought after in case of simple polymeric materials, i.e. ones which are not compounded with additives which may consistently alter the thermo-

degradative behaviour. Only if case such a connection should be determined shall this technique be exploited for any material. Furthermore, for the sake of saving money and time while studying the lifetime of polymeric materials at different temperatures, it could be possible to develop mixed techniques, which combine the activation energy derived from thermogravimetric analysis with the time to failure derived from aging at a specific temperature.

References

[1] S. Turri, "Additives and modification of polymers Introduction to the concept of polymer formulation," *Lect. Notes at Politecnico di Milano*, pp. 0–81, 2017.

[2] M. Nedjar, "Investigation in thermal endurance of polyesterimide used in electrical machines," *J. Appl. Polym. Sci.*, vol. 121, no. 5, pp. 2886–2892, Sep. 2011.

[3] R. Polanský, P. Prosr, and M. Čermák, "Determination of the thermal endurance of PCB FR4 epoxy laminates via thermal analyses," *Polym. Degrad. Stab.*, vol. 105, no. 1, pp. 107–115, Jul. 2014.

[4] A. Joshi and V. Bhanot, "Effect of accelerated aging on the tensile index of a synthetic insulation paper," *NDT E Int.*, vol. 38, no. 5, pp. 394–396, Jul. 2005.

[5] Underwriters Laboratories Inc., "Plastics Testing | Industries | UL." [Online]. Available: https://industries.ul.com/plastics-and-components/plastics/plastics-testing.

[6] Underwriters Laboratories Inc., "The UL Yellow Card for Plastics." [Online]. Available: https://industries.ul.com/plastics-and-components/plastics/plastic-recognition-yellow-card.

[7] LATI S.p.A, "High Performance Thermoplastics | LATI S.p.A." [Online]. Available: http://www.lati.com/.

[8] G. C. Pereira, F. D. Rzatki, G. Mariz, D. O. Barra, C. Ufsc, and S. Catarina, "Study of mechanical and thermo-physical properties of short glass fibers reinforced polybutylene terephthalate upon accelerated aging in refrigerant / lubricant mixture .," *Sl. Conf. Pap.*, no. October, pp. 1–4, 2014.

[9] K. T. Gillen and R. L. Clough, "Prediction of Elastomer Lifetimes from Accelerated Thermal-Aging Experiments," *Elastomer -Service life Predict. Symp. '97*, 1997.

[10] M. C. Celina, "Review of polymer oxidation and its relationship with materials performance and lifetime prediction," *Polym. Degrad. Stab.*, vol. 98, no. 12, pp. 2419–2429, Dec. 2013.

[11] R. Blaine, "A faster approach to obtaining kinetic parameters," *Am. Lab.*, pp. 21–23, 1998.

[12] L. Barral *et al.*, "Thermodegradation kinetics of a hybrid inorganic–organic epoxy system," *Eur. Polym. J.*, vol. 41, no. 7, pp. 1662–1666, Jul. 2005.

[13] A. Brems, J. Baeyens, J. Beerlandt, and R. Dewil, "Thermogravimetric pyrolysis of waste

polyethylene-terephthalate and polystyrene: A critical assessment of kinetics modelling," *Resour. Conserv. Recycl.*, vol. 55, no. 8, pp. 772–781, Jun. 2011.

[14] F. C. R. Lopes, J. C. Pereira, and K. Tannous, "Thermal decomposition kinetics of guarana seed residue through thermogravimetric analysis under inert and oxidizing atmospheres," *Bioresour. Technol.*, vol. 270, no. June, pp. 294–302, 2018.

[15] Y. J. Rueda-Ordóñez and K. Tannous, "Isoconversional kinetic study of the thermal decomposition of sugarcane straw for thermal conversion processes," *Bioresour. Technol.*, vol. 196, pp. 136–144, Nov. 2015.

[16] G. da C. Vasconcelos, R. L. Mazur, B. Ribeiro, E. C. Botelho, and M. L. Costa, "Evaluation of decomposition kinetics of poly (ether-ether-ketone) by thermogravimetric analysis," *Mater. Res.*, vol. 17, no. 1, pp. 227–235, Dec. 2013.

[17] C. Liu, J. Yu, X. Sun, J. Zhang, and J. He, "Thermal degradation studies of cyclic olefin copolymers," *Polym. Degrad. Stab.*, vol. 81, no. 2, pp. 197–205, Jan. 2003.

[18] I. Blanco, L. Abate, and M. L. Antonelli, "The regression of isothermal thermogravimetric data to evaluate degradation Ea values of polymers: A comparison with literature methods and an evaluation of lifetime prediction reliability," *Polym. Degrad. Stab.*, vol. 96, no. 11, pp. 1947–1954, Nov. 2011.

[19] K. M. Wagner, "A Study Of The Thermal Oxidative Degradation Of Polyamide 6,6 – Prediction Of The Thermal Index By A Short Term Analytical Method Versus Long Term Thermal Aging," *Master's Thesis, Washington State University*, 2016.

[20] LATI S.p.A, "Family Details - Lati Material Database." [Online]. Available: https://lambda.lati.com/pDescrizioneFamiglia.aspx?idFam=16.

[21] Underwriters Laboratories, "UL 746B: Polymeric Materials - Long Term Property Evaluations," Fourth Edi., Underwriters Laboratories, 2013.

[22] ASTM International, "ASTM D5423 - Standard Specification for Forced-Convection Laboratory Ovens for Evaluation of Electrical Insulation," no. Reapproved 2005, 2013.

[23] ASTM International, "ASTM D638 - Standard test method for tensile properties of plastics," vol. 08, pp. 46–58, 2003.

[24] International Organization for Standardization, "ISO 527 - Determination of Tensile Properties," 2012.

[25] ASTM International, "ASTM D6110 - Standard Test Method for Determining the Charpy Impact Resistance of Notched Specimens of Plastics 1," pp. 1–17, 2010.

[26] ASTM International, "ASTM D149 - Standard Test Method for Dielectric Breakdown Voltage and Dielectric Strength of Solid Electrical Insulating Materials at Commercial Power," vol. 09, no. Reapproved, pp. 1–13, 2013.

[27] ASTM International, "ASTM E2550 - 17 Standard Test Method for Thermal Stability by Thermogravimetry," 2017.

[28] ASTM International, "ASTM E2958 - 14 Standard Test Methods for Kinetic Parameters by Factor Jump/Modulated Thermogravimetry," 2014.

[29] ASTM International, "ASTM E1641 - 16 Standard Test Method for Decomposition Kinetics by Thermogravimetry Using the Ozawa/Flynn/Wall Method," 2016.

[30] ASTM International, "ASTM E1877 - 17 Standard Practice for Calculating Thermal Endurance of Materials from Thermogravimetric Decomposition Data," 2017.

[31] J. H. Flynn and L. A. Wall, "General treatment of the thermogravimetry of polymers," *J. Res. Natl. Bur. Stand. Sect. A Phys. Chem.*, vol. 70A, no. 6, p. 487, 1966.

[32] J. J. Xu and C. A. Kaminski, "Temperature index of electrical insulations by mTGA," *J. Test. Eval.*, vol. 42, no. 6, 2014.

[33] S. Calorimetry, "ASTM E793 - Standard Test Method for Enthalpies of Fusion and Crystallization by Differential," vol. 85, no. July, pp. 1–5, 2001.

[34] M. Suchitra, "Thermal Analysis of Composites Using DSC," *Adv. Top. Charact. Compos.*, pp. 11–33, 2004.

[35] R. L. Blaine, "Thermal Application Notes - Polymer Heats of Fusion."

[36] International Organization for Standards, "ISO 1133 - Determination of the melt mass-flow rate (MFR) and melt volume flow rate (MVR) of thermoplastics," vol. 2011, 2011.

[37] F. V. Briatico, "Principles of Polymer Processing," *Lect. Notes at Politecnico di Milano*, 2017.

[38] ASTM International, "ASTM E1640 - Standard Test Method for Assignment of the Glass Transition Temperature By Dynamic Mechanical Analysis," pp. 1–6, 2012.

[39] International Organization for Standardization, "ISO 307 - Plastics - Polyamides - Determination of Viscosity Number," 2012.

[40] P. Uribe-Arocha, C. Mehler, J. E. Puskas, and V. Altstädt, "Effect of sample thickness on the mechanical properties of injection-molded polyamide-6 and polyamide-6 clay nanocomposites," *Polymer*, vol. 44, no. 8. pp. 2441–2446, 2003.

[41] N. N. Rammo and A. M. Mahdi, "Thermal Degradation Kinetics of Polyamide 6,6 Cable

Ties by Thermogravimetric Analysis," *Ibn Al-Haitham Journal For Pure And Applied Science*, vol 26 (3), 2013

[42] S. Kumagai, Y. Morohoshi, G. Grause, T. Kameda, and T. Yoshioka, "Pyrolysis versus hydrolysis behavior during steam decomposition of polyesters using 18 O-labeled steam," *RSC Adances*, vol. 00, pp. 1–3, 2013.

[43] L. M. Al-Omairi, "Crystallization, Mechanical, Rheological and Degradation Behavior of Polytrimethylene terephthalate, Polybutylene terephthalate and Polycarbonate blend," *Doctoral thesis at Royal Melbourne Institute of Technology*, 2010.

[44] L. Bottenbruch, *Engineering thermoplastics : polycarbonates polyacetals polyesters cellulose esters*. Hanser Publishers, 1996.

[45] M. Yokouchi, Y. Sakakibara, Y. Chatani, H. Tadokoro, T. Tanaka, and K. Yoda, "Structures of Two Crystalline Forms of Poly(butylene terephthalate) and Reversible Transition between Them by Mechanical Deformation," *Macromolecules*, vol. 9, no. 2, pp. 266–273, 1976.

[46] A. A. Apostolov, S. Fakirov, M. Stamm, R. D. Patil, and J. E. Mark, "Alpha-beta transition in poly(butylene terephthalate) as revealed by small-angle X-ray scattering," *Macromolecules*, vol. 33, no. 18, pp. 6856–6860, 2000.

[47] D. Zhang, M. He, W. He, Y. Zhou, S. Qin, and J. Yu, "Influence of Thermo-Oxidative Ageing on the Thermal and Dynamical Mechanical Properties of Long Glass Fibre-Reinforced Poly(Butylene Terephthalate) Composites Filled with DOPO," *Materials (Basel).*, vol. 10, no. 5, p. 500, 2017.

[48] A. V. Hopper, *Recent developments in polymer research*. Nova Science Publishers, 2007.

[49] P. Gijsman, W. Dong, A. Quintana, and M. Celina, "Influence of temperature and stabilization on oxygen diffusion limited oxidation profiles of polyamide 6," *Polym. Degrad. Stab.*, 2016.

[50] L. M. Nicholson, K. S. Whitley, T. S. Gates, and J. A. Hinkley, "Influence of Molecular Weight on the Mechanical Performance of a Thermoplastic Glassy Polyimide," *Journal of Materials Science*, Volume 35, Issue 24, pp 6111–6121, 2000.

[51] P. J. Flory, "Tensile Strength in Relation to Molecular Weight of High Polymers," *J. Am. Chem. Soc.*, vol. 67, no. 11, pp. 2048–2050, Nov. 1945.

[52] R. Frassine, "Mechanical behaviour and durability of polymers," *Lect. Notes at Politecnico di Milano*, 2018.